ID: 12340

Etappvis schakt i lös lera med nyttjande av konsolspont och hammarband

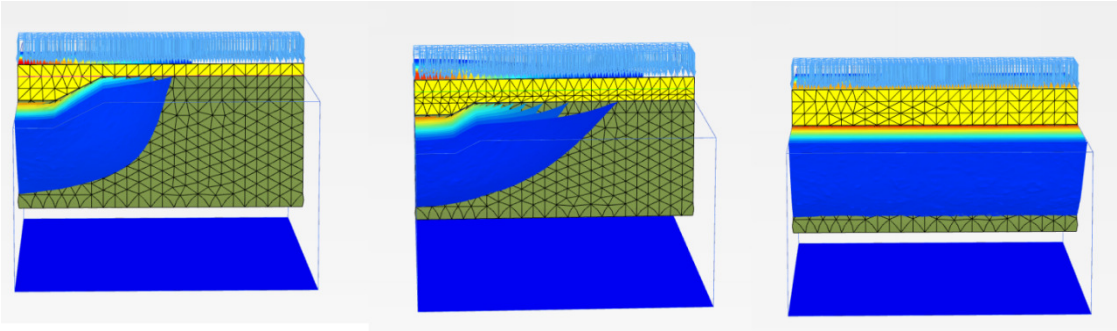

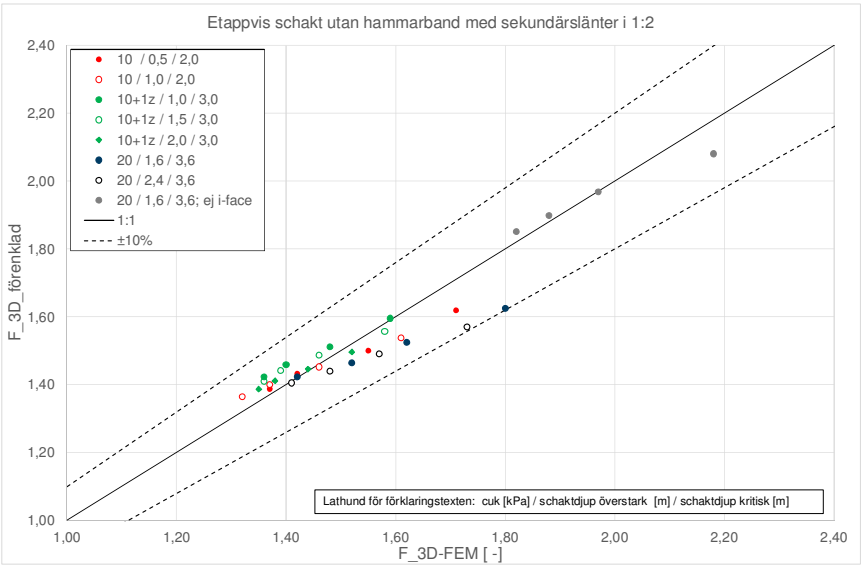

Torbjörn Edstam

Skanska Sverige AB
Teknik

2018

SBUF stödjer
forskning & utveckling
som leder till
praktisk handling

FÖRORD

Under perioden 2009-2010 utförde Skanska Sverige AB, på uppdrag av dåvarande Banverket och Vägverket, entreprenaden ”Bohus-Nödinge, E33”. Utbygganden omfattade bl.a. etappvisa schaktarbeten i lös lera i omedelbar anslutning till ett befintligt trafikerat järnvägsspår längs en ca 600 m lång sträcka.

I föreliggande Slutrapport med tillhörande bilagor, inklusive ett Examensarbete utfört inom ramen för SBUF-projektet, sammanfattas erfarenheterna ifrån de fältmätningar och analyser som utförts. Delar av analyserna utfördes som en del av Examensarbetet, medan övriga analyser utförts relativt nyligen.

Examensarbetet utfördes av Hannes Persson (numera Nordefjäll) och Daniel Sigström, båda numera Skanska Sverige AB.

Till SBUF-projektet har varit kopplat en referensgrupp enligt följande:

- Tara Wood, NCC
- Anders Ryner, GeoTeam (numera Geomind)
- Per-Evert Bengtsson, Statens geotekniska institut (numera PEB Geoteknik)
- Leif Jendeby, Vägverket (numera COWI)
- Anders Hallingberg, Banverket (numera Trafikverket)

Projektet har finansierats av SBUF, Banverket (numera en del av Trafikverket) och Skanska Sverige AB.

Ett stort tack riktas till samtliga ovannämnda personer och finansiärer samt till ett antal kollegor på Skanska Sverige AB (ingen nämnd och ingen glömd) som på olika sätt bidragit till genom- och slutförandet av detta projekt.

Göteborg i september 2018

Torbjörn Edstam

SAMMANFATTNING

Schaktarbeten skall alltid utföras på ett sådant sätt att stabiliteten är tillfredställande. Vid måttliga schaktdjup i lös lera kombineras ofta etappvis (temporär) schakt med en konsolspont som förses med ett hammarband, vars syfte är att omfördela jordtrycket horisontellt. På detta sätt ökar det stabiliserande bidraget från den del av spontväggen som ligger strax intill, men ej mitt för, den lokalt djupare schaktetappen, samtidigt som de schaktinducerade rörelserna begränsas.

I denna Slutrapport sammanfattas erfarenheterna ifrån de fältmätningar, det examensarbete och de efterföljande, mer omfattande analyser, som utförts under det senare år.

Fältmätningarna och Examensarbetet var kopplat till Skanskas entreprenad ”Bohus-Nödinge, E33”, som genomfördes under perioden 2009-2011. Under senare år har modellerats ett antal scenarier som någorlunda efterliknar situationer som ofta råder vid nyttjandet av konsolspont i lös lera. Dessa analyser har utförts i form av finita element metoden, inklusive beaktandet av tredimensionella geometrier och lastförutsättningar, sk 3D-FEM.

De viktigaste erfarenheterna/slutsatserna från ovannämnda aktiviteter är:

- De utförda fältmätningarna och analyserna med 3D-FEM påvisar tydligt att nyttjande av ett kraftigt hammarband leder till avsevärt minskade schaktinducerade rörelser.
- Det är viktigt att på ett korrekt sätt beakta spontväggens anisotropa deformations- och hållfasthetsegenskaper.
- En förenklad beräkningsmodell för beaktande av ”3D-effekter” har utvecklats map ULS/GEO.
- Förutsatt Säkerhetsklass 2 och nyttjande av ovannämnda förenklade beräkningsmodell är lasteffekten i stödkonstruktionen (ULS/STR) så begränsad att normalt förekommande spontplankor, hammarband och i svetsar mellan hammarbandet och spontplankorna kan användas.
- Om man inte beaktar den begränsade råheten spont/lera och vattenspalten på spontväggens aktivsida (vilket avviker ifrån svensk praxis) överskattas totalsäkerhetfaktorn (ULS/GEO) påtagligt samtidigt som lasteffekten i stödkonstruktionen underskattas avsevärt.
- Det är önskvärt att helt undvika nyttjande av spont vid schaktarbeten. Inom ramen för det aktuella SBUF-projektet har begränsade studier utförts, bl.a. med 3D-FEM, varvid konstaterats att dagens branschpraxis delvis är felaktig och dessutom troligen överskattar 3D-effekten när det gäller utformning av etappvis frischakt (slänter). Studierna antyder dock att en förenklad beräkningsmodell för ULS/GEO, likartad den modell som utvecklats för etappvis schakt inom konsolspont, bör ge tillfredsställande noggrannhet, men detta behöver studeras vidare.

INNEHÅLL

1 Inledning

1.1 Bakgrund

Schaktarbeten skall alltid utföras på ett sådant sätt att stabiliteten är tillfredställande. I stadsmiljö uppstår ibland geometriska konflikter med angränsande konstruktioner vilket omöjliggör frischakt med slänter. I sådana fall stöttas schaktväggarna av en spont. I takt med att schaktdjupet ökar krävs en successivt kraftigare stödkonstruktion – exempelvis genom att stötta spontväggen med bakåtförankrade stag eller stämp/strävor. Detta medför dock påtagligt ökande kostnader och långsammare framdrift. Vid måttliga schaktdjup i lös lera, typiskt 2-4 m, tillgrips därför ofta etappvis schakt. Spontväggen är dock förhållandevis böjvek i horisontell led varför ett hammarband, men helst ej stämp eller stag/strävor, nyttjas i syfte att omfördela jordtrycket horisontellt. På detta sätt ökar det stabiliserande bidraget från den del av spontväggen som ligger strax intill, men ej mitt för, den lokalt djupare schaktetappen, samtidigt som de schaktinducerade rörelserna begränsas.

Framtagandet av en lämplig utformning av spontväggen, hammarbandet och den etappvisa schakten innehåller dock många osäkerheter och baseras ofta på tidigare personliga erfarenheter under mer eller mindre kontrollerade former. Numera finns dock kommersiellt tillgängliga avancerade analysverktyg i form av finita element metoden (FEM), vilka även kan beakta tredimensionella geometrier och lastförutsättningar, sk 3D-FEM. Denna typ av analyser är dock förhållandevis tidskrävande, kräver tillgång till kostsam programvara samt god förståelse för hur beräkningsprogrammet fungerar (avseende såväl praktisk hantering som de underliggande teorierna).

1.2 Syfte

Målsättningen med projektets har varit att utveckla en metodik för lämplig utformning av stödkonstruktionen, i form av en konsolspont med hammarband, och det etappvisa schaktarbetet vid temporära schakter. Härvid har syftet varit att utveckla en förenklad beräkningsmodell som medför att tidskrävande analyser med 3D-FEM i möjligaste mån kan undvikas eller reduceras. Således kan den i rapporten föreslagna beräkningsmodellen åtminstone användas vid inledande överslagsberäkningar. Huruvida enstaka kompletterande analyser med 3D-FEM erfordras vid efterföljande detaljprojektering måste dock avgöras av ansvarig geokonstruktör från fall till fall mht de aktuella byggnadstekniska förhållandena.

1.3 Genomförande

Under tidsperioden 2009-2010 utfördes fältmätningar och teoretiska analyser kopplade till Skanskas då pågående entreprenad ”Bohus-Nödinge, E33” på uppdrag av BanaVägiVäst. Arbetet utfördes till stor del inom ramen för ett examensarbete (Persson och Sigström, 2010), vilket även bifogas som Bilaga 1. Schaktarbetena modellerades med FE-programmet PLAXIS 3D FOUNDATION, varvid konstaterades att en del begränsningar i dåvarande version av programvaran medförde att vissa aspekter inte kunde modelleras på ett tillfredsställande sätt.

Under efterföljande år har erfarenheterna ifrån ovannämnda studier nyttjats inom Skanska Teknik vid utformningen av diverse etappvisa schakter i lös lera i Göteborgstrakten. Under denna tidsperiod har nya versioner av PLAXIS 3D FOUNDATION utvecklats (numera benämnda PLAXIS 3D), varvid kunnat konstateras att flertalet av begränsningarna successivt har hanterats. Efter att författaren hade nyttjat PLAXIS 3D 2017 (som blev kommersiellt tillgängligt hösten 2017) i diverse projekt ansågs våren 2018 att tiden var mogen att utföra förnyade systematisk analyser. Vid dessa analyser modellerades ett antal scenarier som någorlunda efterliknar situationer som ofta råder vid nyttjandet av konsolspont i lös lera – åtminstone i de projekt som Skanska Teknik i Göteborg varit engagerade i under senare år.

I denna Slutrapport sammanfattas erfarenheterna och slutsatserna av ovannämnda aktiviteter.

2 Mätningar och analyser i samband med entreprenaden ”Bohus-Nödinge, E33”

2.1 Inledning

De etappvisa schaktarbeten utfördes i lös lera i omedelbar anslutning till ett befintligt trafikerat järnvägsspår längs en ca 600 m lång sträcka.

I samband med schaktarbetena utfördes rörelsemätningar på det befintliga järnvägsspåret inom ramen för det ordinarie kontrollprogrammet. På några utvalda delsträckor utökades dock mätinsatsen i form av ett tillkommande antal mätpunkter, ”kontinuerlig” mätning av dessa då den etappvisa schakten utfördes samt genom mätning mha inklinometer för att se hur sidorörelserna varierade med djupet. Detta kombinerades med modelering av schaktarbetena mha FE-programmet PLAXIS 3D FOUNDATION.

Ovanstående utökade arbeten utfördes till stor del inom ramen för ett examensarbete (Persson och Sigström, 2010) som bifogas som Bilaga 1. Efterföljande avsnitt 2.2-2.5 är i huvudsak en mycket kortfattad sammanfattning av innehållet i den skriften (samtliga figurer i Avsnitt 2 är hämtade därifrån). För detaljer hänvisas till Bilaga 1.

2.2 Schaktarbeten

De studerade delsträckorna och schaktetapprena framgår översiktligt i Figur 1. Längs ena delsträckan saknade konsolsponten (AU14) hammarband medan ett kontinuerligt hammarband (HEB 300) nyttjades inom den andra delsträckan. Som framgår var schaktdjupet begränsat, men på grund av det intilliggande trafikerade spåret i kombination med de utmanande grundförhållandena (ca 1 m fyllning och därunder delvis extremt låg odränerad skjuvhållfasthet; ca 7 kPa i lerans överkant med en tillväxt på ca 1 kPa/m med djupet) krävdes förhållandevis långa spontplankor pga den dimensionerande tåglasten.

Figur 1. *De studerade schaktetapperna.*
Övre bilden: Delsträckan utan hammarband.
Undre bilden: Delsträckan med hammarband.

2.3 Mätningar och mätresultat

De uppmätta horisontalrörelserna, vinkelrätt spontväggen, i toppen av spontplankorna redovisas i Figur 2. Som framgår medför nyttjandet av hammarbandet påtaglig minskade rörelser. I aktuellt fall är rörelserna vid nyttjande av hammarband så små att de är i paritet med mätprecisionen, vilket yttrar sig i form av ”brus”. Motsvarande ”brus” gäller för inklinometermätningarna varför resultaten ifrån dem ej berörs ytterligare. Orsaken till de små uppmätta rörelserna torde vara att den dimensionerande tåglasten dominerar den ”pådrivande lasten”, vilket i sin tur resulterat i den förhållandevis kraftiga stödkonstruktionen.

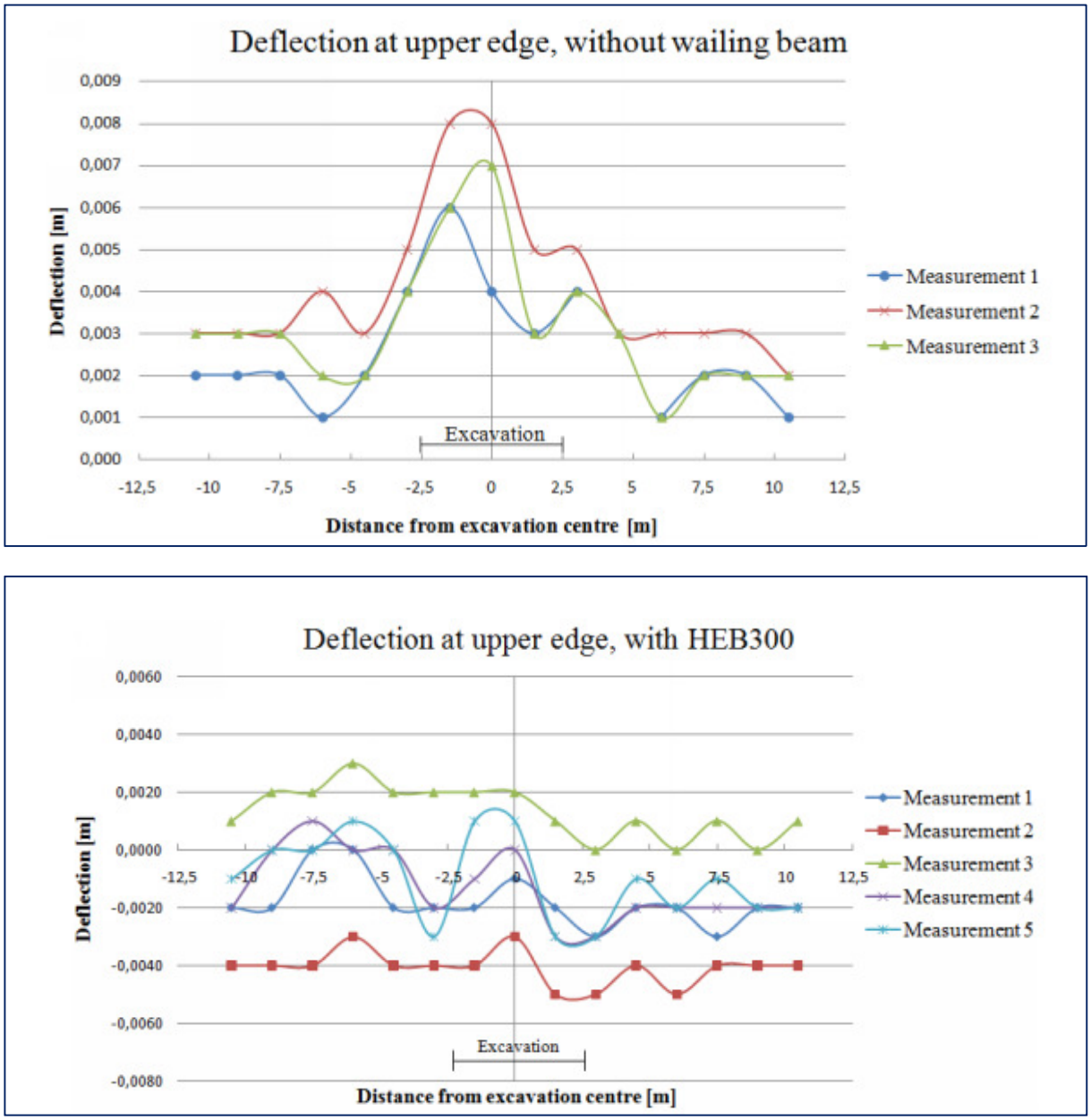

Figur 2. *Uppmätta horisontalrörelser vinkelrätt spontväggen.*
Övre bilden: Delsträckan utan hammarband.
Undre bilden: Delsträckan med hammarband.

2.4 Inledande modelleringar

Modellering av de etappvisa schakterna utfördes mha FE-programmet PLAXIS 3D FOUNDATION (P3DF) som på den tiden (år 2010) var ett av de mest avancerade FE-programmen för geotekniska tillämpningar vid vilka tredimensionella effekter kunde beaktas.

Under genomförandet av examensarbetet framkom ett flertal begräsningar i P3DF, vilka åtminstone delvis kunde hanteras genom ”parameterstudier” och/eller ”pragmatiska förenklingar”, varav några av berörs kortfattat nedan:

- Beräkningstiden vid 3D-beräkningar är väsentligt större än vid 2D-beräkningar (timmar till dagar istället för enstaka minuter), vilket innebär att man inledningsvis behöver ägna en del tid åt att hitta ett lagom finindelat elementnät, modellens yttre begränsningslinjer, osv. Exempelvis medför ett för grovt elementnät felaktiga beräkningsresultat (jämfört med en teoretiskt korrekt – men i praktiken ofta okänd - lösning), normalt i form av underskattade rörelser (SLS = serviceability limit state = bruksgränstillstånd) och en överskattad säkerhetsfaktor (ULS/GEO; ULS = ultimate limit state = brottgränstillstånd; GEO = brott i jorden).

- Begränsad möjlighet att modellera de geometriska förutsättningarna i alla tre dimensioner, vilket innebar att ”sekundärslänten” vinkelrätt mot spontväggen måste modelleras på ett förenklat sätt. Som framgår i efterföljande avsnitt påverkade det ULS/GEO-analyserna.

- I realiteten är spontplankornas böjstyvhet relativt stor i vertikalled, men mycket begränsad i horisontalled (del pga spontplankornas korrugerade tvärsnitt och dels pga att spontlåsen ”glappar”). För att kunna modellera detta krävs ”plate-element” med anisotropa materialegenskaper. Detta kan P3DF förvisso beakta approximativt, men genom ett antal FE-modelleringar av enbart den korrugerade spontväggen framkom att de rekommendationer som ges i ”User Manual” till P3DF påtagligt överskattar spontväggens böjstyvhet i horisontalled. Detta visade sig även vid efterföljande P3DF-modelleringar av ett scenario som var någorlunda likt förhållandena vid schakten för delsträckan utan hammarband, se Figur 3 och Figur 4. I dessa figurer är ”Alt 1” den parameteruppsättning som rekommenderas i ”User Manual” till P3DF och den därmed resulterande utböjningen. Den parameteruppsättning som bedöms vara mest realistisk för en spontvägg uppbyggd av de aktuella spontplankorna benämns dock ”Alt 4” och som framgår leder det till en maximal utböjning som är ca 50 % större än ”Alt 1” - allt annat lika. Noteras bör även att om stödkonstruktionens böjstyvhet i horisontalled antas vara lika stor som den i vertikalled (”Alt 5”) erhålls en maximal utböjning som endast är ca 1/3 av den utböjning som erhålls för den parameteruppsättning som bedöms vara mest realistisk (”Alt 4”).

- Såväl spontväggen (”plate-elements”) som hammarbandet (”beam-elements”) kan enbart tilldelas elastiska egenskaper (om än anisotropa). Detta innebär att vid ULS-beräkningar utbildas brottmekanismer inom vilka enbart jordens fulla skjuvhållfasthet mobiliseras (ULS/GEO men nödvändigtvis inte ULS/STR; STR = brott i konstruktionselement).

Table 4.3. Properties of different sheet pile walls tested in the soil/structure model. Flexural rigidity is depending on the internal moments of inertia in different directions, which are presented. Relations to I_1 within brackets.

Alt	I_1 [m^4]	I_2 [m^4]	I_{12} [m^4]	
1	$2{,}871 \cdot 10^{-4}$	$1{,}436 \cdot 10^{-5}$ (I_1/20)	$2{,}871 \cdot 10^{-5}$ (I_1/10)	PLAXIS manual recommendations
2	$2{,}871 \cdot 10^{-4}$	$3{,}811 \cdot 10^{-8}$ (I_1/7533)	$2{,}871 \cdot 10^{-5}$ (I_1/10)	I_2 from PLAXIS 2D simulations
3	$2{,}871 \cdot 10^{-4}$	$3{,}811 \cdot 10^{-8}$ (I_1/7533)	$2{,}871 \cdot 10^{-7}$ (I_1/1000)	I_1, I_2 from PLAXIS 3D simulations
4	$2{,}871 \cdot 10^{-4}$	$3{,}811 \cdot 10^{-8}$ (I_1/7533)	$2{,}871 \cdot 10^{-6}$ (I_1/100)	I_{12} adjusted
5	$2{,}871 \cdot 10^{-4}$	$2{,}871 \cdot 10^{-4}$ (I_1/1)	$2{,}871 \cdot 10^{-4}$ (I_1/1)	Isotropic

Figur 3. Olika parameteruppsättningar som använts vid modellering av utböjningen hos en spontvägg uppbyggd av AU14-spontplankor.

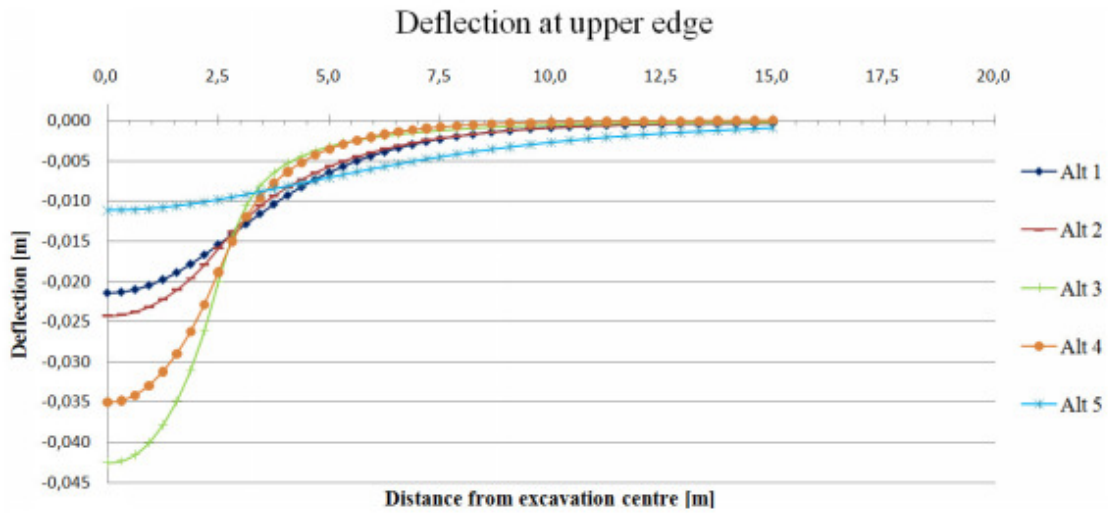

Figure 4.4 The horizontal deflection at the upper edge of the sheet pile wall at different lengths from excavation centre. No wailing beam is used. Five wall settings are tested with different relations between the moments of inertia I_1, I_2 and the torsional rigidity against warping, I_{12}.

Figur 4. Utböjning av en spontvägg vid etappvis schakt för olika antaganden rörande spontväggens böjstyvhet.

2.5 Modelleringar av olika scenarier

Efter att ovan berörda aspekter studerats utfördes ett flertal modelleringar av olika scenarier avseende exempelvis effekterna av schaktetappernas längd, hammarbandens typ och krönlängd samt jordens styvhetsegenskaper. Här återges enbart några utvalda exempel på de beräkningsresultat som anses vara mest intressanta, nämligen hammarbandets påverkan på utböjningen (SLS) samt totalsäkerhetsfaktorn (ULS/GEO).

De tidigare berörda begränsade möjligheterna att modellera geometrier i P3DF innebar att beräkningsmodellen måste förenklas. Detta gjordes genom att all jord ovanför nivån för schaktbotten inom den etappvisa schakten ersattes med yttre laster (vertikalspänning i nivå schaktbotten motsvarande tyngden av ovanliggande jord och trafiklast; horisontalspänning mot spontväggarna motsvarande medelvärdet av vilojordtrycket och det aktiva jordtrycket). Den resulterande beräkningsmodellen framgår i Figur 5.

Effekten på utböjningen (SLS) vid nyttjande av olika typer av hammarband - allt annat lika - framgår i Figur 6. Som förväntat minskar utböjningen ju styvare hammarband som nyttjas och förutsatt ett HEB300-hammarband förefaller den maximala utböjningen kunna halveras jämfört med att inget hammarband nyttjas.

Effekten på brottmekanismen och därmed totalsäkerheten (ULS/GEO) utan respektive med nyttjande av hammarband visualiseras i Figur 7. Utan hammarband utgörs den kritiska brottmekanismen av att spontväggen ”lägger sig” (roterar kring spontväggens underkant) inom och strax bortom delsträckan för den etappvisa schakten, varvid totalsäkerhetsfaktorn uppgår till ca 1,7. Med nyttjande av hammarband utgörs den kritiska brottmekanismen av kollaps i jorden i anslutning till ”sekundärslänten” vinkelrätt spontväggen, varvid totalsäkerhetsfaktorn uppgår till ca 1,9. Det förenklade sättet att modeller ”sekundärslänten” bidrar dock sannolikt till att underskatta totalsäkerhetsfaktorn (ULS/GEO) vid nyttjande av hammarbandet, men det förutsätter att hammarbandet väljs så kraftigt mht ULS/STR att den erhållna brottmekanismen blir kritisk.

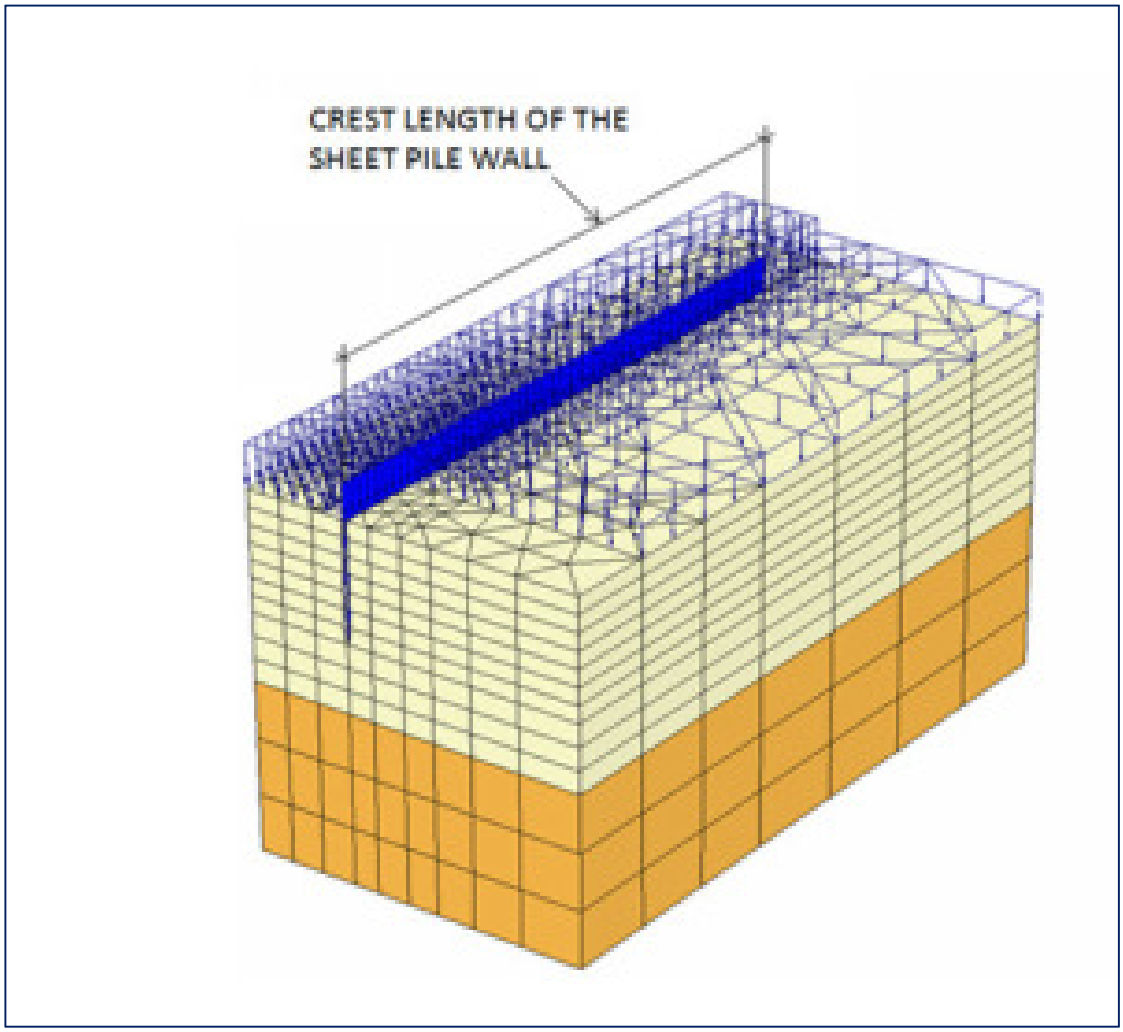

Figur 5. *Beräkningsmodellen i P3DF vid modelleringen av ett av de studerade scenarierna. I förgrunden syns halva schaktetappen (pga nyttjande av symmetri för att reducera beräkningstiden) vilken modellerats genom att deaktivera de yttre laster som motsvarar jordtrycket mot sponten och den blivande schaktbotten innan schakten utförs.*

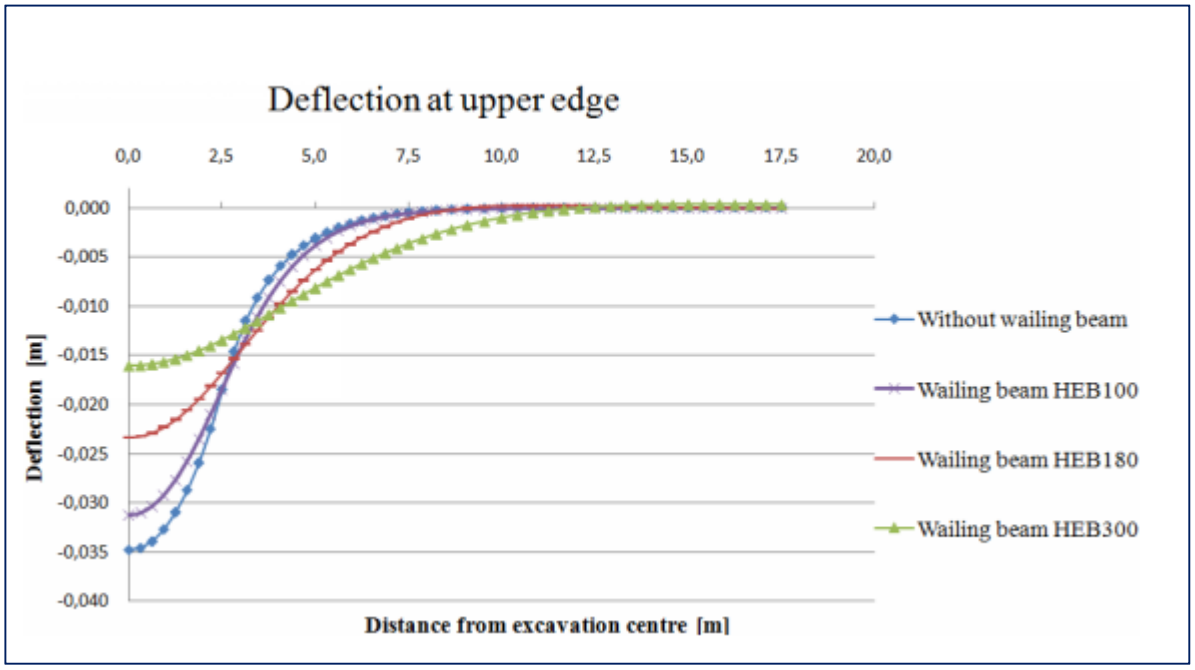

Figur 6. *Spontväggens utböjning vid nyttjande av hammarband med olika böjstyvhet.*

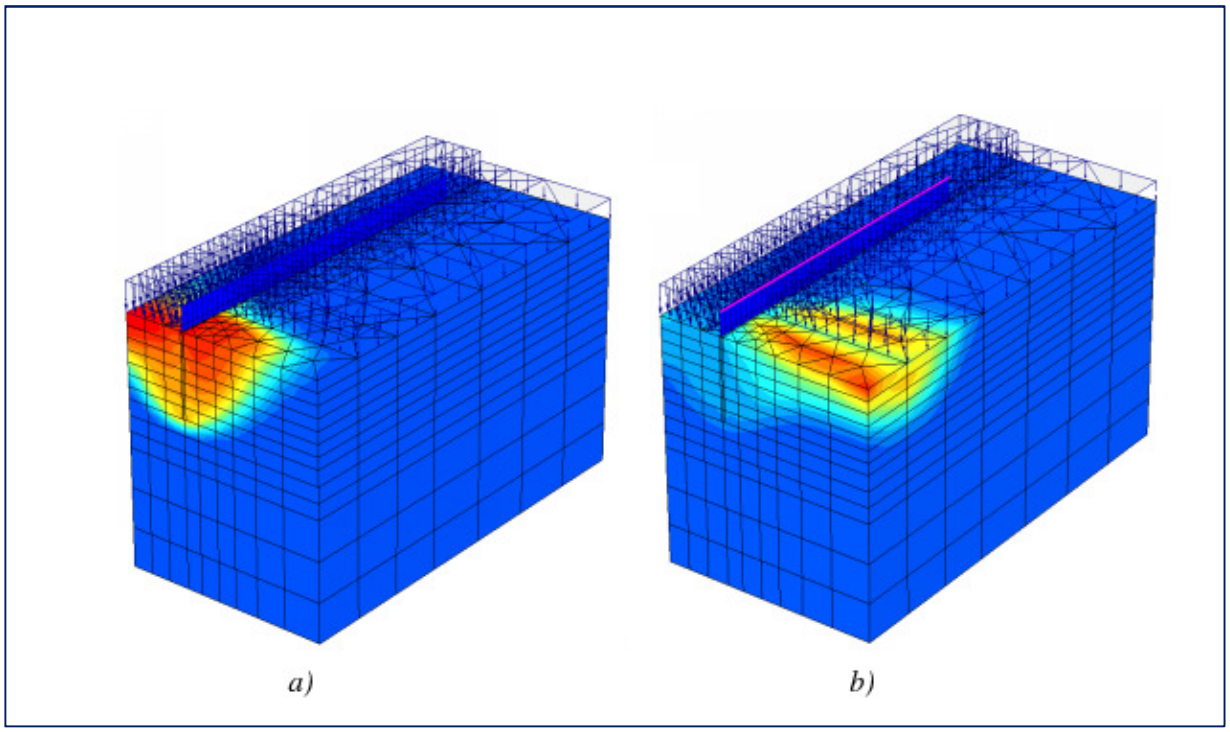

Figur 7. *Visualisering av brottmekanismen (ULS/GEO) utan (till vänster) respektive med (till höger) hammarband.*

3 Analyser under senare år

3.1 Inledning

Erfarenheterna ifrån bl.a. analyserna av tidigare berörda entreprenad ”Bohus-Nödinge, E33” har under senare år nyttjats inom Skanska Teknik i de fall när etappvis schakter i lös lera har utförts inom konsolspont. Numera föreskrivs i stort sett alltid att konsolsponten förses med ett kraftigt hammarband.

Nya versioner av PLAXIS 3D FOUNDATION har utvecklats (numera benämnda PLAXIS 3D), varvid vissa av de tidigare begränsningarna har hantertas, jfr Avsnitt 2.4. I ett antal år har det varit möjligt att geometriskt modellera den tidigare berörda ”sekundärslänten” vinkelrätt spontväggen. Från och med PLAXIS 3D 2017 (som släpptes hösten 2017) har det även varit möjligt att modellera såväl spontväggen (”plate-elements”) som hammarbandet (”beam-elements”) med en anisotrop elastoplastisk materialmodell.

Våren 2018 ansågs att tiden blivit mogen att slutföra det aktuella SBUF-projektet och sammanställa erfarenheterna i denna Slutrapport. Som ett led i detta har ett antal analyser utförts med PLAXIS 3D 2017 (version 2017.01) under senare tid, varvid fokus varit att ta fram en förenklad beräkningsmodell med fokus på ULS för ett antal scenarier som någorlunda efterliknar sådana scenarier som ofta uppkommer vid nyttjandet av konsolspont – åtminstone i de projekt som Skanska Teknik i Göteborg varit engagerade i. Således är den föreslagna beräkningsmodellen inte alltid direkt tillämpar för kvantitativa ULS-beräkningar, men i sådana fall bör det redovisade tillvägagångssättet vara användbart som inspiration vid planering och genomförande av systematiska modelleringar med 3D-FEM av andra scenarier än de studerade.

De ursprungliga planerna på att utveckla en förenklad beräkningsmodell avseende SLS har dock skrinlagts. Detta beror dels på att 3D-modelleringar är så tidskrävande att den geometriska modellen måste begränsas av ”fiktiva randvillkor” som inte avspeglar de verkliga grundförhållandena (exempelvis lerans utbredning i djup och plan) och dels på att de konstitutiva modeller som erfordras för att någorlunda efterlikna lerans spännings-töjningsrespons, vid fokus på SLS, är så komplexa att beräkningstiden blir påtaglig (även om man skulle nyttja ”fiktiva randvillkor”). Som tydligt framgår i Avsnitt 2 bör ett kraftigt hammarband dock alltid nyttjas om de schaktinducerade rörelserna behöver begränsas (självklart är en kortare schaktetapp även en effektiv åtgärd).

3.2 Inledande översiktlig studier av 3D-effekter vid frischakt i lera mht ULS

Oavsett om den etappvisa schakten utförs inom en spontvägg (spontplankor utan/med hammarband och eventuellt stämp) eller som frischakt (slänter) bidrar anslutande överstarka delsträckor till stabiliteten. Nyttjande av en spontvägg leder dock till ökad komplexitet jämfört med frischakt. Därför har en begränsad genomgång gjorts av litteratur som behandlar hur ”3D-effekter” kvantitativt kan tillgodoräknas på ett förhållandevis enkelt sätt vid frischakt i lera,

varvid syftet var att hitta inspiration till hur 3D-effekter skulle kunna nyttjas vid etappvis schakt inom en spontvägg.

I Sverige är den metod som redovisas i Skredkommissionen (1995) att betrakta som branschpraxis, se Figur 8. Efter en mer detaljerad genomgång av relevanta avsnitt av den skriften, inklusive diskussioner med några av delförfattarna, och studium av bl.a. den artikel som där refereras till (Gens et al, 1988) anses att ekvationen längst ned i Figur 8 inte är korrekt (gissningsvis pga av att ”tryckfelsnisse” varit framme). Oavsett om ekvationen är korrekt eller ej är en viktig förutsättning för att tillvägagångssättet i Figur 8 skall vara direkt tillämpbart att angränsade överstarka delsträckor är oändligt överstarka. Detta påtalas förvisso i Skredkommissionen (1995) och dessutom föreslås där en förenklad metod som skall beakta situationer där så inte är fallet. Efter modelleringar mha 3D-FEM av stabilitetsförhållandena för några relativt enkla geometriska förhållanden, exemplifierat i Figur 9, är dock bedömningen att inte heller den metoden är tillförlitlig och dessutom överskattar 3D-effekten.

Oavsett den exakta matematiska formuleringen av en förenklad beräkningsmetod som skall kunna hantera 3D-effekter vid etappvis schakt måste den beakta stabilitetsförhållandena inom såväl den kritiska delsträckan (beskriven av $F_{2D\_kritisk}$, $L_{kritisk}$) som närliggande överstarka delsträckor (beskriven av $F_{2D\_överstark}$). En av de enklast möjliga ekvationerna för att i princip beakta detta är:

$$\frac{F_{2D\_kritisk} \cdot L_{kritisk} + F_{2D\_överstark} \cdot L_{överstark}}{L_{kritisk} + L_{överstark}} = F_{3D} \qquad \textit{Ekv. 1}$$

Om man förutsätter att denna förenklade ekvation är tillämpbar gäller för kvoten $F_{2D\_överstark}/F_{2D\_kritisk}$ =1,0 att $L_{överstark}$ är oändligt lång (vilket är identiskt med plant töjningstillstånd i 2D). Med ökande kvot minskar $L_{överstark}$, men teoretiskt minskar den aldrig till exakt noll på grund av ändyteeffekten (3D-effekten). Således är $L_{överstark}$ en ”modellparameter” som saknar exakt geometrisk betydelse men den kan trots det vara användbar i en förenklad beräkningsmodell enligt Ekv. 1 vars syfte är att i möjligaste mån undvika tidskrävande modelleringar med 3D-FEM. Denna idé testades för etappvis frischakt i lera genom att några hypotetiska (men realistiska) scenarier modellerades med 3D-FEM map ULS(GEO), varefter $L_{överstark}$ ”bakåträknades” mha Ekv. 1. Eftersom ett relativt tydligt samband erhölls mellan $L_{överstark}$ och kvoten $F_{2D\_överstark}/F_{2D\_kritisk}$ nyttjades motsvarande tillvägagångssätt även för etappvis schakt i lera inom konsolspont, se Avsnitt 3.3.4.

1. Beräkna säkerhetsfaktorn utan beaktande av ändyteeffekter, $F_{2\text{-}Dim}$

$$F_{2-Dim} = \frac{M_{(\tau_{fu} \cdot l \cdot r)}}{M_{(W \cdot a + Q \cdot b)}}$$

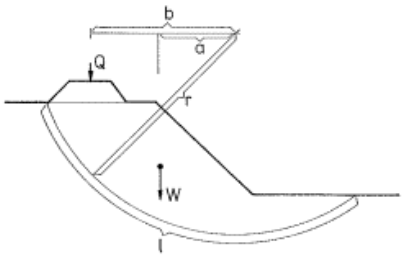

2. Beräkna säkerhetsfaktorn med plana ändytor, F_p

$$F_p = \frac{M_{(\tau_{fu} \cdot l \cdot r \cdot L)} + 2\,M_{(\tau_{fu} \cdot A \cdot c)}}{M_{(W \cdot a + Q \cdot b)L}}$$

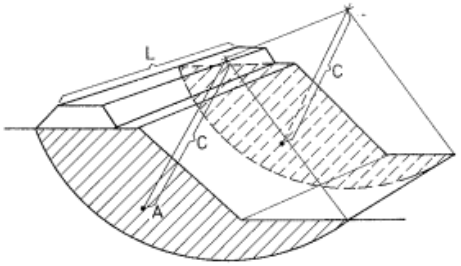

3. Beräkna den 3-dimensionella säkerhetsfaktorn, $F_{3\text{-}Dim}$

$$F_{3-Dim} = F_{2-Dim} + 0{,}75\left(\frac{F_p}{F_{2-Dim}} - 1\right)$$

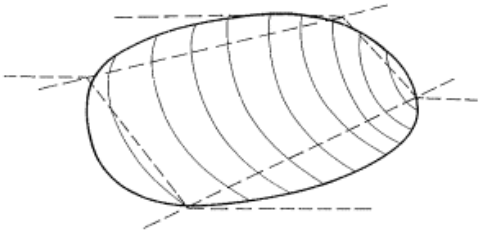

Figur 8. Beräkning av säkerhetsfaktorn vid nyttjande av 3D-effekten enligt rådande svensk branschpraxis (Skredkommissionen, 1995).

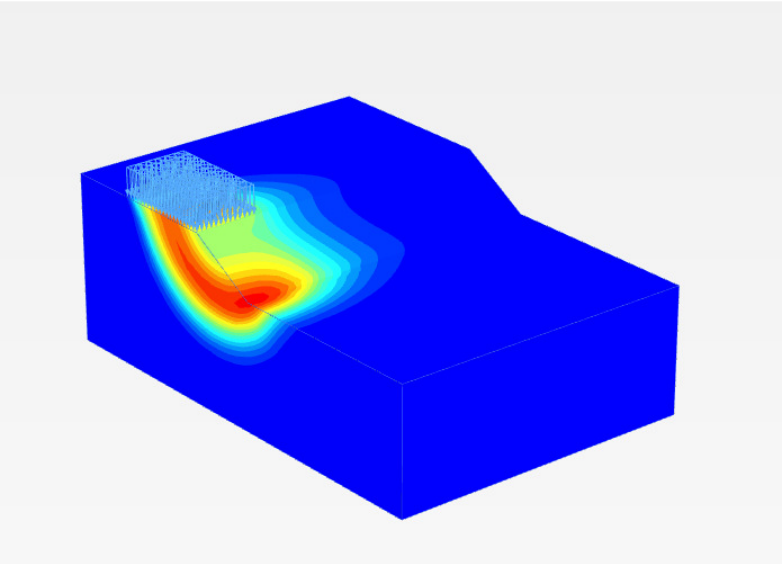

Figur 9. *Exempel på utbildad 3D-brottmekanism vid frischakt i lera (i aktuellt scenario beror 3D-effekten på en ytlast med begränsad utbredning parallellt med släntkrönet).*

3.3 Analyser mha 3D-FEM av etappvis schakt i lera inom konsolspont mht ULS

3.3.1 Studerade scenarier

Ett antal olika kombinationer avseende grundförhållanden, schaktgeometri samt utformning av stödkonstruktionerna har analyserats mha 3D-FEM i syfte att någorlunda täcka in ett antal vanligen förekommenade situationer enligt nedan.

Grundförhållanden och materialegenskaper:

Lera till stor djup (”svävande” spont) med tre alternativa hållfasthetsprofiler c_u:

- 10 kPa
- 10+1z kPa (z= i 0 i markytan)
- 20 kPa

Lerans tunghet 16 kN/m^3. Hydrostatisk grundvattensituation med gvy i markytan. K_0=0,7.

Leran modellerad som ett odränerat tvåfas Mohr-Coulomb material med E=250c_u och ν=0,2.

Schaktgeometri:

Den kritiska schaktetappens totalsäkerhetsfaktor förutsatt 2D-förhållanden (plant töjningstillstånd) uppgår genomgående till ca $F_{tot,2D} \approx 1,20$. Detta motsvarar 2,0-3,6 m schaktdjup beroende på aktuell hållfasthetsprofil.

Sekundärslänterna vinkelrätt spontväggen har genomgående lutningen 1:2 på ömse sidor om den kritiska schaktetappen.

De intilliggande överstarka delsträckornas schaktdjup är 1,0-2,0 m mindre än inom den kritiska schaktetappen.

Den kritiska schaktetappens längd varierar mellan ca 5,0 och 18,0 m.

Schaktbredden (vinkelrätt spontväggen) uppgår till 30 m.

Stödkonstruktioner:

Spontväggen utgörs av 12 m långa AU14 S355 spontplankor med egenskaper enligt ”Alt 4” i Figur 3, men med dimensionerande momentkapacitet 399 kNm/m vid böjning kring en horisontell axel (med beaktande av låsglidning) samt 1,5 kNm/m vid böjning kring en vertikal axel (antaget mycket lågt schablonvärde).

I vissa scenarier förutsätts hammarband och vissa scenarier förutsätts det inte. I de fall hammarband nyttjas utgörs det genomgående av HEB300 S355 med dimensionerande momentkapacitet 660 kNm.

Övrigt:

Råheten mellan spont och lera uppgår till 0,5.

Mellan leran och sponten finns en vattenspalt med vattenytan i nivå med ök lera (tillika markytan).

Omedelbart bakom spontväggen finns en 5,0 m bred, men långsträckt ytlast med intensiteten 10 kPa

FE-modell:

Den nyttjade FE-modellen framgår av Figur 10 och Figur 11. Eftersom fokus är på ULS är underkant lera förlagd 4 m under spontfoten medan det horisontella avståndet från spontväggen på aktivsidan är förlagd 15 m bortom spontväggen. Spontväggens krönlängd är vald till 25 m. Samtliga dessa mått är valda på basis av inledande tester, varvid brottmekanismens utbredning och totalsäkerhetens storlek studerades. Elementnätets finhet (ca 90000 element och ca 130000 noder) bestämdes genom motsvarande inledande tester. På detta sätt kunde beräkningstiden begränsas till några enstaka timmar per scenario.

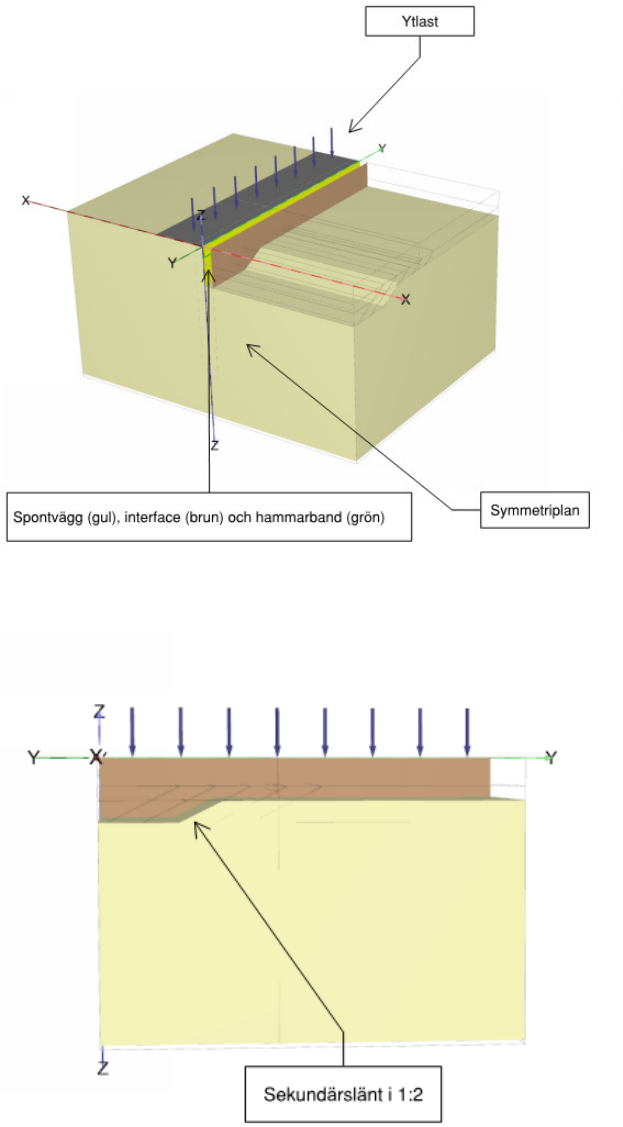

Figur 10. *FE-modellen ur några olika perspektiv. Utöver det i den övre figuren markerade verkliga symmetriplanet har även modellens övriga vertikala begränsningsytor tilldelats randvillkor motsvarande symmetriplan.*

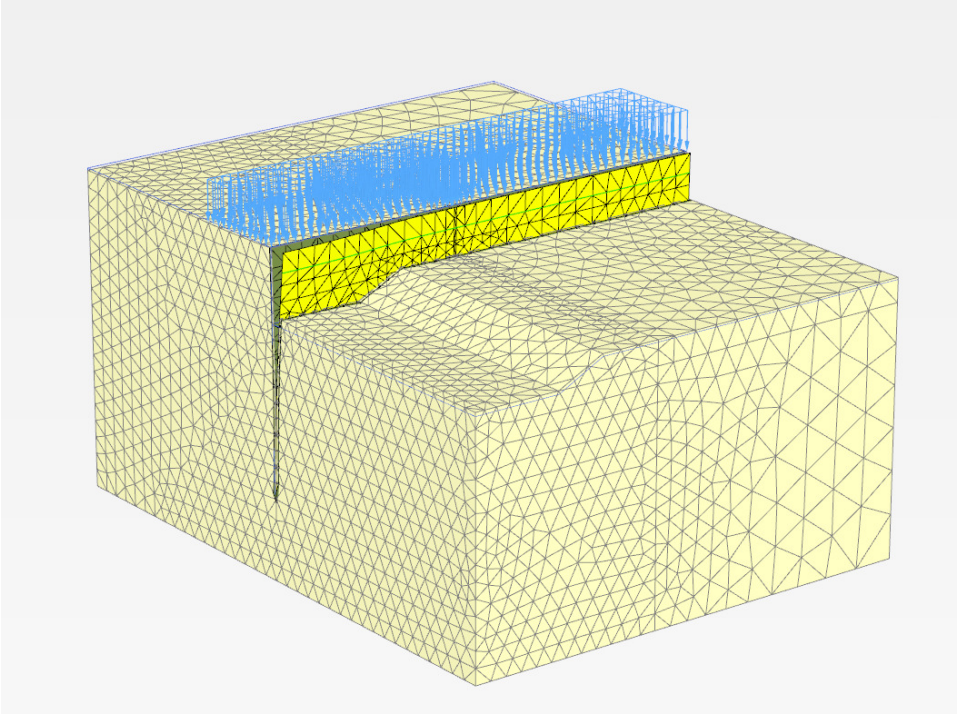

Figur 11. FE-modellen med elementnätet vid ett av de studerade scenarierna.

3.3.2 Beräkningsresultat – visuella illustrationer

Beräkningarna resulterade naturligtvis ett antal kvantitativa resultat, men inledningsvis redovisas diverse ”utdatafigurer” eftersom dessa ger en visuell uppfattning om de aktuella brottmekanismernas utbredning och form.

Som tidigare nämnts kan man betrakta en långsträckt schakt (dvs 2D, plant töjningstillstånd) som ett extremfall av en etappvis schakt när det gäller kvoten mellan den överstarka och den kritiska delsträckans 2D-säkerhetsfaktor. I Figur 12 framgår hur denna kvot påverkar brottmekanismens utbredning och som förväntat minskar dess utbredning med ökande kvot.

Effekten av varierande schaktlängd illustreras i Figur 13. Som framgår ”genar” brottmekanismen vid ökande schaktlängd vilket i de aktuella exemplen innebär att brottmekanismen ”slår upp” genom markytan i respektive en bit bortom den sekundära schaktslänten vinkelrätt spontväggen.

Hammarbandets effekt på brottmekanismen framgår i Figur 14. Som förväntat medför nyttjande av ett hammarband att mekanismens utbredning ökar. I sammanhanget bör påminnas om att det här genomgående förutsatts hammarbandet av typen HEB300.

Spontväggens horisontella rörelsemönster i ULS illustreras i Figur 15. Som framgår är horisontalrörelsen störst i spontväggens överkant inom den del som ingår i brottmekanismen.

I de studerade scenarierna är nivåskillnaden och lutningen på sekundärslänten vinkelrätt spontväggen vald så att 2D-stabiliteten för denna slänt inte blir kritisk, dvs en brottmekanism som den i Figur 7 (högra mekanismen) uppkom inte. I vissa scenarier kunde dock skönjas (mha de inkrementella rörelsevektorerna) en brottmekanism som utgörs av en kombination av att spontväggen roterar kring sin underkant samtidigt som jordvolymen i anslutning till sekundärslänten rör sig mot den kritiska schaktetappen. Således har sekundärsläntens geometri en viss påverkan på brottmekanismen och därmed på totalsäkerheten.

För vissa scenarier var de ovan beskrivna brottmekanismerna inte lika tydliga som i Figur 12 till Figur 15. Detta bedöms åtminstone delvis bero på spontväggens begränsade horisontella utbredning. I sådana fall testades andra randvillkor i spontväggens ”bortre ände”, varvid konstaterades att sådana förändringar har förhållandevis begränsad påverkan på ULS-resultaten i flertalet fall.

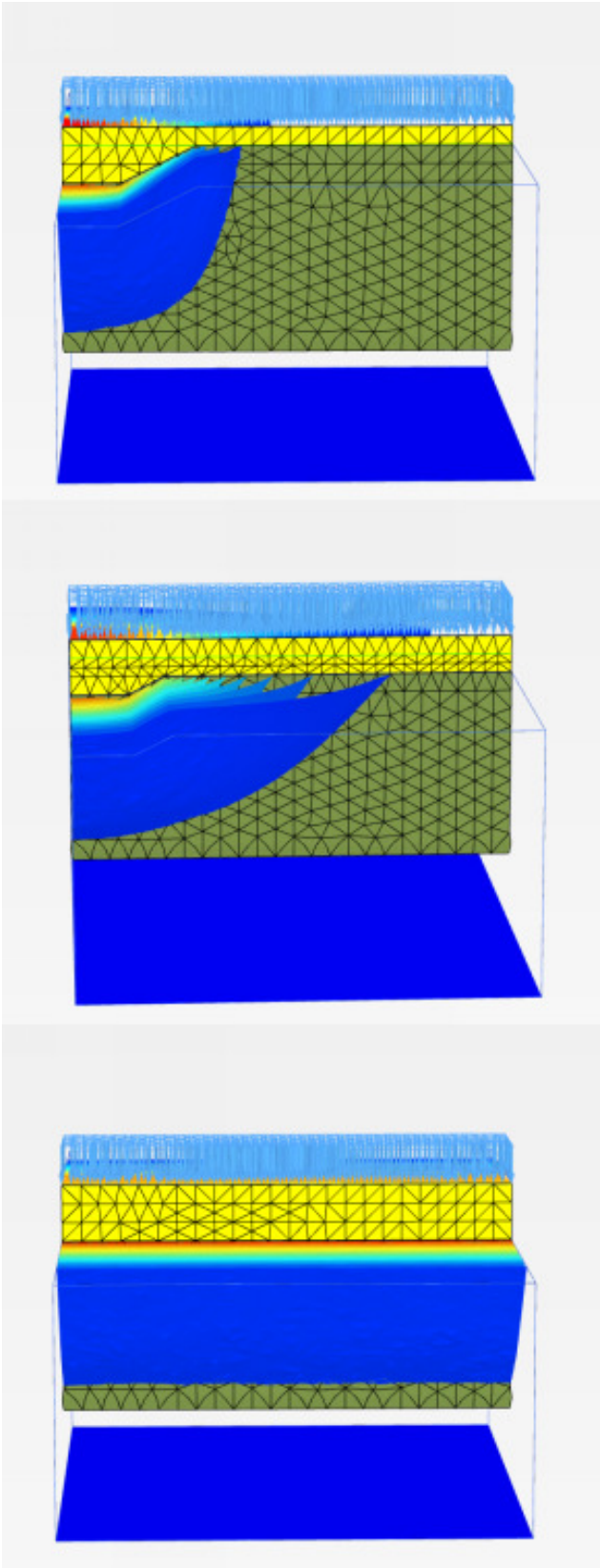

Figur 12. Brottmekanismens ungefärliga utbredning vid varierande 2D-säkerhet för den överstarka delsträckan jämfört med den kritiska delsträckan – allt annat lika.

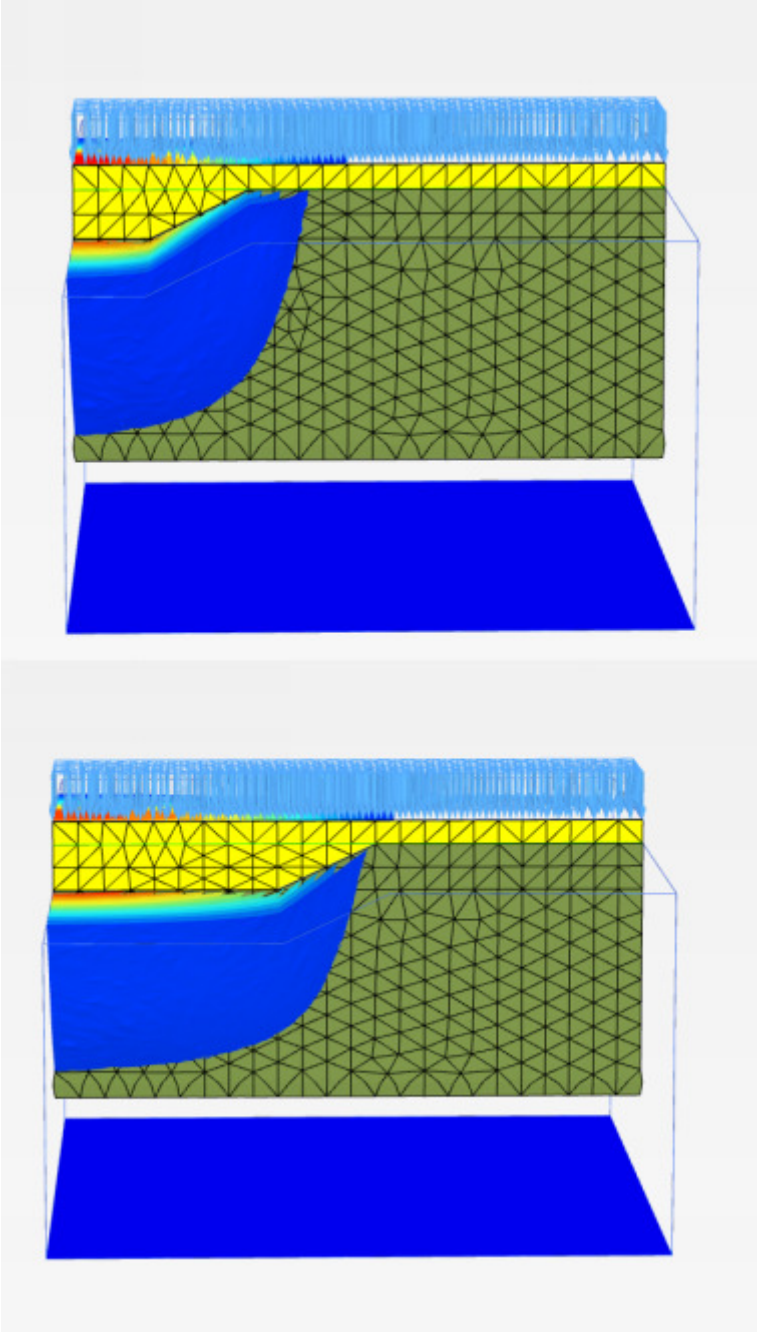

Figur 13. Brottmekanismens ungefärliga utbredning vid olika schaktetapplängd – allt annat lika.

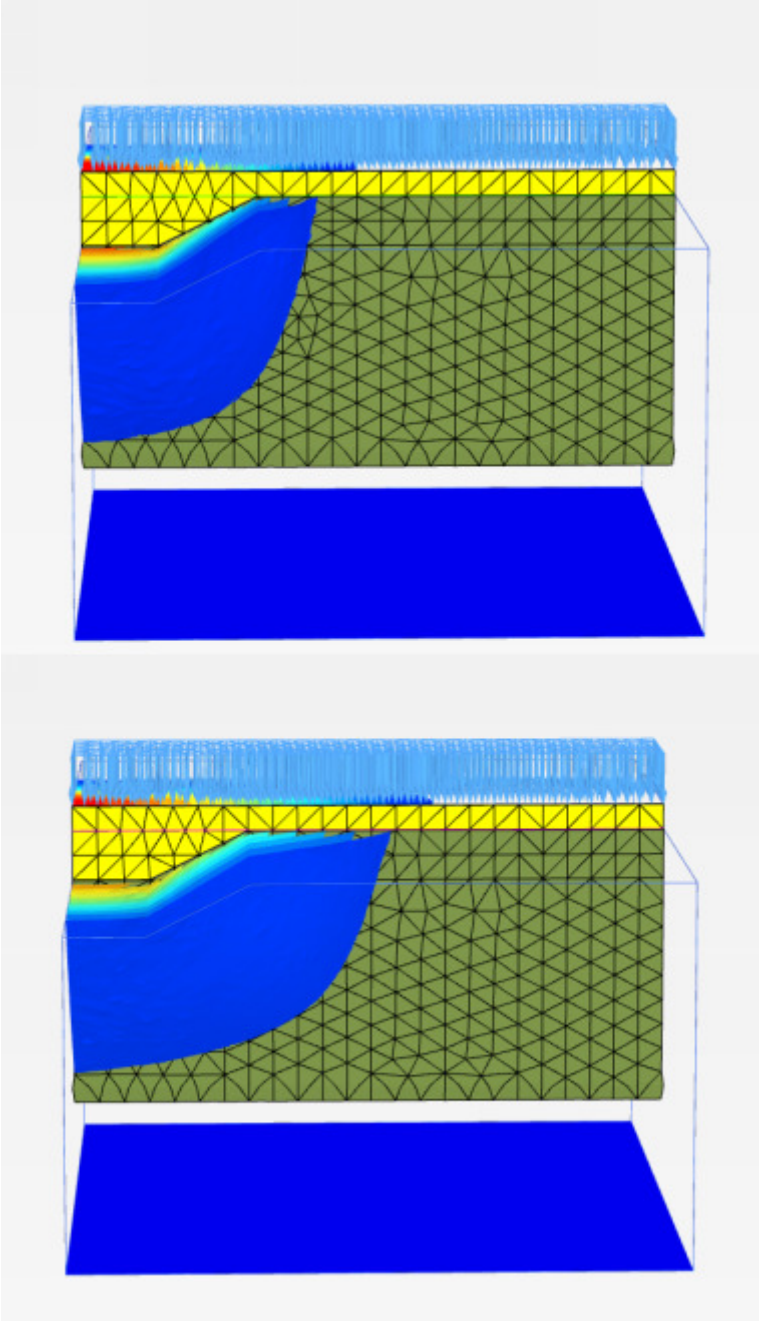

Figur 14. Brottmekanismens ungefärliga utbredning utan respektive med HEB300 hammarband – allt annat lika.

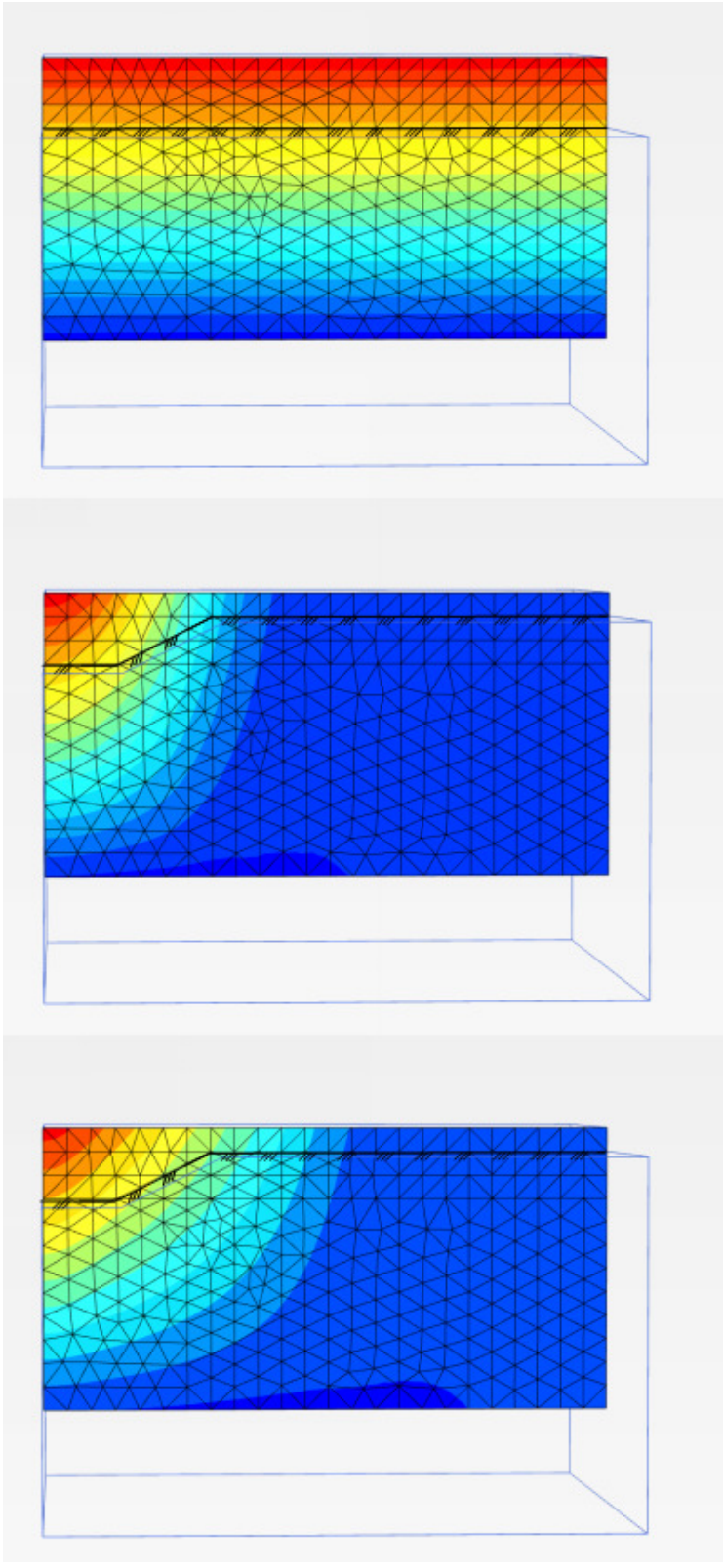

Figur 15. Spontväggens horisontella utböjning i brottstadiet (röd=stor rörelse; blå=liten rörelse; schaktbotten är schematiskt illustrerad).
Överst: Schaktetapp med oändlig horisontell utbredning (2D)
Mitten: Schaktetapp med begränsad längd utan nyttjande av hammarband.
Nederst: Schaktetapp med begränsad längd med nyttjande av hammarband.

3.3.3 Beräkningsresultat – kvantitativ redovisning

Vid beräkning av totalsäkerhetsfaktorn (ULS/GEO mha ”ϕc-reduction”) visade det sig att ”totalsäkerhetskurvorna” aldrig uppnår något maxvärde, se exemplet i Figur 16. Vid jämförelse av ”totalsäkerhetskurvorna” erhållna vid modelleringa av 2D-situationer i både PLAXIS 2D (där maxvärden erhölls) respektive PLAXIS 3D noterades dock att en relativt god överensstämmelse erhålls genom att utvärdera totalsäkerhetsfaktorn enligt Figur 16. Detta tillvägagångssätt har även fördelen att det är ett någorlunda objektivt sätt att utvärdera säkerheten. Samtliga erhållna ”totalsäkerhetskurvor” är sammanställda i Bilaga 2.

Den utvärderade totalsäkerhetsfaktorn för samtliga scenarier är sammanställd i Figur 17. Som förväntat minskar säkerhetsfaktor med ökad schaktlängd i samtliga studerade scenarier (notera den valda definitionen på den schabloniserade schaktetapplängden enligt Figur 18). Vidare framgår att nyttjande av ett hammarband HEB300 vid etappvis schakt ökar totalsäkerhetsfaktorn med ca 0,05 á 0,20. Den minsta effekten erhålls vid långa schaktetapper vilket i flertalet fall beror på att hammarbandets dimensionerande momentkapacitet uppnås. I några fall tillkommer dock en viss påverkan ifrån det begränsade avståndet till spontväggens ”bortre rand”. Avslutningsvis framgår att stabiliteten kraftigt överskattas i de fall (benämnda ”…ej i-face”) för vilka den begränsade råheten spont/lera och vattenspalten på aktivsidan inte beaktas.

I Figur 19 redovisas kvoten mellan den utvärderade totalsäkerhetsfaktorn och totalsäkerhetsfaktorn vid en oändligt långsträckt schaktetapp (2D). För de studerade scenarierna utan nyttjande av hammarband medför ett etappvis schaktförfarande att totalsäkerhetsfaktorn ökar med faktorn 1,1 á 1,5 jämfört med en oändligt långsträckt schakt (2D). Motsvarande värden vid nyttjande av hammarband HEB300 är 1,15 á 1,65.

För de scenarier utan nyttjande av hammarband för vilka totalsäkerhetsfaktorn 1,50 eller högre uppnåtts (dvs minst Säkerhetsklass 2) uppgår det maximala böjmomentet i sponten till ca 200-300 kNm/m (dvs lägre än spontplankornas dimensionerande momentkapacitet) när säkerhetsfaktorn uppgår till ca 1,50 (dvs vid Säkerhetsklass 2). Motsvarande värden med nyttjande av hammarband HEB300 är ca 100-250 kNm/m. I de fall när den begränsade råheten spont/lera och vattenspalten på aktivsidan inte beaktas uppgår det maximala böjmomentet i sponten dock endast till ca 40-50 kNm/m.

För de scenarier med nyttjande av hammarband HEB300 för vilka totalsäkerhetsfaktorn 1,50 eller högre uppnåtts mobiliseras hammarbandets dimensionerande momentkapacitet i vissa fall redan innan säkerhetsfaktorn uppgår till ca 1,50. Tvärkraftens variation längs hammarbandet, vilket dimensionerar svetsarna som fäster hammarbandet till spontplankorna, uppgår maximalt till ca 30-50 kN/m. I de fall när den begränsade råheten spont/lera och vattenspalten på aktivsidan inte beaktas uppgår det värde dock endast till ca 10-20 kN/m.

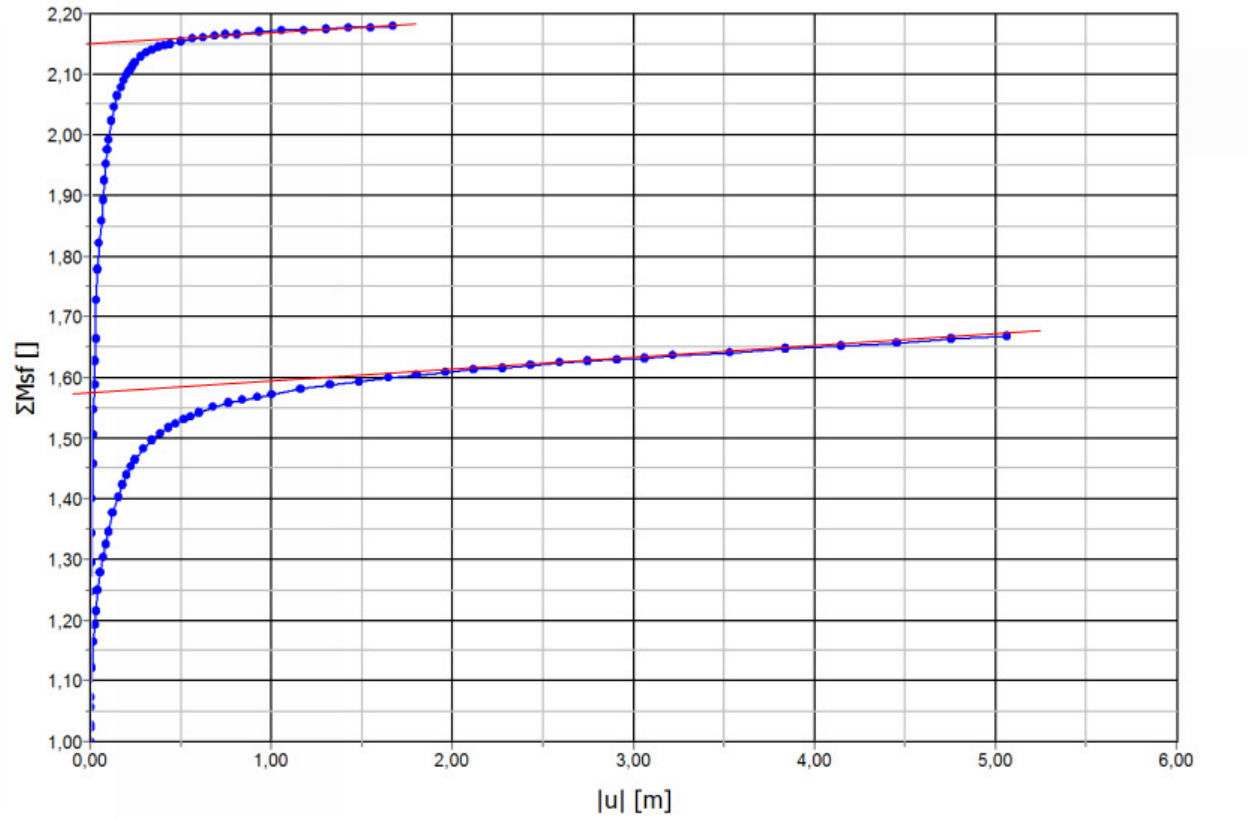

Figur 16. Exempel på utvärdering av totalsäkerhetsfaktorn. Blå kurvor är de beräknade ”totalsäkerhetskurvorna” medan de röda linjernas skärningspunkt med ordinatan utgör den utvärderade totalsäkerhetsfaktorn.

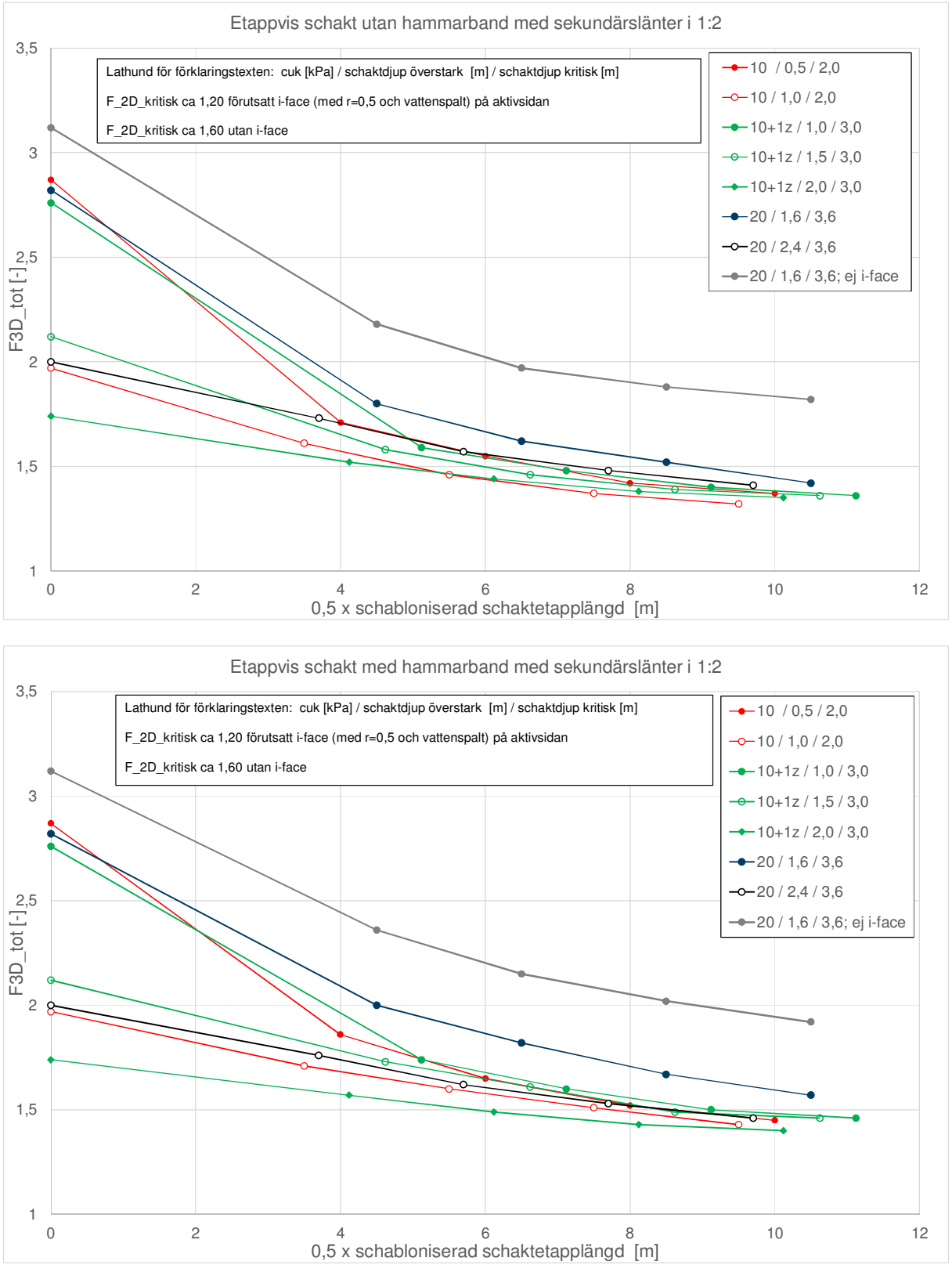

Figur 17. Beräknad totalsäkerhetsfaktor för samtliga studerade scenarier som funktion av halva den schabloniserade schaktetapplängden.
Övre bilden: Utan hammarband
Undre bilden: Med hammarband HEB300

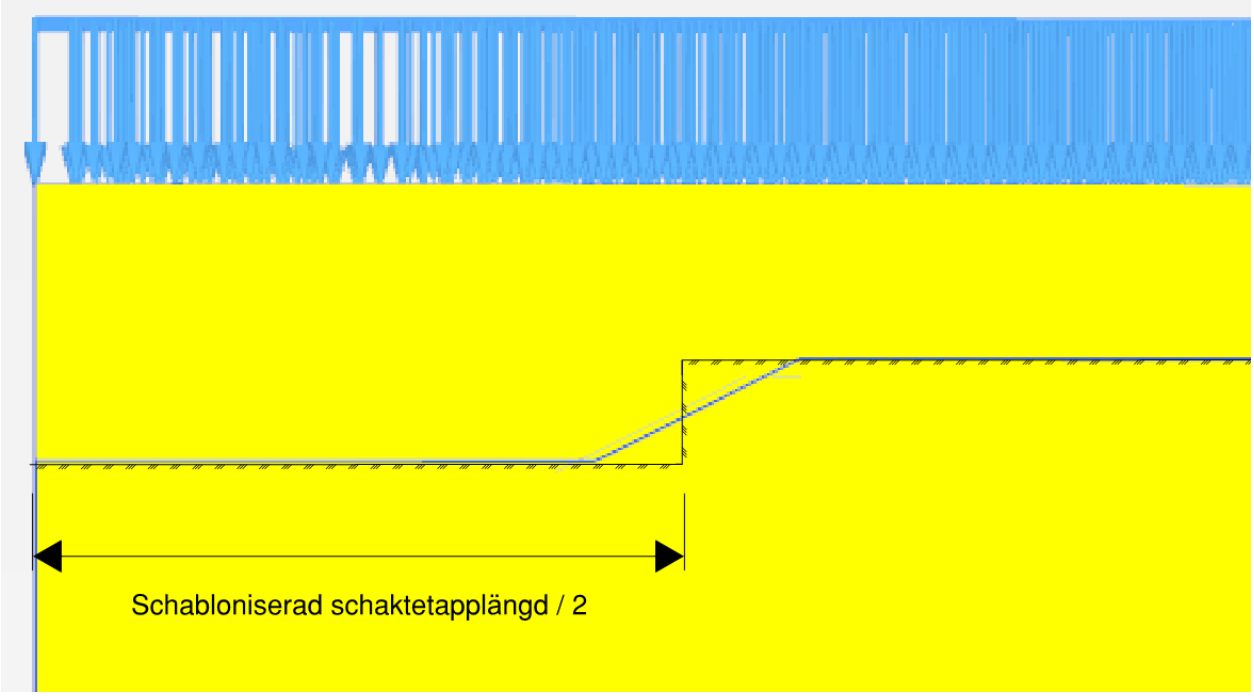

Figur 18. Definition av schabloniserad schaktetapplängd.

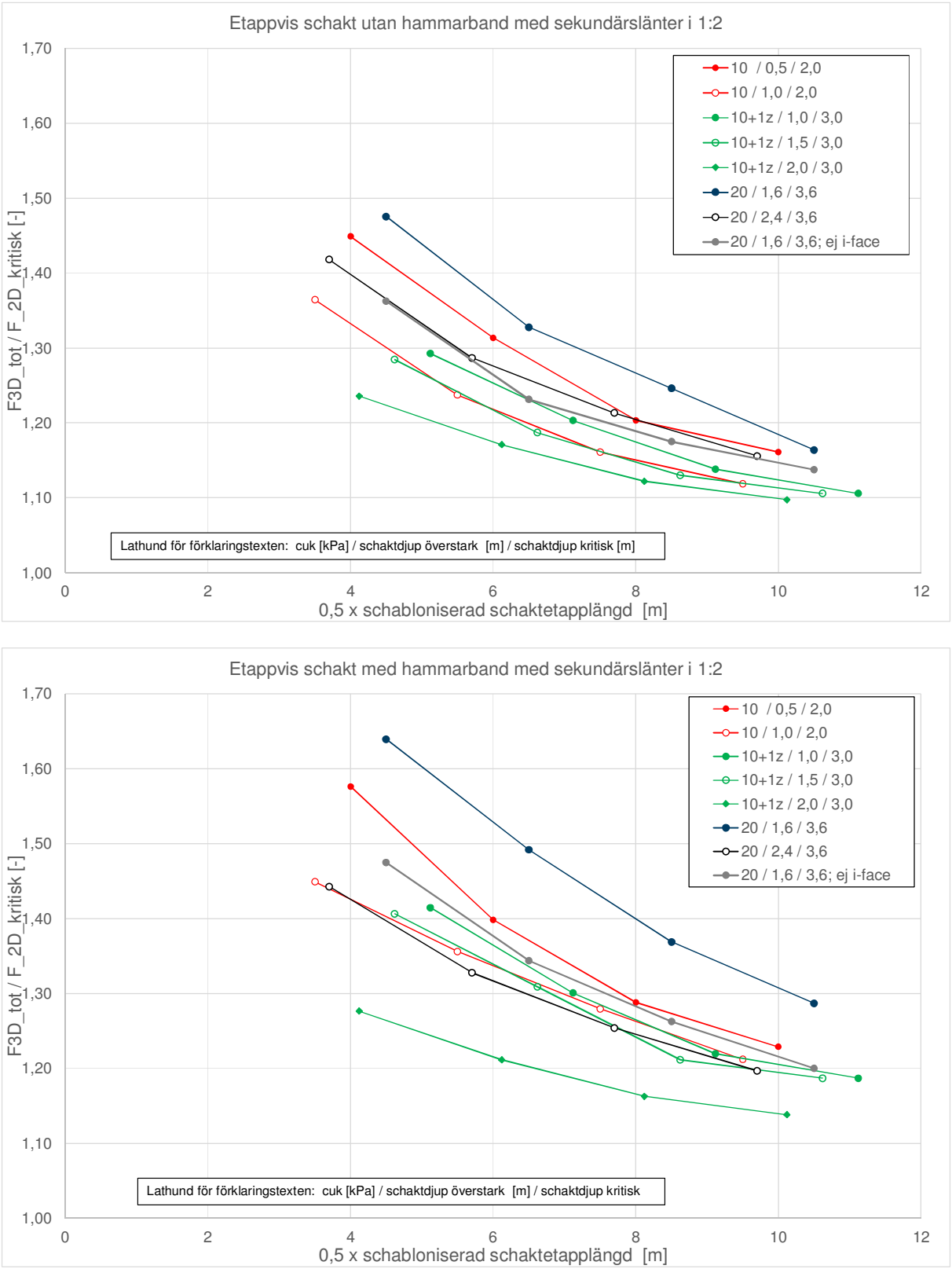

Figur 19. *Kvoten mellan beräknad totalsäkerhetsfaktor för samtliga studerade scenarier och den kritiska schaktetappens 2D-säkerhetsfaktor som funktion av halva den schabloniserade schaktetapplängden.*
Övre bilden: Utan hammarband
Undre bilden: Med hammarband HEB300

3.3.4 Beräkningsresultat – förslag på en förenklad 3D-modell mht ULS

ULS/STR

Lasteffekten i stödkonstruktionen påverkas delvis av styvhetsförhållandet mellan stödkonstruktion och omgivande jord vilket i sin tur beror av hur hårt ansträngd jorden är. I de studerade scenarierna har använts en enkel Morh-Coulomb modell för jorden. Den ansatta styvheten på jorden bedöms dock vara relativt låg ($250c_u$) och i vissa scenarier har uppkommit en fullt utvecklad brottmekanism jorden vid totalsäkerhetsfaktorn 1,50.

Som framgår i Avsnitt 3.3.3 överstiger det maximalt mobiliserade böjmomentet i spontplankorna aldrig ca 200-300 kNm/m vilket är betydligt lägre än den dimensionerande momentkapaciteten (ca 400 kNm/m) för de klenaste spontplankor (typ PU12 eller AU12) som numera används. Således anses att denna aspekt ej behöver studeras mer ingående i syfte att optimera utformningen mht ULS/STR.

Det mobiliserade maximala böjmomentet i HEB300 hammarbandet uppgår i vissa scenarier till den dimensionerande momentkapaciteten. Ett HEB300 hammarband är relativt kraftigt, men som framgår i Figur 2 och Figur 6 är ett så kraftigt hammarband lämpligt för att erhålla en påtaglig SLS-effekt. Ett pragmatiskt sätt att hantera detta map ULS/GEO är att bortse ifrån hammarbandets stabilitetshöjande effekt (som framgår i Figur 17 förefaller effekten vara relativt begränsad map ULS/GEO) och enbart nyttja det mht SLS.

Därmed kvarstår dimensioneringsförutsättningarna för svetsarna mellan hammarbandet och spontplankorna. Som framgår i Avsnitt 3.3.3 uppgår den maximala ”linjelasten” mot hammarbandet till ca 50 kN/m (tryck mitt för den kritiska delsträckan men drag bortom densamma), vilket enbart erfordrar enklare ”standardsvetsar”. Således anses att inte heller denna aspekt behöver studeras mer ingående i syfte att optimera utformningen mht ULS/STR.

ULS/GEO

Som framgår av föregående avsnitt borstes pragmatiskt (och något konservativt) ifrån hammarbandets stabilitetshöjande effekt mht ULS. Vidare nyttjas principen i Avsnitt 3.2, varvid $L_{överstark}$ ”bakåträknats” mha Ekv. 1. Detta förfarande resulterar i Figur 20. Som förväntat framgår hur $L_{överstark}$ minskar när kvoten $F_{2D\_överstark}$ /$F_{2D\_kritisk}$ ökar, jfr även Figur 12. Sambandet är dock inte entydigt och för en godtyckligt vald kvot $F_{2D\_överstark}$ /F_{2D} minskar $L_{överstark}$ med ökande schaktetapplängd. Även det är som förväntat, jfr Figur 13.

I samtliga analyserade scenarier har förutsatts 12 m långa spontplankor eftersom kortare spontplankor sällan nyttjas vid svävande spontväggar – åtminstone inte vid de förutsatta förhållandena. Det förefaller dock rimligt att spontplankornas längd delvis påverkar brottmekanismens horisontella utbredning inom de överstarka delsträckorna – allt annat lika. Ett

approximativt sätt att beakta detta kan vara att istället för $L_{överstark}$ använda ”lutningen” N med definition enligt Figur 21. Detta förfarande resulterar i Figur 22. Som förväntat ökar N när kvoten $F_{2D\_överstark}$ /F_{2D} ökar och för en godtyckligt vald kvot $F_{2D\_överstark}$ /F_{2D} ökar N med ökande schaktetapplängd. Linjär regression resulterar i det approximativa sambandet som redovisas i figuren. Detta approximativa samband återges även i Figur 20.

Genom att kombinera det approximativa sambandet för N i Figur 22 (vilket resulterar i ett approximativt värde på $L_{överstark}$) med $L_{kritisk}$, $F_{2D,kritisk}$ och $F_{2D,överstark}$ kan ett approximativt värde på F_{3D} beräknas mha Ekv. 1. I Figur 23 jämförs den resulterande approximativa totalsäkerheten med den som erhållits med 3D-FEM. Som framgår är skillnaden inom ± 10%. Förutsatt att hammarband nyttjas finns dock en begränsad ”dold säkerhet” vid tillämpning av den förenklade metoden.

Sammantaget bedöms att den förenklade metoden enligt Ekv. 1, i kombination med det approximativa sambandet för N (och därmed $L_{överstark}$) kan nyttjas för beräkning av totalsäkerhetfaktorn (ULS/GEO) vid etappvis schakt inom konsolspont med nyttjande av hammarband. Detta förutsätter dock byggnadstekniska förhållanden som inryms i de scenarier som analyserats. Om förhållandena är annorlunda och/eller konsekvenserna är stora vid ett eventuellt brott bör den approximativa metoden dock endast användas vid inledande överslagsberäkningar, vilka dock behöver kompletteras med enstaka 3D-analyser vid efterföljande detaljprojektering. Självklart skall ett kontroll- och åtgärdsprogram nyttjas när schaktarbetena utförs, men så skall göras för i stort sett alla schakter som utförs inom spont.

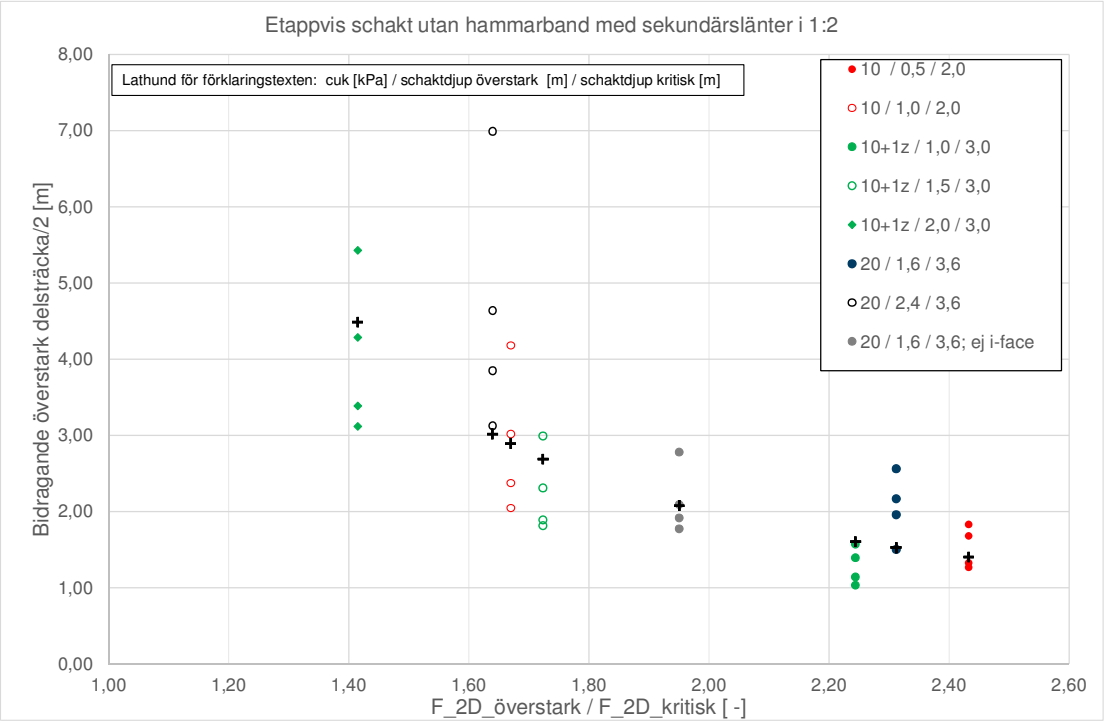

Figur 20. *Bidragande överstark delsträcka för samtliga studerade scenarier utan hammarband som funktion av kvoten mellan de överstarka och de kritiska schaktetappernas 2D-säkerhetsfaktorer. Den bidragande överstarka delsträckan definieras i Ekv. 1 och är ”bakåträknad” mha densamma samt resultatet från 3D FE-analyserna.*

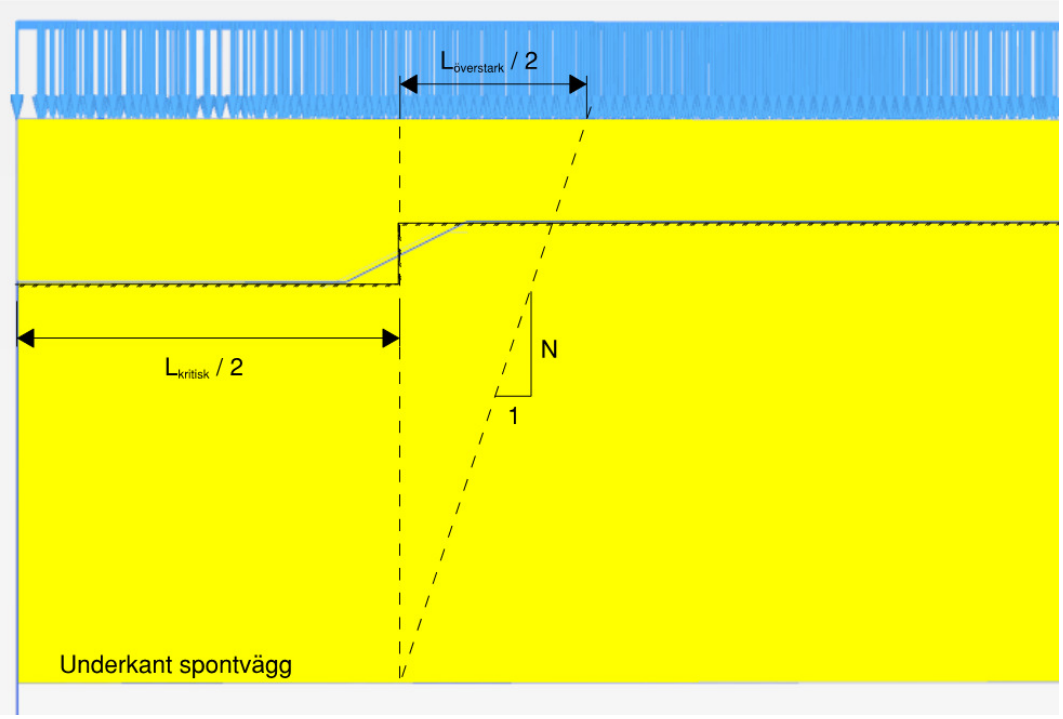

Figur 21. *Definition av lutningen N.*

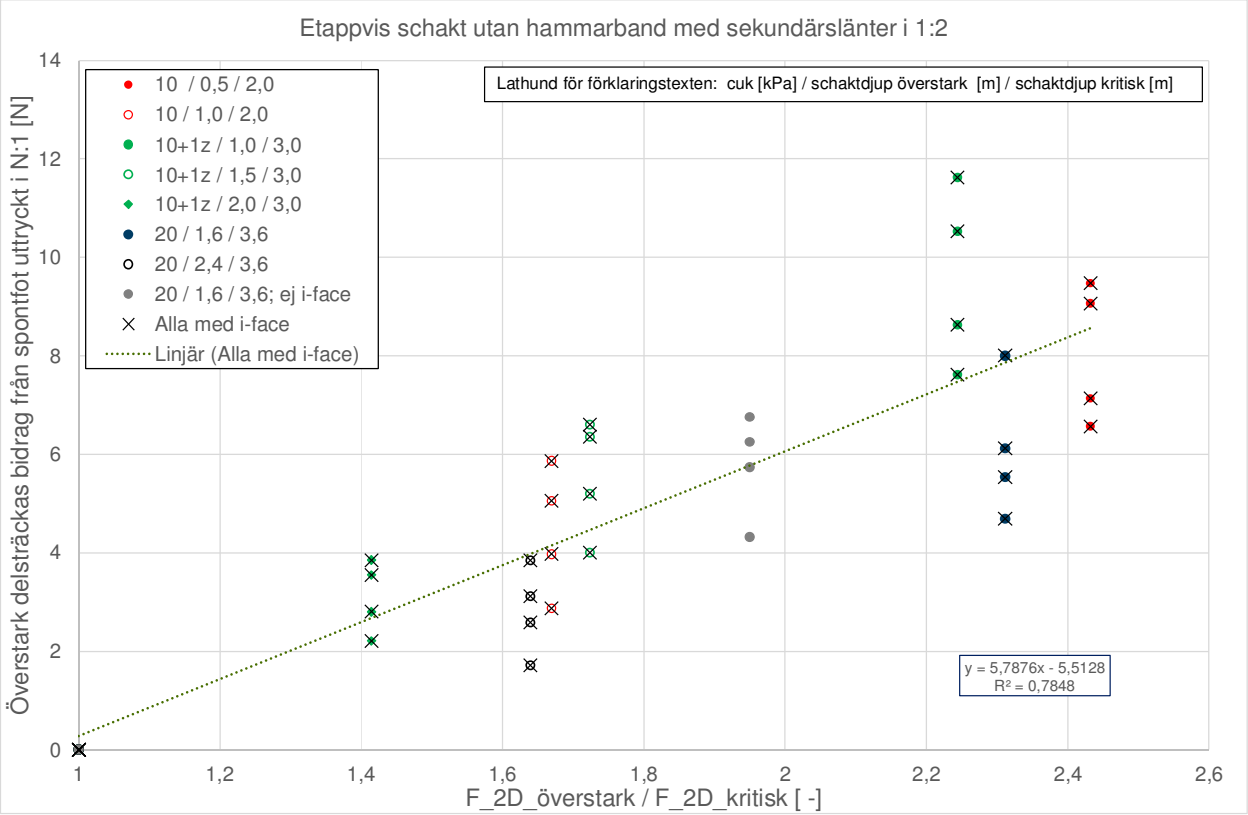

Figur 22. *Samma information som i Figur 20, men med den bidragande överstarka delsträckan ”normaliserad” mht spontplankornas längd och därmed uttryckt i form av en begränsningslinje med lutningen N:1 från spontfoten till ursprunglig markyta.*

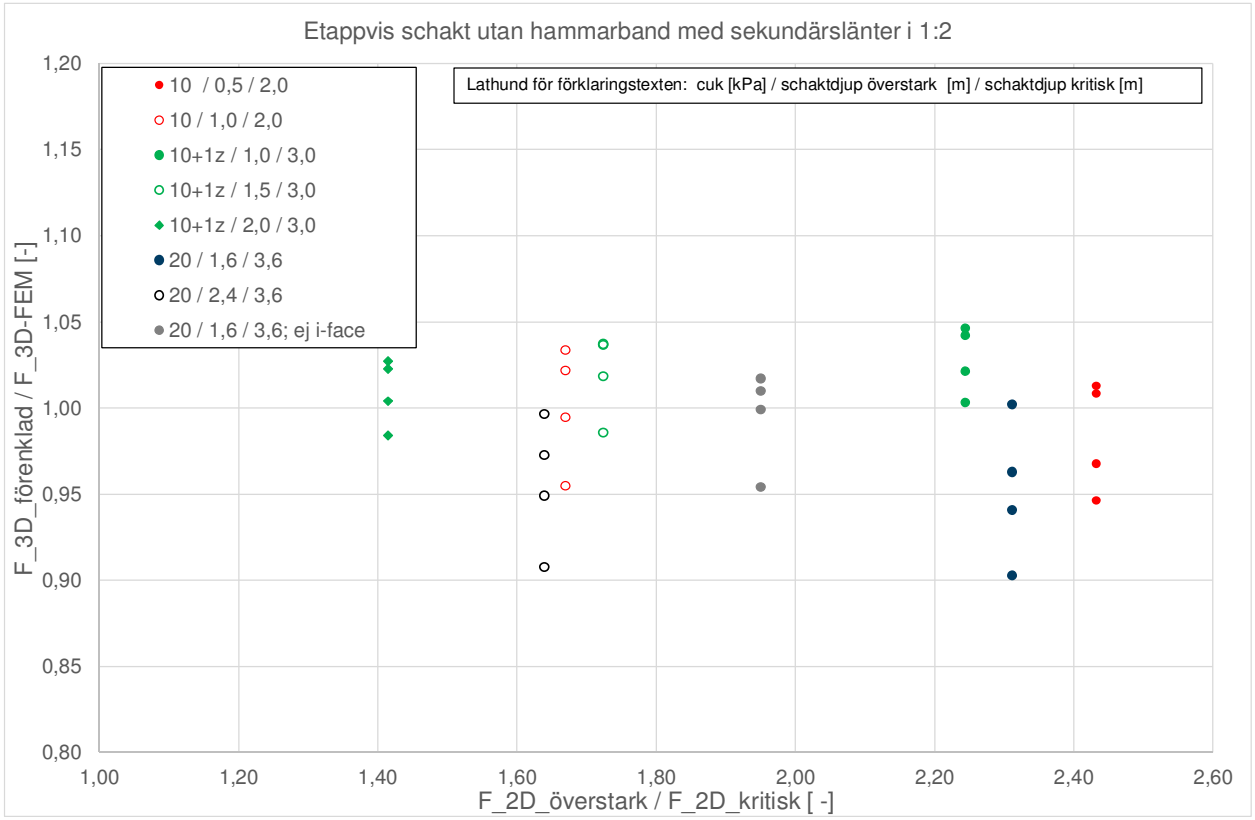

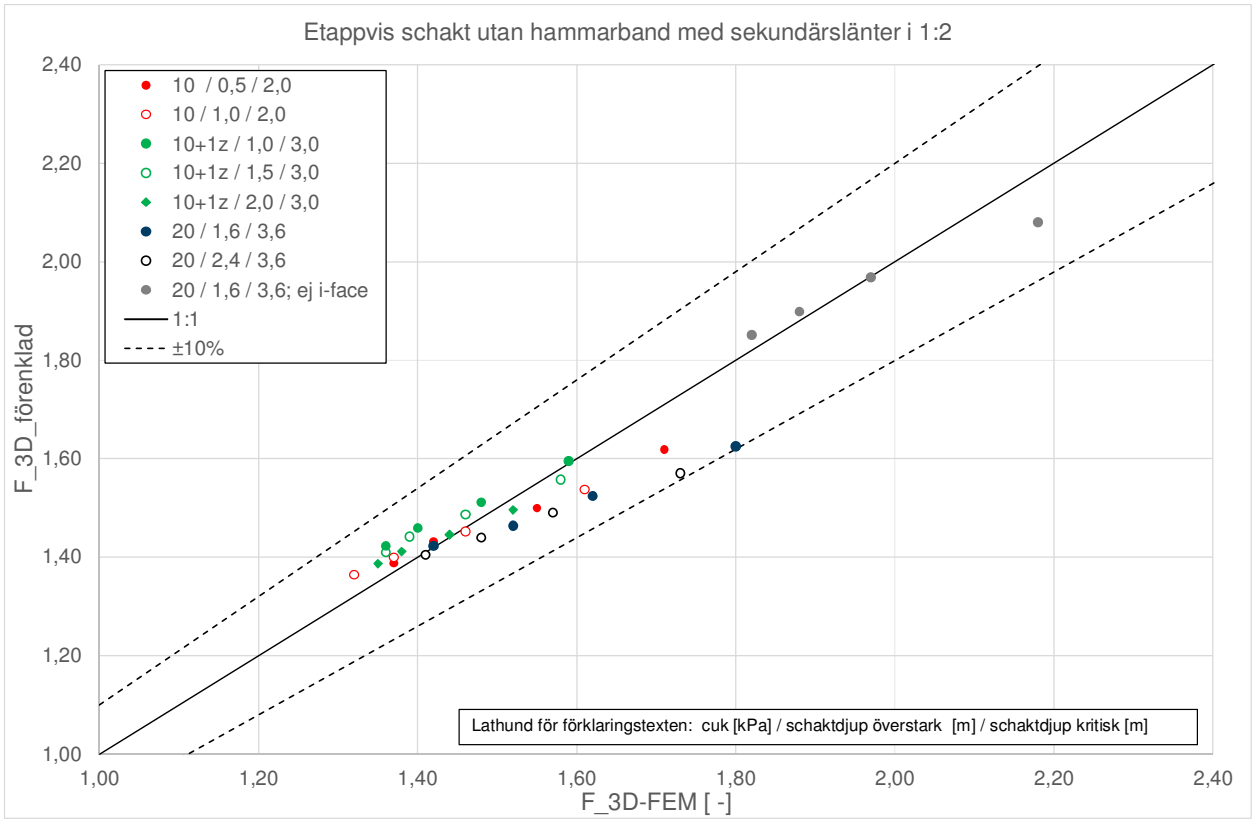

Figur 23. Totalsäkerhetsfaktor enligt förenklad metod och enligt 3D FE-analys.

4 Övergripande slutsatser och rekommendationer

4.1 Angående analyser med 3D-FEM

Beräkningstiden vid 3D-beräkningar är väsentligt större än vid 2D-beräkningar (timmar till dagar istället för enstaka minuter), vilket innebär att man i inledningen av mer omfattande analyser med 3D-FEM behöver ägna en del tid åt att hitta ett lagom finindelat elementnät, beräkningsmodellens yttre geometriska begränsningslinjer, osv.

4.2 Angående SLS

De utförda fältmätningarna och analyserna med 3D-FEM påvisar tydligt att nyttjande av ett kraftigt hammarband vid temporära etappvisa schakter i lös lera leder till avsevärt minskade schaktinducerade rörelser.

Det är viktigt att på ett korrekt sätt beakta spontväggens anisotropa egenskaper, varvid de schablonmässiga rekommendationer som eventuellt återfinns i ”User Manual” inte bör tillämpas okritiskt.

I det bifogade Examensarbetet redovisas SLS-responsen för ett antal scenarier som analyserats mha 3D-FEM. Resultaten ger förvisso en kvalitativ/relativ bild av hur olika förutsättningar påverkar den schaktinducerade responsen. Det har dock inte gått att utveckla en förenklad beräkningsmodell som kan användas för en tillförlitlig bedömning av kvantitativ SLS-respons.

4.3 Angående ULS

Ett antal scenarier har analyserats med 3D-FEM varvid följande har konstateras:

- En förenklad beräkningsmodell för beaktande av ”3D-effekter” har utvecklats map ULS/GEO, se Avsnitt 3.3.4. Om de aktuella förhållandena avviker ifrån de modellerade scenarierna och/eller konsekvenserna är stora vid ett eventuellt brott bör den förenklade metoden endast användas vid inledande överslagsberäkningar, vilka dock enbart behöver kompletteras med enstaka 3D-analyser vid efterföljande detaljprojektering.

- Förutsatt Säkerhetsklass 2 är lasteffekten i spontväggen (ULS/STR) så begränsad att den understiger lastkapaciteten hos samtliga idag normalt förekommande spontplankor. Lasteffekten i hammarbanden är i vissa fall dock större än lastkapaciteten, vilket pragmatiskt hanterats genom att bortse ifrån hammarbandens effekt i den ovannämnda förenklade beräkningsmodellen. Lasteffekten i svetsarna mellan hammarbandet och spontplankorna är så begränsad att enbart ”standardsvetsar” erfordras.

- I några scenarier har den begränsade råheten spont/lera och vattenspalten på spontväggens aktivsida inte beaktats. Dessa antaganden, vilka avviker ifrån svensk praxis (SS-EN 1997:1), leder till en avsevärt högre totalsäkerhetfaktor (ULS/GEO) och avsevärt lägre lasteffekter (ULS/STR) än vad som annars varit fallet.

4.4 Angående fortsatt arbete

Den föreslagna förenklade beräkningsmodellen baseras på de scenarier som analyserats mha 3D-FEM. Huruvida beräkningsmodellen är tillförlitlig även för andra scenarier går självklart inte att avgöra innan de har studerats. Därför är det önskvärt att ytterligare scenarier systematiskt analyseras med 3D-FEM. Sådana scenarier skulle exempelvis omfatta andra längder på spontplankorna och delvis andra grundförhållanden än de hittills studerade.

Det är självklart önskvärt att helt undvika nyttjande av spont vid schaktarbeten. Idag saknas dock enkla beräkningsmetoder som leder till en säker utformning av etappvis frischakt (slänter). Inom ramen för det aktuella SBUF-projektet har begränsade studier utförts, bl.a. med 3D-FEM, varvid konstaterats att dagens branschpraxis delvis är felaktig och dessutom troligen överskattar 3D-effekten, se Avsnitt 3.2. De studierna antyder dessutom att en förenklad beräkningsmodell för ULS/GEO, likartad den modell som utvecklats för etappvis schakt inom konsolspont, bör ge tillfredsställande noggrannhet vid frischakt (slänter). Dessa aspekter behöver dock studeras vidare.

5 Referenser

Gens, A, Hutchinson, JN, Cavounidis, S. (1988). Three-dimensional analysis of slides in cohesive soils. Geotechnique, Vol. 38, No. 1.

Persson, H. Sigström, D. (2010). Staged excavation in soft clay supported by a cantilver sheet pile wall - Numerical analysis and field measurements of the effect of using a wailing beam. Chalmers tekniska högskola. Institutionen för Bygg- och miljöteknik. GEO. Geologi och geoteknik. Examensarbete 2010:41

Skredkommissionen (1995). Anvisningar för släntstabilitetsutredningar. Ingenjörsvetenskapsakademien, IVA. Skredkommissionen. Rapport 3:95. Linköping.

SS-EN 1997:1 (2005). Eurokod 7: Dimensionering av geokonstruktioner – Del 1: Allmänna regler.

CHALMERS

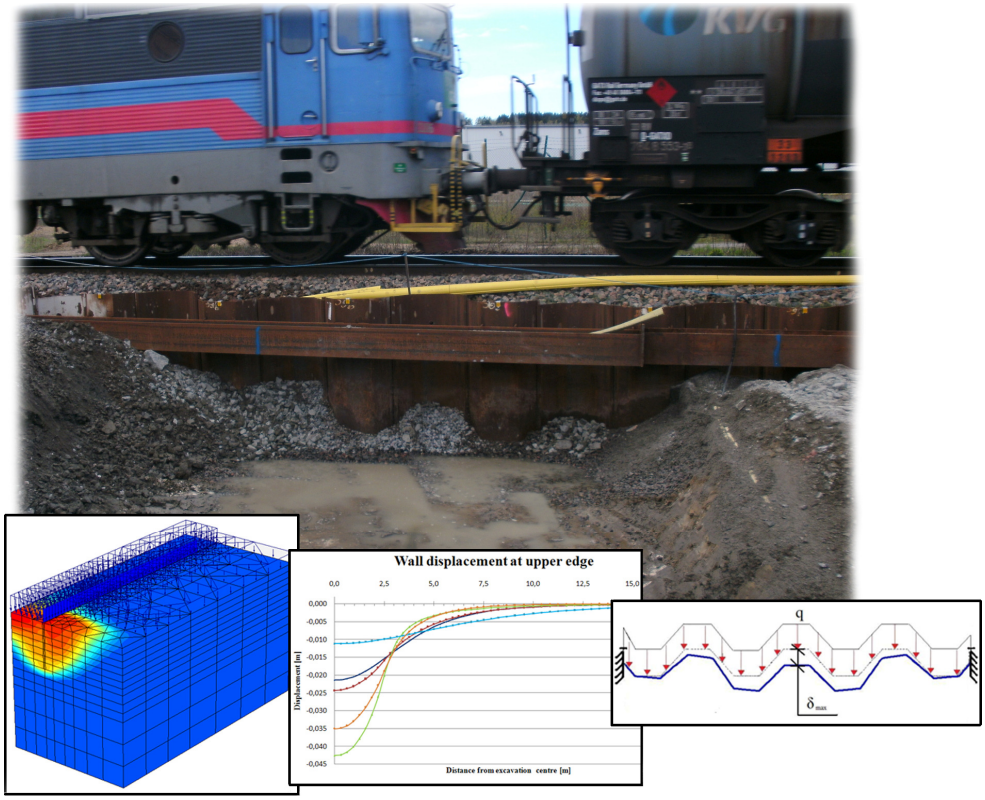

Staged excavation in soft clay supported by a cantilever sheet pile wall

-Numerical analysis and field measurements of the effect of using a wailing beam

Master of Science Thesis in the Master's programme Geo and Water Engineering

HANNES PERSSON

DANIEL SIGSTRÖM

Department of Civil and Environmental Engineering
Division of GeoEngineering
Geotechnical Engineering
CHALMERS UNIVERSITY OF TECHNOLOGY
Göteborg, Sweden 2010
Master's Thesis 2010:41

MASTER'S THESIS 2010:41

Staged excavation in soft clay supported by a cantilever sheet pile wall

-Numerical analysis and field measurements of the effect of using a wailing beam
Master's Thesis in the *Geo and Water Engineering*

HANNES PERSSON

DANIEL SIGSTRÖM

Department of Civil and Environmental Engineering
Division of GeoEngineering
Geotechnical Engineering
CHALMERS UNIVERSITY OF TECHNOLOGY
Göteborg, Sweden 2010

Staged excavation in soft clay supported by a cantilever sheet pile wall
-Numerical analysis and field measurements of the effect of using a wailing beam

Master's Thesis in the Master´s Programme *Geo and Water Engineering*

HANNES PERSSON
DANIEL SIGSTRÖM

© HANNES PERSSON, DANIEL SIGSTRÖM, 2010

Examensarbete / Institutionen för bygg- och miljöteknik,
Chalmers tekniska högskola 2010:41

Department of Civil and Environmental Engineering
Division of GeoEngineering Geotechnical Engineering
Chalmers University of Technology
SE-412 96 Göteborg
Sweden
Telephone: + 46 (0)31-772 1000

Cover:
Staged excavation along the railway track in Bohus and results from simulations in PLAXIS. Photograph taken by Daniel Sigström 5 May 2010.

Reproservice, Chalmers University of Technology
Göteborg, Sweden 2010

Staged excavation in soft clay supported by a cantilever sheet pile wall
-Numerical analysis and field measurements of the effect of using a wailing beam

Master's Thesis in the Master´s Programme Geo and Water Engineering

HANNES PERSSON
DANIEL SIGSTRÖM
Department of Civil and Environmental Engineering
Division of GeoEngineering
Geotechnical Engineering

Chalmers University of Technology

ABSTRACT

Staged excavation is a useful method that in a cost effective way minimize the deflection of a sheet pile wall. No well established design method exists today, and the three dimensional behavior of the sheet pile wall is hard to predict. The purpose of this master´s thesis is to investigate the three dimensional side effects from the surrounding soil volumes when apply staged excavation and to determine behavior of sheet pile wall. It also aims to investigate the effect of adding a wailing beam to the sheet pile wall and analyze which parameters that are affecting the retaining system. To do this, the flexural rigidities are determined, as well as the torsional rigidity against warping. This study shows that the flexural rigidity for bending around a vertical axis is much lower than for bending around a horizontal axis. A three dimensional model is built in PLAXIS 3D Foundation, where the staged excavation is simulated. In this model, different material properties of the sheet pile wall are tested, as well as a number of wailing beams. A parameter study is also performed in order to investigate the influence of a number of parameters that could affect the horizontal deflection of the sheet pile wall as well as the factor of safety in the soil. This study shows that a stiffer wailing beam can reduce the deflection radically, and at the same time increase the influence distance, while a weaker wailing beam only have a marginally effect of the deflection. The results are then evaluated in field study at contract E33, included in the infrastructure project BanaVäg i Väst, north of Gothenburg. The deflections are measured at the staged excavations performed along the railway, and the result shows that there is a clear effect of using a stiff wailing beam. The result also shows that the flexural rigidities found in the simulations are realistic, since the shape of the deflection shows good agreement with the simulated case.

Key words: Staged excavation, cantilever sheet pile wall, wailing beam, deflection, flexural rigidity, torsional rigidity, PLAXIS

Etappvis schakt i lös lera med konsolspont
-Numeriska simuleringar och fältmätningar av effekten med hammarband

Examensarbete inom Geo and Water Engineering

HANNES PERSSON
DANIEL SIGSTRÖM
Institutionen för bygg- och miljöteknik
Avdelningen för Geologi och Geoteknik
Geoteknik
Chalmers tekniska högskola

SAMMANFATTNING

Genom att tillämpa etappvisa schakter kan man på ett kostnadseffektivt sätt minska de schaktinducerade rörelser som uppkommer i en spont. I dagsläget finns inga etablerade designmetoder för dimensionering av etappvisa schakter. Det saknas även kunskap om hur sponten beter sig i tre dimensioner. Detta examensarbete syftar till att studera jordens tredimensionella sidoeffekter vid etappvis avschaktning och att utvärdera effekten av att använda ett hammarband på en konsolspont. Det syftar även till att analysera vilka parametrar som påverkar stödkonstruktionens beteende samt att studera spontens egenskaper i olika riktningar. Spontens böj- och vridstyvhet studeras i olika riktningar, både utifrån teorier om korrugerade stålprofiler och simuleringar i PLAXIS. Denna studie visar att egenskaperna skiljer sig markant åt i spontens olika riktningar. För att kunna analysera jordens sidoeffekter samt spontens tredimensionella beteende vid etappvis avschaktning, görs numeriska beräkningar i en modell i PLAXIS 3D Foundation. I modellen görs simuleringar med olika materialegenskaper för sponten och hammarbandet. En parameterstudie utförs för att utreda vilka parametrar som påverkar spontens horisontella utböjning samt jordens säkerhetsfaktor. Studien visar att det är fördelaktigt att välja ett styvare hammarband då detta på ett effektivt sätt reducerar utböjningarna. Då den horisontella utböjningen på sponten reduceras leder detta till att influensområdet ökar, vilket innebär att en större del av de omkringliggande jordvolymerna påverkas. Fältmätningar har genomförts för att verifiera resultaten från simuleringarna. Dessa gjordes på Skanska Sveriges etapp E33, som är en del i infrastrukturprojektet BanaVäg i Väst. Mätningarna visar att hammarbandet gör effekt då den gör hela stödkonstruktionen styvare. De visar även att de framtagna värdena på spontens egenskaper är realistiska, då spontens beteende överensstämmer väl med spontens verkliga beteende.

Nyckelord: Etappvis schakt, konsolspont, hammarband, utböjning, böjstyvhet, vridstyvhet, PLAXIS

Contents

Preface

This master's thesis has been carried out during the spring 2010 in cooperation between the Division of GeoEngineering at Chalmers University of Technology and Skanska Teknik. The report is a part of a SBUF project (Swedish construction industry's organisation for research and development) which is operated by Skanska Teknik.

First of all we would like to thank our supervisor at Skanska Teknik, Ph.D Torbjörn Edstam, for showing great interest in our thesis and for introducing us to the subject. We are very grateful for his advices and for guidance during the whole project.

We wish to thank Ph.D Anders Kullingsjö at Skanska Teknik for his valuable thoughts during the project and our examiner at Chalmers, Professor Claes Alén.

We would also like to thank the involved persons at Skanska Sverige AB for all help during the field measurement at contract E33 in Bohus.

Göteborg, June 2010

Hannes Persson

Daniel Sigström

Notations

Roman upper case letters

A_w	Webb area of the beam
B	Torsional rigidity
D	Required driven depth of the sheet pile wall under excavation bottom
E	Young's modulus
G	Shear modulus
I	Moment of inertia
K_0	Lateral earth pressure ratio
K_A	Lateral earth pressure ratio in the active case
M_{Rd}	Design value of the moment capacity
p_a	Resulting passive earth pressure
p_p	Resulting active earth pressure
V_{Rd}	Design value of shear capacity

Roman lower case letters

c´	Cohesion
c_u	Undrained shear strength
f_{yc}	Characteristic strength of steel
p_w	Groundwater pressure
w	Bending resistance
w_x	Elastic section modulus

Greek letters

δ_v	Vertical deflection
δ_h	Horizontal deflection
δ_{max}	Maximal deflection
ε	Strain
ε^p	Plastic strain
ε^e	Elastic strain
γ	Unit weight of the soil
κ	Curvature
σ_h	Horizontal effective stress
σ'_v	Vertical effective stress
σ_1	Major principal stress
σ_3	Minor principal stress
φ	Friction angle
τ_f	Defining shear stress failure line
ψ	Dilatancy angle
υ	Poisson´s ratio

1 Introduction

1.1 Background

This master's thesis is based on a project that is included in the infrastructure project BanaVäg i Väst. The project includes construction of a new double track railway, Norge/Vänerbanan, and a four lane highway, E45, between Göteborg and Trollhättan. Skanska Sverige AB is the contractor at the section between Bohus and Nödinge, called contract E33. This includes a construction phase where a new track is to be built right next to an existing track. In order to keep this track in traffic during the construction, a sheet pile wall is installed along the existing track. To avoid the use of ground anchors, staged excavations was performed, where side effects from the surrounding soil volumes are used to support the sheet pile wall. A wailing beam was used at some sections on the sheet pile wall to make the wall stiffer. Since no guidelines exist for these types of design, the geotechnical engineers at Skanska Teknik, who was responsible for all the temporary retaining structures, made the design using conservative assumptions and experiences from other projects. This resulted in a restrictive design where the three dimensional behavior of the sheet pile wall was hard to predict, due to the design was made with a two dimensional model. It was also unclear which parameters that were affecting the deflections of the wall, and thereby it was hard to determine the geometries of the staged excavations. When designing sheet pile walls, it is mostly done for elongated excavations which means that the design can be solved as a two dimensional problem. But in design cases where the three dimensional effects have to be evaluated in order to optimize the design, advanced softwares are needed.

This master's thesis is a part of a SBUF project (Swedish construction industry's organisation for research and development) which is operated by Skanska Teknik.

1.2 Purpose

The purpose with this master's thesis is to study the effects of using a wailing beam on a sheet pile wall, with focus on staged excavations. It also aims to give a deeper knowledge of the three dimensional side effects of the soil and the mechanical behavior of the retaining structure. The effects are regarding horizontal deflections of a sheet pile wall, the influence of the surroundings and how the global factor of safety in the soil is affected by the retaining system. A parametric study is done in order to evaluate which parameters that affect the behavior of the system.

1.3 Delimitation

The simulations are based on the conditions that are prescribed at Skanska Sverige AB´s contract, E33. This concerns the soil properties, geometries and the chosen retaining structure which is a cantilever sheet pile wall with a wailing beam. The excavation method that is analyzed and discussed in this thesis is staged excavation. The situations that are analyzed are regarding horizontal deflections of the sheet pile wall, influence distance of the curvature and the safety factor in the soil. Only numerical simulations are performed at Serviceability limit state and an Ultimate limit state analysis of structural elements is beyond the scope of this thesis.

1.4 Method

In order to simulate the mechanical behavior of the sheet pile wall, numerical analysis will be done in the FE-software PLAXIS 3D Foundation version 2.2. To evaluate the results a field study is performed at the construction site at Skanska Sverige AB´s contract E33. The results from the simulations are also compared with the design model and made by Skanska Teknik during the design phase. The properties of the sheet pile wall in every direction are determined by using PLAXIS. A parametric study is done in order to analyze which parameters that affect the mechanical behavior of the sheet pile wall.

2 Review of previous work

This chapter gives a theoretical background to this master's thesis which includes a general description of sheet pile wall design, failure mechanisms and an introduction to the theories about staged excavation. The design method by Skanska Teknik is also described as well as the theories of the Finite Element Method, FEM.

2.1 Sheet pile wall design

Retaining structures are used in excavations and enables vertical slopes. The alternative is to excavate slopes with enough inclination, resulting in a sufficient total stability of the entire system. In many cases that kind of slopes are impossible to create due to lack of space at the construction site and impact of the surrounding area, e.g. buildings and roads. A number of methods are available to avoid large deformations and also to get sufficient factor of safety, both regarding failure in the sheet pile wall and global failure in the soil. Different types of struts and anchors could be necessary in order to fixate the sheet pile wall to avoid uneconomical dimensions.

In Swedish practise when designing retaining structures the *Handbook for design of sheet pile walls* (Ryner *et al*., 1996) is used. It is primary based on the theory of earth pressure developed by Rankine (1857). When designing sheet pile walls according to Ryner et al., (1996) the partial coefficient method is used, both in Serviceability limit state and Ultimate limit state. This is a statistical method to handle uncertainties of external loads, material properties, calculation methods and action effects.

2.1.1 Cantilever sheet pile walls

The principle with a cantilever sheet pile wall is that it is not anchored or strutted. It has to be driven to a depth under the excavation bottom where the active and the passive earth pressures balancing each other, i.e. moment and horizontal equilibrium occurs. The required depth of the sheet pile wall under the excavation bottom is based on moment equilibrium, defined in Equation (2.1).

$$\boldsymbol{P_P \times h_p > P_A \times h_A} \tag{2.1}$$

where the parameters are defined in Figure 2.1. Horizontal equilibrium is assumed to be satisfied with an extra 20 % of embedding. A cantilever sheet pile wall rotating around a point at the lower part of the sheet pile wall.

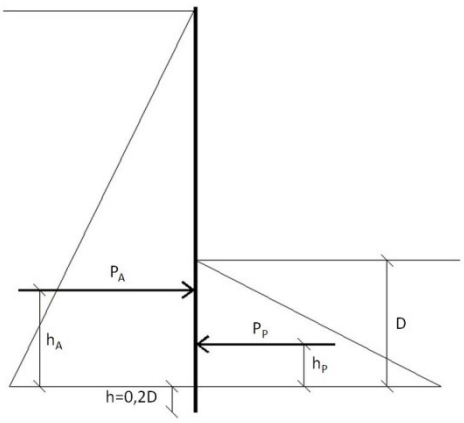

Figure 2.1 Earth pressure against a cantilever sheet pile wall, (Ryner et al., 1996).

2.1.2 Ultimate limit state design

The different types of failure that sheet pile walls should be designed for, in Ultimate limit state, can be divided into two main groups, failure in soil or failure in structural elements, (Ryner et al., 1996). Failure in soil is the most common and examples of this are presented in Figure 2.2.

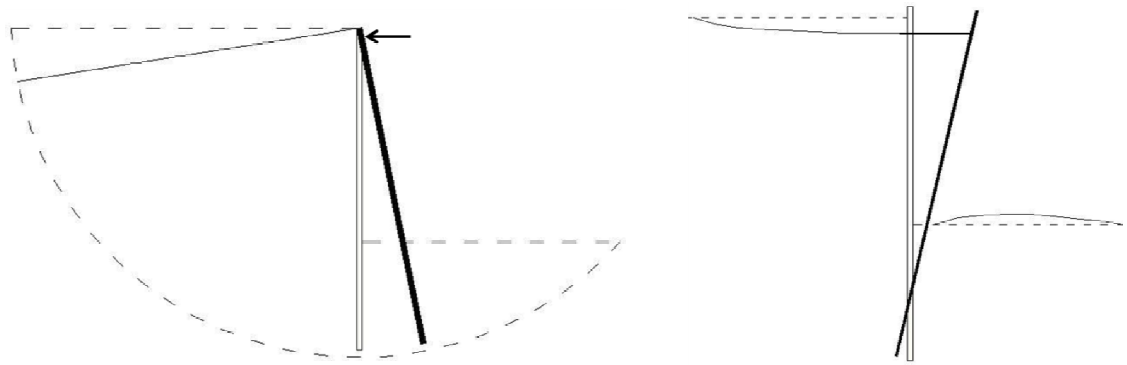

Figure 2.2 Failure mechanisms in the soil that has to be controlled in Ultimate limit state design.

Examples of failure in structural elements are failure in the sheet pile wall and failure in wailing beam, see Figure 2.3.

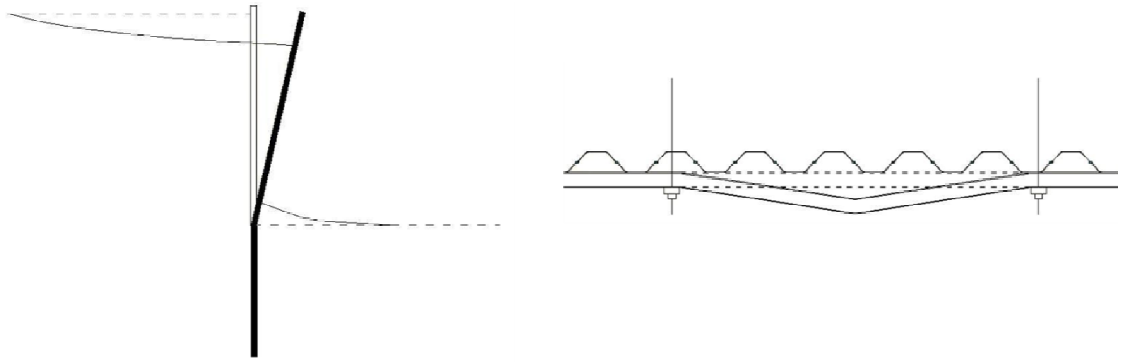

Figure 2.3 Failure mechanisms in structural elements that have to be controlled in Ultimate limit state design, (Ryner et al., 1996).

2.1.3 Serviceability limit state design

In the Serviceability limit state the design focus on acceptable displacements around or in the sheet pile wall. According to Ryner et al., (1996), settlements and horizontal displacements in the soil are related to strain in struts and deflection of the sheet pile wall, see Figure 2.4. This could also be caused by bottom heave.

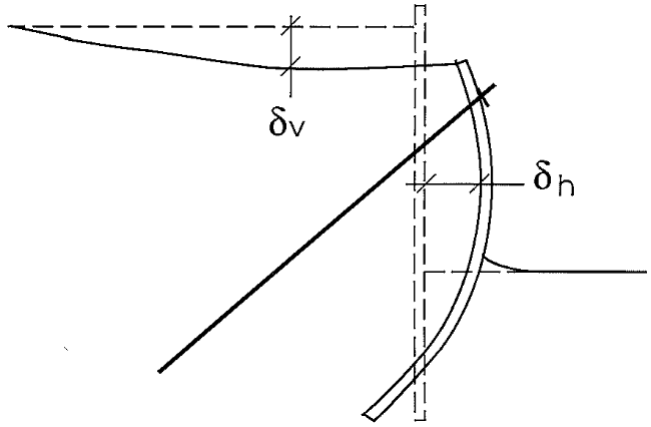

Figure 2.4 Settlements and deflection of a sheet pile wall, (Ryner et al., 1996).

2.1.4 Staged excavations

Staged excavations are used as a complement when satisfying stability cannot be reached. The principle is that one segment at a time is excavated. Then the excavation is refilled with another material or a concrete slab is casted and then the excavation front is moving forward, see Figure 2.5.

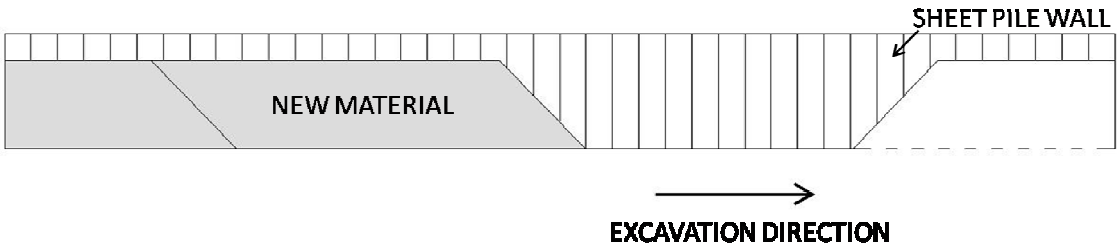

Figure 2.5 Sequence of staged excavations.

No well established analytical design method exists today in order to predict the side effects from the surrounding soil volumes. The design methods are instead based on conservative predictions of these side effects and experiences from earlier projects.

2.2 Skanska Tekniks model during the design phase

At contract E33, the restrictions concerning horizontal and vertical deformations of the existing railway track were strict. Thereby the deflections in the sheet pile wall had to be minimized. Due to a high surface load, the net earth pressure was acting on the active side, i.e. an equilibrium state could never occur. The proposed construction method by the Swedish Traffic Administration was to implement an anchored sheet pile wall. This is an expensive design and to reduce the cost, alternative methods was evaluated by Skanska Teknik during the tender process. The final design method was to implement staged excavation and a cantilever sheet pile wall with a wailing beam. This would keep the deflections within the limits and give a satisfying safety factor. During the design, conservative analytical models and numerical simulations in two dimensions were applied. In this section, the underlying theories and the assumptions made by Skanska Teknik are presented.

2.2.1 Theories and assumptions

By excavating one segment at a time, the surrounding soil volumes will stabilize the system. This means that the maximum horizontal deflection will occur in the middle of the excavated segment, cross section A-A in Figure 2.6. The mechanical behavior which is developed is called horizontal arching.

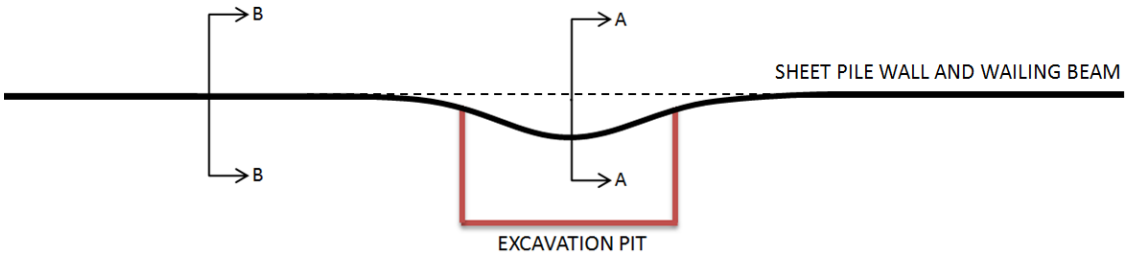

Figure 2.6 The horizontal deflection of the sheet pile wall seen from above. By horizontal arching in the retaining structure the loads induced by the excavation is distributed to the soil outside the excavation pit.

The deflection varies along the sheet pile wall. In cross section A-A it will tilt into the excavation. In cross section B-B, which is located far from the excavation, the wall is unaffected, see Figure 2.7.

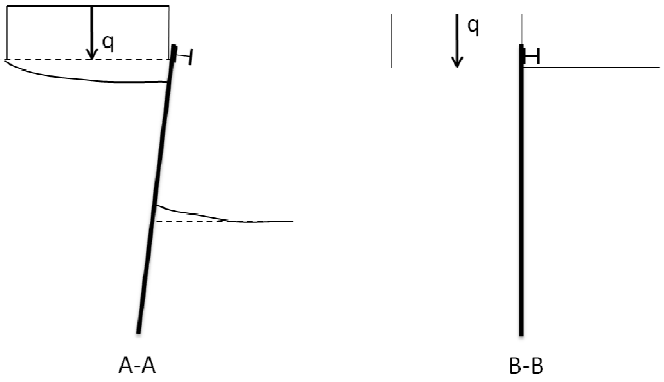

Figure 2.7 Cross sections from Figure 2.6. A-A shows a section inside the excavation and B-B shows a section outside the influence distance.

By using this excavation method, the sheet pile wall is used to distribute the loads induced by the excavation to the soil outside. During this process, shear forces are spread to the outer soil volume. Where the displacements have its maximum, the relative deformations between the grains are zero, and thereby also the shear forces. In opposite, the shear forces have its maximum where the maximum relative deformation occurs. This happens at edge of the excavation, in cross section $B^- A^-$ and $A^+ B^+$, see Figure 2.8.

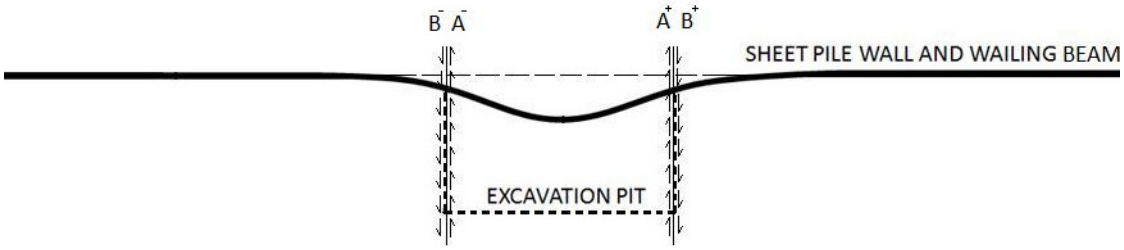

Figure 2.8 The maximum shear forces are developed at the edge of the excavation pit where the relative deformations have its maximum.

In the sections along the wall, slip surfaces are developed where shear forces are transferred. The slip surfaces are formed as straight failure lines with an inclination of 45 degrees and are based on Rankine´s method of plane slip surface, see Figure 2.9. Inside the excavation in Figure 2.9 a), the shear forces counteract the deflection of the wall and will increase the stability in this area. Outside the excavation the shear forces are reversed, which contributes to a lower stability in this area, see Figure 2.9 b).

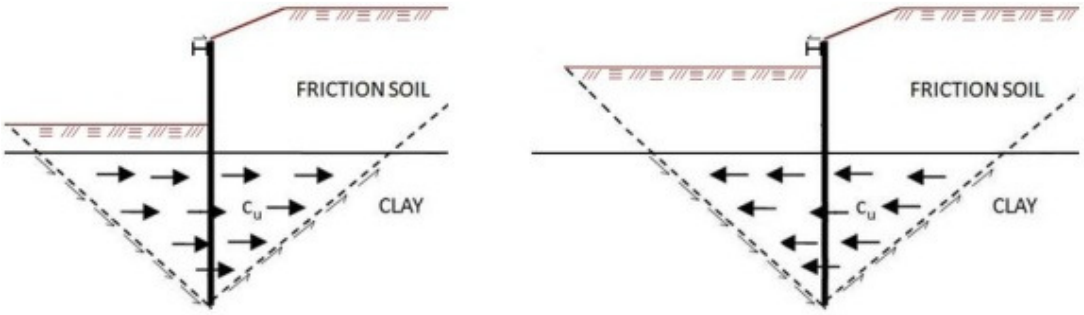

a) *b)*

Figure 2.9 *Cross section from Figure 2.8. Slip surfaces that are developed inside the influence area. Modified after (Edstam, 2010).*

a) Cross section showing the distribution of shear forces, c_u, inside the excavation, between A^- and A^+. In the excavation centre c_u is zero.

b) Cross section showing the distribution of shear forces, c_u, outside B^- and B^+. Outside the influence distance, c_u, is zero.

At a point in a sufficient distance from the excavation pit, all shear forces have been transferred and no deformations occur. This is called the influence distance. The sheet pile wall has a low flexural rigidity around the vertical axis. To increase this, a wailing beam is often used. This will decrease the maximum deflection. How the reaction force in the wailing beam is distributed is hard to predict, and the assumption made by Skanska Teknik is illustrated in Figure 2.10. p_A and p_B are the forces acting against the wailing beam inside and outside the excavation respectively.

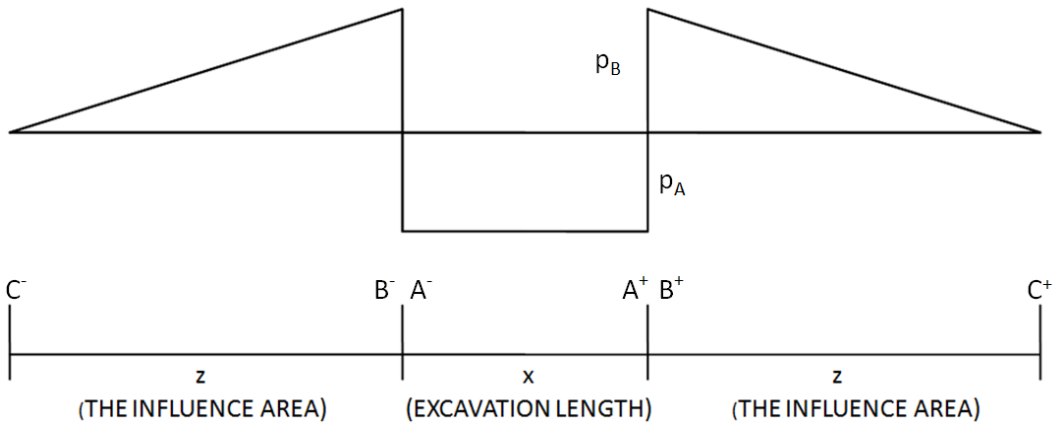

Figure 2.10 *The reaction force that is assumed to be acting against the wailing beam. (Edstam, 2010).*

2.2.2 Model

When designing a sheet pile wall for staged excavation, the conventional 2 dimensional method is not sufficient. Since the side effects cannot be considered in a two dimensional analysis, fictive loads and springs are introduced in the two dimensional model in order to account for these three dimensional effects.

The design approach was to simulate a two dimensional model concerning horizontal arching that took the wailing beam and the three dimensional side effects from the soil into account. From the first analysis it was concluded that the major failure mechanism was dominated by a small horizontal translation and a rotation of the sheet pile wall around a point just above the lower edge of the sheet pile wall.

The assumed horizontal side effect is the sum of the mobilized shear strength in the soil. This corresponds to the area filled with arrows in Figure 2.9, where c_u is the mean characteristic shear strength. Note that it has to be taken into account if the shear strength, c_u, varies with depth. The shear strength that is mobilized in the friction soil is harder to estimate why it was neglected.

In the two dimensional model, the side effects from the soil is transformed to a triangulate line load. This line load is acting from the upper edge of the clay to the lower edge of the sheet pile wall, and is defined as P_{cl}. A point load, $P_{wailing\ beam}$, represents the influence of the wailing beam, see Figure 2.11.

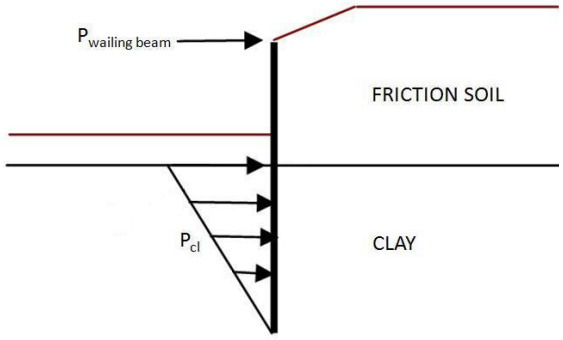

Figure 2.11 Cross section illustrating the model in Ultimate limit state design which brings the side effects from the clay and the wailing beam into account, (Edstam, 2010).

In order to determine the excavation length and the influence area, an iteration of the forces $P_{wailing\ beam}$ and P_{cl} was done in order to reach an equilibrium state with a reasonable displacement pattern. When the equilibrium state was reached, the stresses in the wailing beam were analyzed separately.

This procedure resulted in a Ultimate limit state design with a safety factor of 1,5. This analysis was done in PLAXIS 2D. To evaluate the deflections in Serviceability limit state, a spring model was used. The predicted side effect from the surrounding clay was replaced with springs. This includes also the impact of the wailing beam, see Figure 2.12.

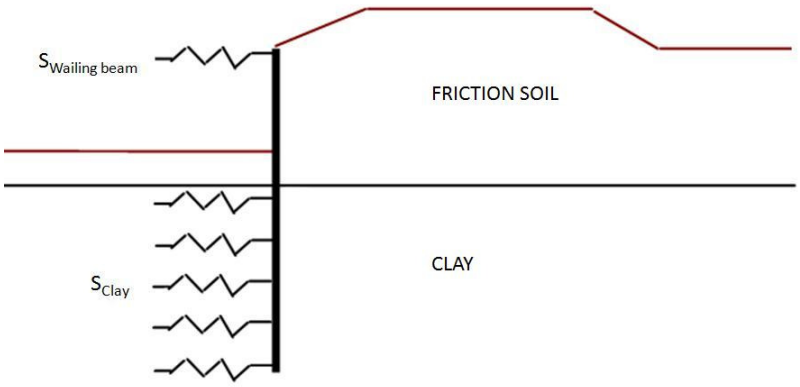

Figure 2.12 Cross section illustrating the design model in Serviceability limit state, (Edstam, 2010).

2.3 Numerical modelling and FEM

When the complexity of a geotechnical problem is increasing, it could be preferable to use a numerical model. This is based on calculations that use algorithms to solve partial differential equations which are functions of several variables. These variables are material parameters, stresses, and strains etc, which in geotechnical engineering often show very complex correlation. The Finite Element Method (FEM) is a technique to find the solutions to this kind of equation systems. This is done by collecting the variables into matrices and vectors in computer programs and by numerical methods solve the system.

The use of this kind of tools does not only require knowledge about the theory behind numerical methods and skills to handle computer software, but also good knowledge and experience about the subject. In this case it is important to understand the soil mechanics and structural engineering and to be able to see the limitations of the model (Potts et al., 2002). Generalisation and simplifications of the reality are often needed to build the model, and to do this, understanding and experience in geotechnical engineering is essential. This is also needed in order to evaluate the calculation results. If this is not done properly, the output will be misleading, which can get serious consequences.

3 Finite Element Analysis in PLAXIS

The development of commercial finite element software in geotechnical engineering started in the late 80´s, and is today widely spread. In many ways it differ from FEM applications in other engineering fields, since geotechnical engineering involves many specific and often very complex issues (Potts et al., 2002).

This chapter includes an introduction to PLAXIS 3D Foundation. It also includes the creation of the model. Then a study to find the three dimensional properties of the sheet pile wall, is presented.

3.1 PLAXIS 3D Foundation

PLAXIS was started at Delft University in 1987 as a finite element code for analysing the lowland riverbanks of the Netherlands. Until 2001, the modelling was two dimensional, when PLAXIS 3D Tunnel was released. Three years later, PLAXIS 3D Foundation came, developed for a broader spectrum of foundation constructions and geotechnical application such as stability, settlements and deformation calculations.

When taking the step from 2D to 3D analysis, the possibilities, but also the complexity increases. This also includes a major increase in size of the calculations. If a detailed calculation takes a couple of minutes to perform in 2D, the same calculation in 3D could take hours. Despite this, for some problems the need of consider 3D aspects requires this type of heavier calculations in 3D. Modelling side effects of staged excavation is one of these cases. PLAXIS 3D Foundation consists of three main parts which is *Model*, *Calculation* and *Output mode*.

3.1.1 Model mode

In the *Model mode*, the geometry is built. Soil layer boundaries and material properties are set. Construction element, such as walls and beams are placed in the model and interface properties are defined. Finally, the mesh is generated and refined to a proper level. The choice of soil model is very important, and will be described more in Chapter 3.6.

3.1.2 Calculation mode

In the *Calculation mode*, a number of calculation phases can be defined. Different load cases and geometries are set to simulate a realistic building sequence. For every step, different groundwater conditions can be set, and construction elements could be activated. Excavation is simulated by deactivation of cluster. The calculation type must be defined and could be *plastic*, *consolidation* or *phi/c reduction*. The *consolidation* analysis is used when modelling time dependent behaviours such as development and dissipation of excess pore pressures and settlement calculation when creep deformations are requested. The *plastic* calculation is used to analyse the elastic-plastic deformations according to small deformation theory (Brinkgreve, 2007). Deformations and stresses are calculated for all nodes in Serviceability limit state. The result is depending on the choice of material model.

The *phi/c reduction* is a safety analysis that will calculate the global factor of safety and is executed by stepwise reduction of the strength parameters of the soil. This iteration process proceeds until failure occur somewhere in the model. The safety factor is then calculated by the relation between the input strength parameters and the stepwise reduced strength parameters when failure occurs. The safety factor, M_{sf}, is

defined as the value of the soil strength parameters at a given stage in the safety analysis, see Equation (3.1).

$$\Sigma Msf = \frac{\tan \varphi_{input}}{\tan \varphi_{reduced}} = \frac{c_{input}}{c_{reduced}} \tag{3.1}$$

Note that *phi/c reduction* will not reduce the strength parameters of the structural elements. In order to design structural elements in Ultimate limit state, the bending moments and shear forces has to be studied separately. By comparing the action effects with the calculated capacity, a safety factor for every structural element can be determined. This calculation cannot be performed by PLAXIS.

3.1.3 Output mode

In the third main part of PLAXIS is the output mode and is used for post processing of the calculation result. Deformations, strains and pore-pressures are visualized for every phase of the calculation and for construction elements bending moments and shear forces can be studied. Curves for e.g. safety factor analysis could be plotted.

3.2 Geometry

When making a model, the creation process is important. This means that the complete process needs to be presented and discussed. Many assumptions need to be explained and simplifications need to be motivated. If the process is not transparent, the outcome could always be challenged.

The starting point for the model was the construction of the double track railway close to the existing track between Gothenburg and Trollhättan, at contract E33. First, the outer boundaries were determined. The calculations made by Skanska Teknik had indicated an excavation length of about 5 meter along the sheet pile wall and an influence distance in the wall of about 12 meter outside the excavation for the case when a wailing beam is used. The size of the model was chosen according to this and is presented in Figure 3.1.

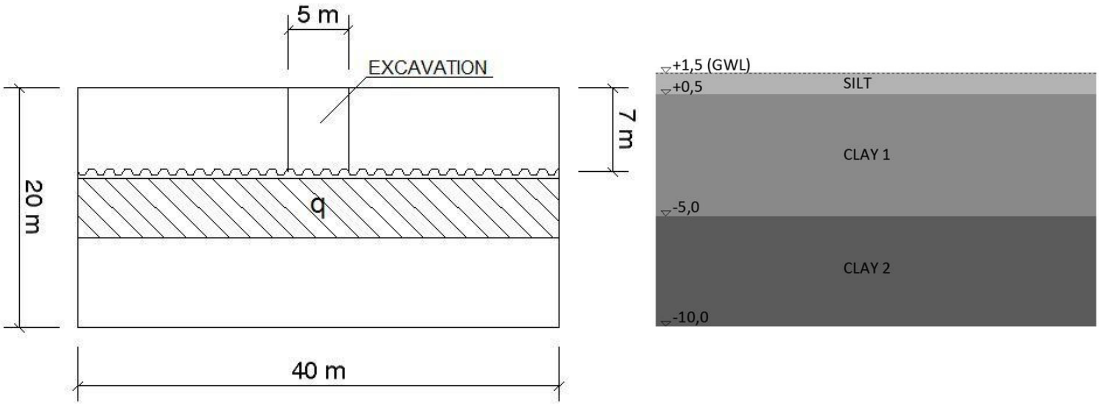

Figure 3.1 The geometry for the model in plan is shown to the left. To the right the profile is presented.

It has to be verified that the size is appropriate and that the influence area is not larger than the model. If the size of the model is too small, the boundary conditions will affect the result and if the size is too large, the calculation time is increasing. In the

first model the lower edge, in the bottom of the geometry, was set to z = -20 meter in PLAXIS. In adept to optimize the model, this boundary was stepwise moved to -10 meter, and the result from these calculations was compared with the result from the model with the lower boundary at -20 meter. Since there were no differences between the results, even in an extreme load case, the smaller model to -10 meter could be used further on.

3.3 Simplifications and assumptions

To make the model more valid for a general case the model was simplified. As shown in Figure 3.2 the layer of silt is replaced with a distributed load.

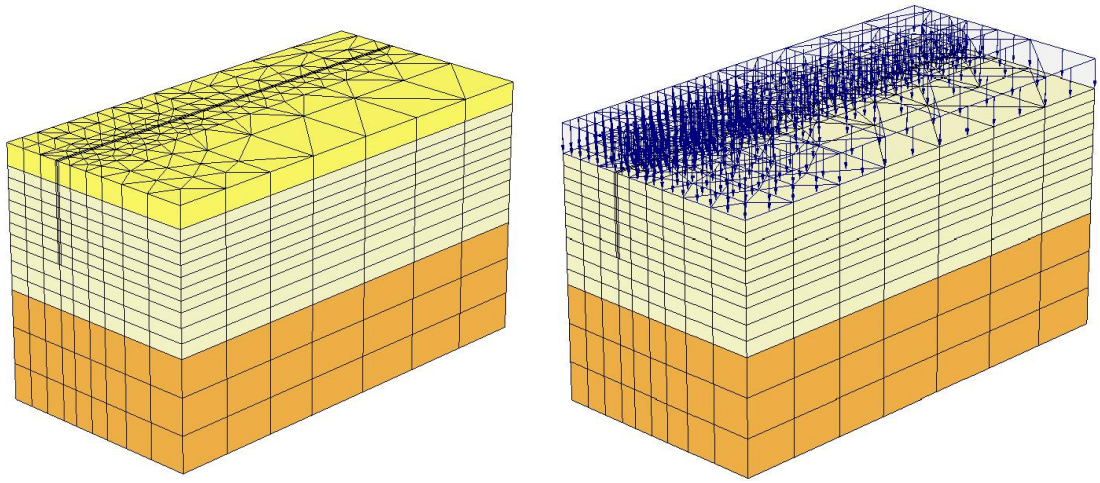

Figure 3.2 The layer of silt is replaced with a distributed load.

This was done to simplify the calculations but also because the interest is not what happens locally in the silt layer, but what the load of the silt layer causes in the under laying soils. Therefore, the silt is replaced with a vertical load, Q, acting directly on the clay.

$$Q = \gamma \cdot H \tag{3.2}$$

where γ is the unit weight of the silt and H is the thickness of the silt layer. To simulate the horizontal earth pressure, a distributed surface load is working on the sheet pile wall, σ_h.

$$\sigma_h = \sigma'_v \cdot K_{mean} + p_w \tag{3.3}$$

where,

$$K_{mean} = \frac{K_0 + K_A}{2} \tag{3.4}$$

$$K_0 = 1 - sin\varphi \tag{3.5}$$

$$K_A = tan^2(45 - \frac{\varphi'}{2}) \tag{3.6}$$

K_A is however adjusted according to the roughness of the interface, which is set to 1, and is taken from tables. p_w is the load corresponding to the hydrostatic groundwater

pressure. The reason for using K_{mean} is that K_0 determines the horizontal component before there is any displacements in the sheet pile wall and K_A when the deformations are large enough to mobilize full strength in the silt. To consider both these aspects a mean value of K_0 and K_A is used during the simulations in PLAXIS.

3.4 Boundary conditions

When modelling the sheet pile wall, the effect of the boundary conditions needs to be considered. This is not only a limitation; it can also be used as a tool to optimize the calculation process. To decrease the size of the model in a symmetric geometry, the model could be cut in symmetry sections. This will leave only half of the original geometry, reducing the number of elements needed and thereby also the calculation time. In this model, two symmetry cuts are used, see Figure 3.3. Only one fourth of the original geometry is remaining and the results from the calculation will not be affected.

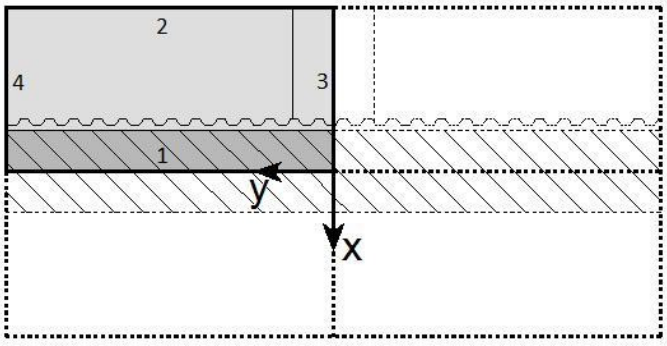

Figure 3.3 The original geometry is cut in two symmetry sections, reducing the size of the model to one fourth. The numbers are used to identify the sides.

The cut along side 1 is not a perfect symmetry cut, since the excavation only is made on one of the sides. However, this will only marginally affect the result.

On side three, the wall will have its maximum deflection. The sheet pile wall is fixed for rotation in this symmetry cut, and moment is transferred over this section. This boundary is thereby considered free to move along the edge, in the x- and z- direction. In the y- direction the wall cannot move. This is the default configuration in PLAXIS 3D Foundation.

On side four, the sheet pile wall must end on a sufficient distance from the boundary. The sheet pile wall must be free to move, unaffected by this boundary. When the free end of the wall is ending close to the boundary, the boundary condition will affect the movement of the wall. In reality, it is the shear strength of the soil that is preventing the wall to move. When the wall is ending close to the boundary, this will not be the case. Since the boundary condition allows free movement along the side without friction, the wall in the model will have a larger displacement than the real case. However, this assumption will be on the safe side. The opposite extreme would instead be to lock the displacements at the boundary, which is possible in PLAXIS. For this configuration, no nodes can move along the side, in either direction. This configuration has been tested for the current model, and the result showed very small differences with the model with free displacements along the boundary. The realistic

behaviour of the sheet pile wall is somewhere in this interval, which means that the used approximation is valid in this case.

3.5 Mesh generation

In order to make finite element calculations, the base geometry in PLAXIS 3D Foundation has to be divided into smaller elements, so called finite element mesh. Each element includes a certain number of nodes which form the equation system for the calculations. The more number of nodes, the larger equation system the computer has to solve. In 2D, each node has two degrees of freedom, i.e. the nodes can move in x and y-direction, see Figure 3.4.

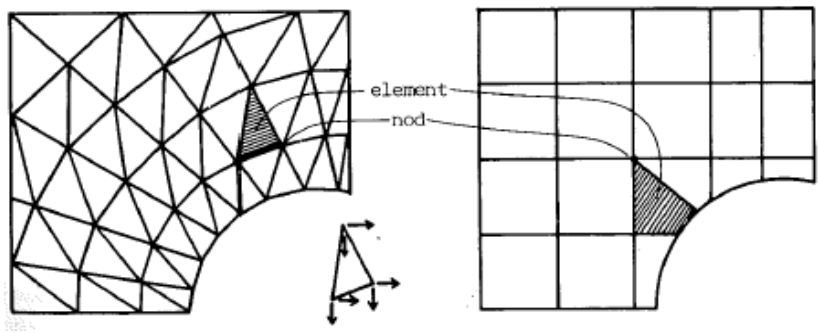

Figure 3.4: Elements and nodes in a 2D- model. Each node has two degrees of freedom, described by the arrows in the smaller figure, (Wiberg, 1974).

When modelling in three dimensions, each node has three degrees of freedom which results in a larger equation system due to the fact that the each node can also move in z- direction.

The FEM-analysis is proceeding in three steps, see Figure 3.5. The first step is to divide the model into smaller parts by G*enerate elements* into the model, where each element is relatively easy to solve individually. The next step is analysing the element in the *Element analysis*. The last step is the *System analysis* where all the elements get connected to a system by boundary conditions, (Wiberg, 1974).

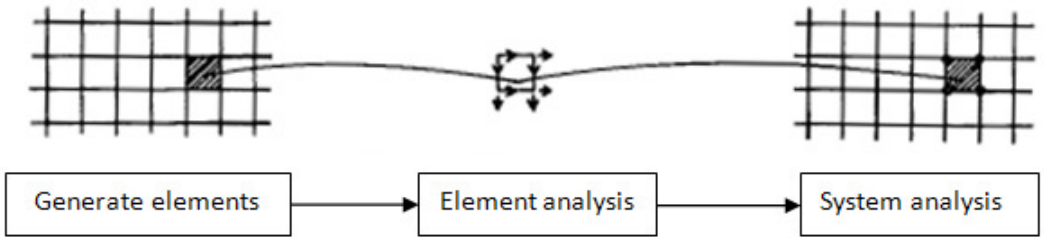

Figure 3.5 Steps in FEM-analysis (Wiberg, 1974).

FEM- analysis is an approximated calculation method and the sources of error are many and often unavoidable (Wiberg, 1974). The number of nodes in the model has a considerably impact of the result from the calculations. A higher number of elements, which generating a larger number of nodes, gives results with more accuracy, better

approximation, than a model with less nodes. When designing more complex models it is preferable to have higher number of nodes than in more simple cases.

The default settings for the cluster size in PLAXIS 3D Foundation is *Coarse mesh*. This may be enough size when modelling simple cases and the accuracy of the calculation do not need to be high. The equation system is easier for the computer to solve and the calculation time is relatively short.

If the accuracy needs to be higher, a refinement of the cluster is necessary. If the whole model should be refined, the function *Global coarseness* changes the element size in both horizontal and vertical direction with the intervals *Very coarse* to *Very fine*.

The two dimensional refinement, on the horizontal plane, is done first. It is of great importance that the two dimensional mesh is not too fine when proceeding to the 3-dimensional mesh. This is because a very fine two dimensional mesh generates a large number of 3D elements and nodes, and thus excessive calculation time.

The user is responsible to judge if the finite element mesh is enough sufficient or if a global/ local refinement is necessary (Brinkgreve et al. 2007). Using the geometry defined above, the mesh in the horizontal plane is adjusted to an appropriate level. For areas where most deformations are expected, the mesh has to be finer. The areas around the sheet pile wall and the excavation is refined incrementally until an appropriate coarseness is found. By adjusting the local element size factor in the geometry points and the geometry lines the coarseness can be controlled by the user. Areas far from the excavation and the sheet pile wall are left with a coarse mesh.

To verify that the model consists of enough number of nodes, simulations are done where the number of nodes is increased gradually. The result is compared regarding the factor of safety and the total displacement, see Figure 3.6. The simulations are based on the model geometry from the case study in this report accept from the excavation width, which here is 10 meter.

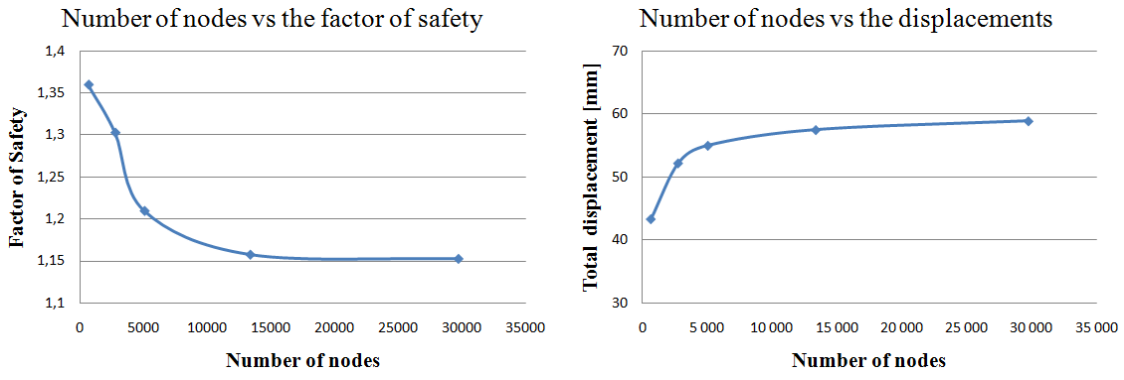

a) *b)*

Figure 3.6 *Results from the 3D simulation with different number of nodes*

a) Number of nodes vs. the factor of safety

b) Number of nodes vs. total displacement

The calculations verifies that the results differs with increased number of nodes but flatten out when reach a higher number of nodes. The model used in this thesis consists of about 14 000 nodes. The results in Figure 3.6 are verifying that the difference is sufficiently small from a model with 30 000 nodes and that the calculations of the model with 14 000 nodes will give enough accuracy in this case.

To verify the accuracy of the calculations, the results are compared to calculations in PLAXIS 2D. By simulate an excavation along the entire sheet pile wall in the 3D model, it can be seen as a 2D simulation. Both the safety factor and the displacements showed good correlation, verifying the accuracy.

The calculation time should also be considered. To be able to use the model in the most effective way, the calculation time for one simulation including a large number of phases should not exceed 15 hours. This allows the user to configure the settings and phases during the day and start the calculations before leaving in the late afternoon. Next morning, after approximately 15 hours, the simulation should be finished, and ready for processing. After that, the cycle will be restarted. Therefore, the number of nodes should be chosen regarding both the accuracy needed and also to the time available for each simulation.

In order to compare the differences in calculation time between the simulations with different number of nodes, a study was made. Each simulation was made with identical calculation phases and the result is presented in Figure 3.7.

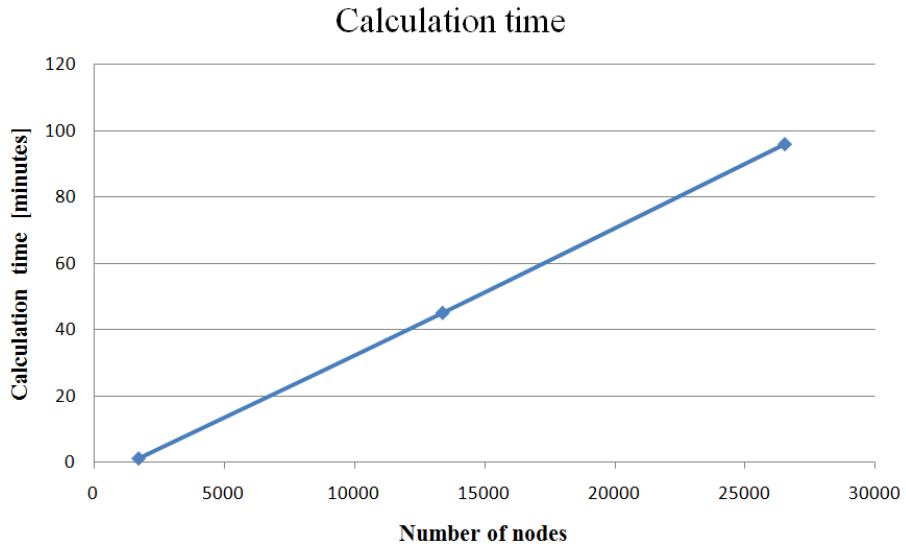

Figure 3.7 Calculation time when simulating with different number of nodes in PLAXIS 3D Foundation.

The calculation time increased linearly with number of nodes from 1 minute calculation time when simulating with 1 700 nodes to 96 minutes with 27 000 nodes.

3.6 Soil settings

PLAXIS 3D Foundation can handle a number of soil models, were the Mohr-Coulomb model is the most commonly used and also the model used in most of the simulations in this thesis. The model is a linear elastic, perfectly-plastic model, meaning that the material is behaving ideal elastic until all the shear strength have been mobilised (Brinkgreve, 2007). When the yield criterion is reached, all load

increments will lead to plastic strains. No hardening parameter is used, which means that the yield condition does not change as a result of plastic straining (Potts et al., 2002). The material properties in the Mohr-Coulomb model are defined in Table 3.1.

Table 3.1 Material properties of the soil in Mohr-Coulomb model(Brinkgreve, 2007).

Parameter	Unit	Definition
E, Young´s modulus	kPa	The modulus of elasticity
ν, Poisson´s ratio	-	The strain change perpendicular to the load direction
φ, Friction angle	°	The internal friction angle of the soil
c, Cohesion	kPa	Intermolecular attraction in fine-grained soils
ψ, Dilatancy angle	°	The volume change of the soil during shearing

The strain consists of a plastic and an elastic part, which for one dimension is shown below.

$$\varepsilon^{tot} = \varepsilon^{e} + \varepsilon^{p} \tag{3.7}$$

For elastic deformations, Hooke's law in Equation (3.8) is valid.

$$\sigma = E^{e} \cdot \varepsilon^{e} \tag{3.8}$$

To be able to evaluate if strains will be plastic or elastic, a yield criterion is expressed as a function of stress, cohesion, and friction angle, see Equation (3.9).

$$f(\sigma, c, \varphi) = 0 \tag{3.9}$$

This defines an area in the stress space where all load increments will lead to plastic strains, (Kullingsjö, 2007). For soils, Mohr- Coulomb´s criteria of failure is used which is defined in Equation (3.10).

$$\tau_f = c + \sigma \cdot \tan\varphi \tag{3.10}$$

where τ_f defines the shear stress failure envelope, c is the cohesion and φ is the friction angle, see Figure 3.8. The soil stress, according to Mohr- Coulomb´s model, is related to the difference between σ_1 and σ_3, which represent the major and the minor principle stress respectively.

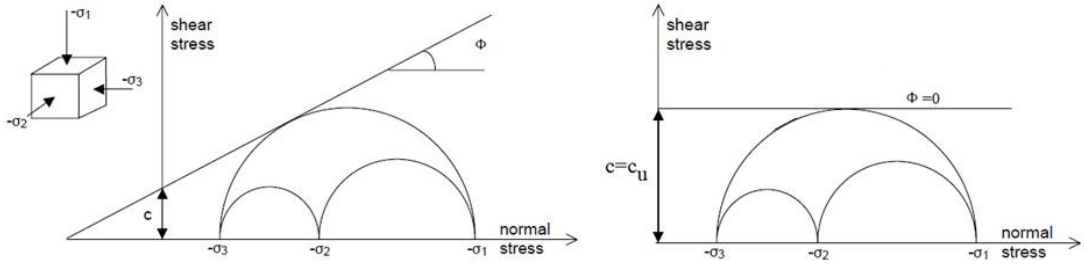

Figure 3.8 Mohr- Coulomb´s criteria of failure in two dimensions, (Brinkgreve, 2007).

The Mohr-Coulomb´s failure envelope indicates that stress points under the line are in an elastic state. When the stress circles touch the failure line, failure will occur, i.e. the soil goes from elastic to plastic state (Sällfors, 2001).

When taking the third dimension into account, the failure surface in Mohr- Coulomb´s model occurs as a cone with a base of a hexagon, see Figure 3.9. Inside the surface elastic deformations will be developed which are depending on the given Young´s modulus, E and Poisson´s ratio, υ. When an element of the soil has reached the stress surface, the elastic deformations goes to elastic-plastic deformations and the point cannot be exposed of increased loads. This is the same scenario that occurs in the two dimensional case.

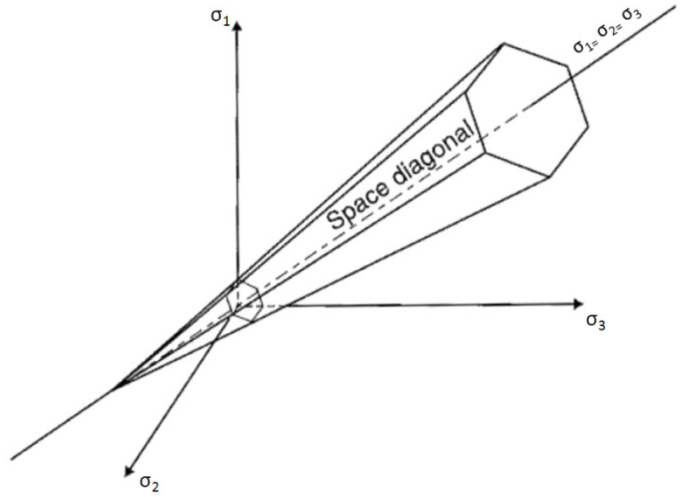

Figure 3.9 Failure surface for Mohr-Coulomb´s model in three dimensions for cohesion less soils,(Potts et al., 2002).

It is important to remember that this model only is an approximation of the real soil behaviour. In Figure 3.10 (a), a soil sample is compressed isotropically up to some confining stress σ_3. Then the axial pressure σ_1 increased whilst the radial stress is kept constant. Figure 3.10 (b) shows the corresponding test result using a Mohr-Coulomb model.

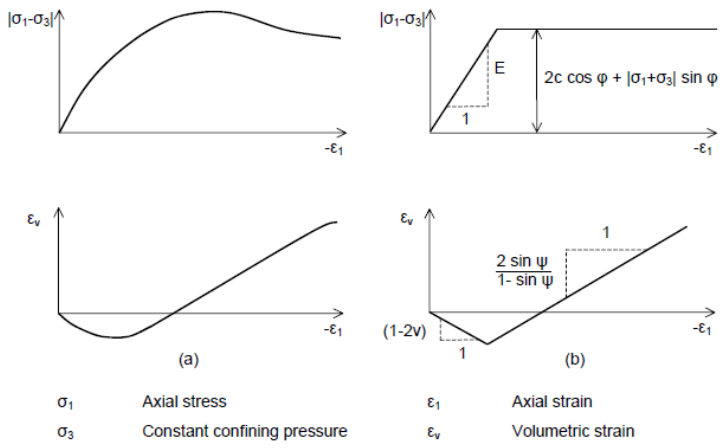

Figure 3.10 Results from standard drained triaxial tests (a) and elastic-plastic model (b), (Brinkgreve, 2007).

3.7 Sheet pile wall settings

The sheet pile wall is modeled as linear- elastic and can therefore never go to failure. To simulate retaining structures, PLAXIS 3D Foundation uses the construction element *Wall*. To get a satisfying behavior of the wall in three dimensions, the behavior in different directions must be realistic. Since a wall element for practical reasons must be drawn as a straight line, its corrugated shape must be simulated using anisotropic material properties. This will give the wall different flexural rigidity in different directions. In PLAXIS 3D Tunnel, the wall could only have isotropic properties, meaning that the flexural rigidity is the same in all directions. This is not a realistic behavior of a corrugated sheet pile wall. In PLAXIS 3D Foundation this problem was solved, and the wall could have anisotropic properties. Now, the challenge was to find the properties that would simulate a realistic behavior of the sheet pile wall to be used in the soil/structure model in the parametric study. This means that the properties of the corrugated sheet pile wall with its anisotropic geometry must be transformed to a wall with isotropic geometries and anisotropic properties. The procedure for doing this is discussed in the following chapter. The local system of axis and properties in all directions are shown in Figure 3.11. The sheet pile wall parameters in PLAXIS 3D Foundation is presented in Table 3.2.

Table 3.2 Material properties for the sheet pile wall with linear elastic behaviour(Brinkgreve, 2007).

Parameter	Unit	Definition
d, equivalent thickness	m	The cross section area of the wall across its major axial direction per 1 m width
E_1, Young's modulus	kPa	Modulus of elasticity in first axial direction
E_2, Young's modulus	kPa	Modulus of elasticity in second axial direction
G_{12}, shear modulus	kPa	In plane shear modulus
G_{13}, shear modulus	kPa	Out-of-plane shear modulus related to shear deformation over first direction
G_{23}, shear modulus	kPa	Out-of-plane shear modulus related to shear deformation over second direction

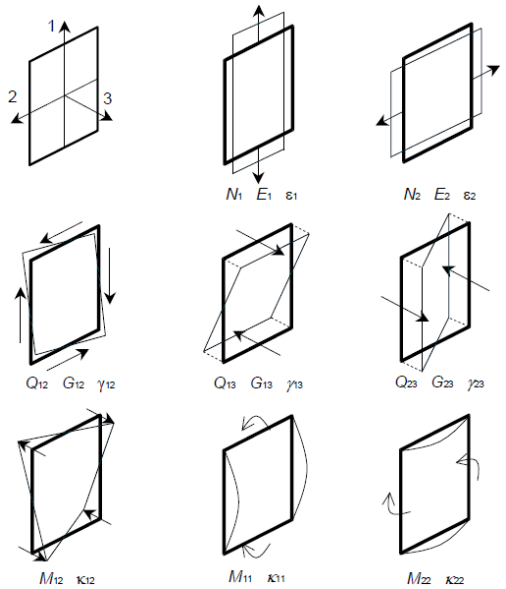

Figure 3.11. The local system of axes in the wall element and various quantities,(Brinkgreve, 2007).

The flexural rigidities must be found in each direction. For a sheet pile wall, bending around the first and the second axis is of most importance, together with the resistance against torsion. To describe this, each column of

Figure 3.11 shows parameters that affects the flexural rigidity in each direction. The procedure for determine these is described under the following sections.

3.7.1 The flexural rigidity around the second axis

The flexural rigidity around the second axis is usually what is of interest in a 2D analysis. The parameters are described in

Figure 3.12.

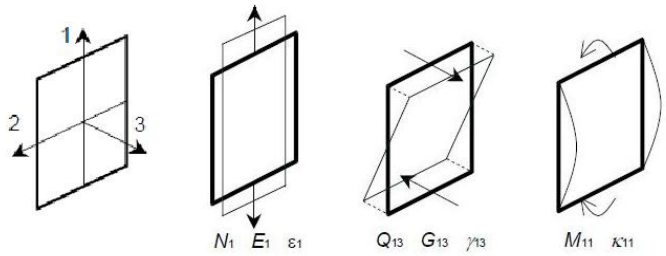

Figure 3.12 Definition of the parameters describing flexural rigidity around the second axis,(Brinkgreve, 2007).

When subjected to a moment force, M_{11}, the resistance is determined by Young´s modulus E_1 and the shear modulus G_{13}.

$$E_1 = \frac{12 \cdot E_{steel} \cdot I_1}{d^3} \tag{3.11}$$

$$G_{13} = \frac{E_{steel} \cdot A_{13}}{2 \cdot (1+\upsilon) \cdot d} \tag{3.12}$$

where I_1 is the moment of inertia around the second axis. A is the cross section area per 1 meter wall that is effective against shear forces. These two properties can be found in specifications from manufactures. For A_{13}, which is working over the vertical direction, the value is approximated to 1/3 of A, according to (Brinkgreve, 2007).

In three dimensions the behaviour of the wall is much more complex, and more material parameters are needed to describe the behaviour. Also the flexural rigidity around the first axis needs to be defined.

3.7.2 The flexural rigidity around the first axis

This direction is usually not of interest then looking at a 2D case, but when simulating in three dimensions the flexural rigidity around the first axis is important. The parameters are described in Figure 3.13.

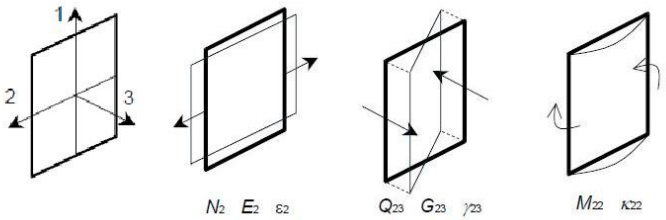

Figure 3.13 Definition of the parameters describing flexural rigidity around the first axis, (Brinkgreve, 2007).

The flexural rigidity in this direction is determined by E_2 and G_{23} and is defined in Equation (3.13) and (3.14). These equations are according to PLAXIS 3D Foundation user manual, (Brinkgreve, 2007).

$$E_2 = \frac{12 \cdot E_{steel} \cdot I_2}{d^3} \tag{3.13}$$

$$G_{23} = \frac{E_{steel} \cdot A_{23}}{2 \cdot (1+\upsilon) \cdot d} \tag{3.14}$$

where A_{23} is effective against shear deformation over the horizontal direction and is 1/10 of the value of A, (Brinkgreve, 2007). According to PLAXIS user manual, (Brinkgreve, 2007), I_2 can be defined as $I_1/20$. This recommendation can be questioned since the flexural rigidity in this direction is much weaker. The flexural rigidity is also influenced by the interaction between the single sheet piles. Slip in the interlocks makes the wall much weaker compared to a solid wall and this effect is hard to estimate. Also assumptions regarding angle displacement in the interlocks will affect the behaviour. If not weld, which usually is the case, sliding is only prevented by friction in the interlocks, and the friction coefficient is unknown. Even if the interlocks are welded the stiffness is hard to estimate.

If slip in the interlocks and angle displacements are neglected, PLAXIS 2D could be used to determine the flexural rigidity around the first axis. A particular sheet pile wall geometry is chosen, and modeled as a corrugated beam, fully fixed in both ends. The deflection is then calculated when a load is acting on the beam, and is bending it in its weakest direction, around the first axis, see Figure 3.14. The value of E is set to Young's modulus of steel, 210 GPa, and the geometry is chosen according to standard dimension for some sheet pile wall. This will simulate the deformation pattern of the sheet pile wall in its weakest direction. For the given geometry the value of the maximum deflection, δ_{max} is calculated.

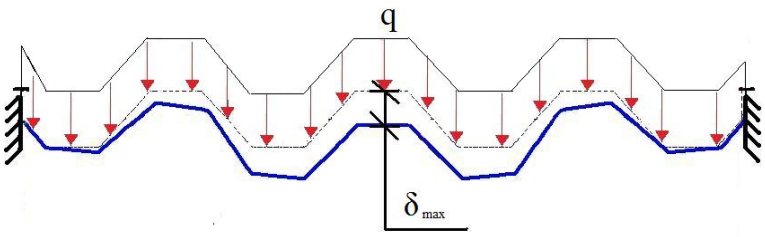

Figure 3.14. Simulation of a corrugated beam in PLAXIS 2D. The maximum deflection, δ_{max}, is calculated for a distributed load q.

This can now be transformed to a homogenous beam with anisotropic material properties, illustrated in Figure 3.15. The properties for this beam are adjusted so that the maximum deflection, δ_{max}, is the same as for the corrugated wall in Figure 3.14.

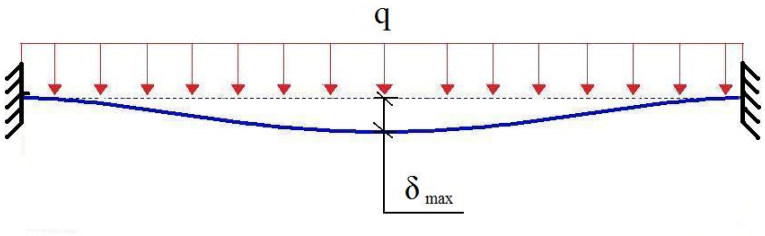

Figure 3.15 Simulation of a homogenous beam in PLAXIS 2D. The maximum deflection, δ_{max}, is calculated for a distributed load q.

For the beam in Figure 3.15, the maximum deflection can be expressed by Equation (3.15).

$$\frac{w \cdot L^4}{384 \cdot E_{steel} \cdot I_2} = \delta_{max} \tag{3.15}$$

or again,

$$I_2 = \frac{L^4 \cdot w}{384 \cdot E \cdot \delta_{max}} \tag{3.16}$$

E_2 can now be calculated from Equation (3.13) and will be the equivalent modulus for the rectangular, isotropic geometry that can be used in further simulations in PLAXIS 3D Foundation.

3.7.3 Torsional rigidity against warping

The parameters affecting the torsional rigidity against warping is defined in Figure 3.16.

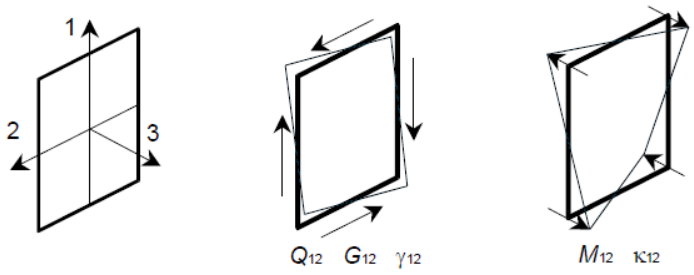

Figure 3.16 Definition of the parameters affecting the torsional rigidity against warping, (Brinkgreve, 2007).

When bending is the most important type of deformation, the in plane shear modulus G_{12}, can be defined by Equation (3.17).

$$G_{12} = \frac{6 \cdot E_{steel} \cdot I_{12}}{(1+\nu) \cdot d^3} \tag{3.17}$$

To determine G_{12}, the moment of inertia against torsion, I_{12}, has to be defined. This requires deeper studies of the theories behind the behavior. The shear modulus, G, can in general terms be described by Equation (3.18).

$$G = \frac{E}{2\cdot(1+\nu)} \tag{3.18}$$

If G is multiplied by the moment of inertia, I, the torsional rigidity, B, is defined.

$$\frac{EI_{12}}{2\cdot(1+\upsilon)} = B \tag{3.19}$$

The torsional moment M_{12} can be expressed by product of the torsional rigidity and the curvature κ.

$$[M_{12}] = \left[\frac{EI_{12}}{2\cdot(1+\upsilon)}\right][\kappa_{12}] \tag{3.20}$$

Theories about corrugated plates can be found in *Theories and Application of Plate Analysis*, (Szilards, 2004) where a sinus-shaped corrugated plate is discussed, see Figure 3.17.

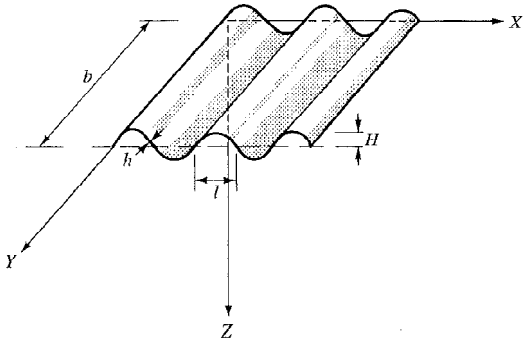

Figure 3.17 A corrugated plate with various quantities, (Szilards, 2004).

According to these theories, the torsional rigidity, B, for this corrugated plate can be estimated from Equation (3.21).

$$B = \frac{s}{l}\frac{E\cdot h^3}{12\cdot(1+\upsilon^2)} \tag{3.21}$$

where

$$S = l\cdot\left(1+\frac{\pi^2\cdot H^2}{4\cdot l^2}\right) \tag{3.22}$$

The value of S is depending on the geometry of the corrugated plate and the quantities are defined in Figure 3.17.

B is equal to the expression of $G\cdot I$ in Equation (3.19) and can be written together with Equation (3.21).

$$\frac{EI_{12}}{2\cdot(1+\upsilon)} = \frac{s}{l}\cdot\frac{E\cdot h^3}{12\cdot(1+\upsilon^2)} \tag{3.23}$$

or again

$$I_{12} = \frac{s}{l}\cdot\frac{h^3}{6\cdot(1-\nu)} \tag{3.24}$$

This expression gives a rough estimation of I_{12}, since the geometry of the sheet pile wall is not sinus-shaped, and the value is used as a starting value for further simulations. To verify this PLAXIS 3D Foundation is used to simulate a wall in 3D, similar to the simulation done in PLAXIS 2D above. In the model, a corrugated wall was built with E-modulus equal to E_{steel}. Deformations are then calculated for a number of fixing cases. The result is compared with similar calculations of a homogenous wall with isotropic geometry and anisotropic properties. The material settings of this wall are taken from previous steps, but the value of I_{12} is adjusted to make the deformations match the deformations of the sheet pile wall. The reason for doing this is to transform the settings of the corrugated sheet pile wall to a homogenous, rectangular wall with anisotropic material properties. The input values will then be used in the parametric study in the soil/structure model. The three dimensional models of the corrugated wall and the equivalent plate is presented in Figure 3.18.

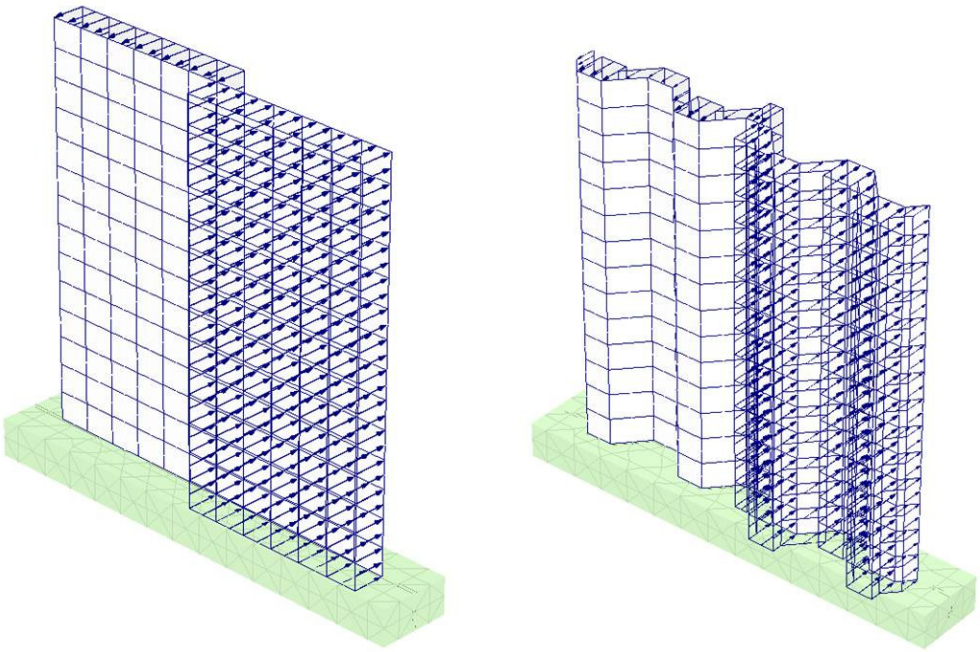

a) *b)*

Figure 3.18. a) The solid wall subjected for a load q, warping the wall.

b) The corrugated wall subjected for the same load.

3.8 Wailing beam settings

The wailing beam is used to distribute the loads induced by the excavation to the surrounding soil. For anisotropic beams, e.g. a HEB-profile, the properties are different in different directions. The properties are often provided by steel manufacturers or can be found in tables. The material properties for beams with elastic behaviour are defined in Table 3.3.

Table 3.3 Material properties for the wailing beam, (Brinkgreve, 2007).

Parameter	Unit	Definition
A	m^2	Beam cross section area
γ	kN/m^3	The unit weight
E	kN/m^2	Young´s modulus in axial direction
I_2	m^4	Moment of inertia against bending around the second axis
I_3	m^4	Moment of inertia against bending around the third axis
I_{23}	m^4	Moment of inertia against oblique bending (zero for symmetric beam profiles)

The stiffness properties and the curvature of the beam visualised in Figure 3.19.

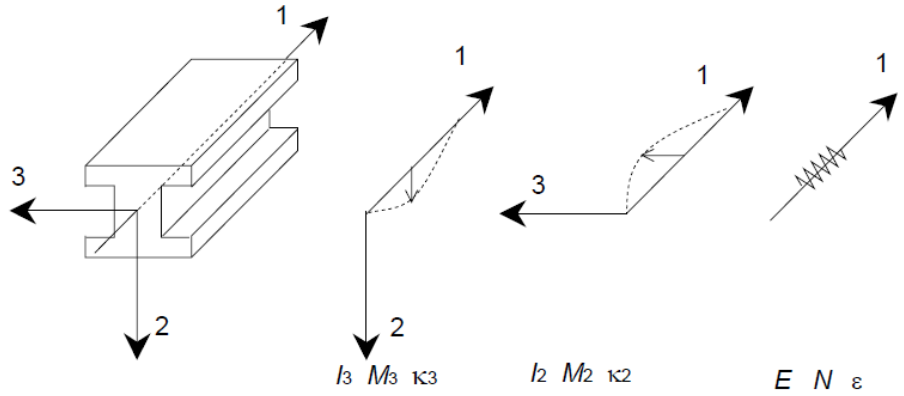

Figure 3.19 The local system of axes in the wall element and various quantities (Brinkgreve, 2007).

The wailing beam is modelled as linear elastic and can therefore never go to failure. The action effects can be determined and used as a design value during Serviceability limit state. For Ultimate limit state design it is possible, as mentioned in *3.1.2*, to receive the action effects on the beam during the stepwise *phi/c reduction* in the soil.

4 Parametric study

The purpose is to investigate which parameters that affect the design of a sheet pile wall used for staged excavation. To do this, a generalized model is used for simulation in PLAXIS 3D Foundation, called the soil/structure model. In this model, the staged excavation is simulated. The parametric study will consist of two base cases. The first case is without a wailing beam and the second is a model with a wailing beam added to the sheet pile wall. All the simulations are done in PLAXIS 3D Foundation Version 2.2 if nothing else is declared.

4.1 Introduction

The configuration for these base cases are presented in this introduction. The two base cases have equal settings besides that the second base case has a wailing beam weld to the upper edge of the sheet pile wall. One parameter at the time is then varied to investigate the influence in the model. All simulations in the soil/structure model are configured with settings according to the base case if nothing else is declared.

4.1.1 Mesh

The geometry of this model is defined in chapter 3.2 and the mesh is generated so that the number of nodes will match Figure 3.6. This resulted in a model with 13367 nodes, see Figure 4.1.

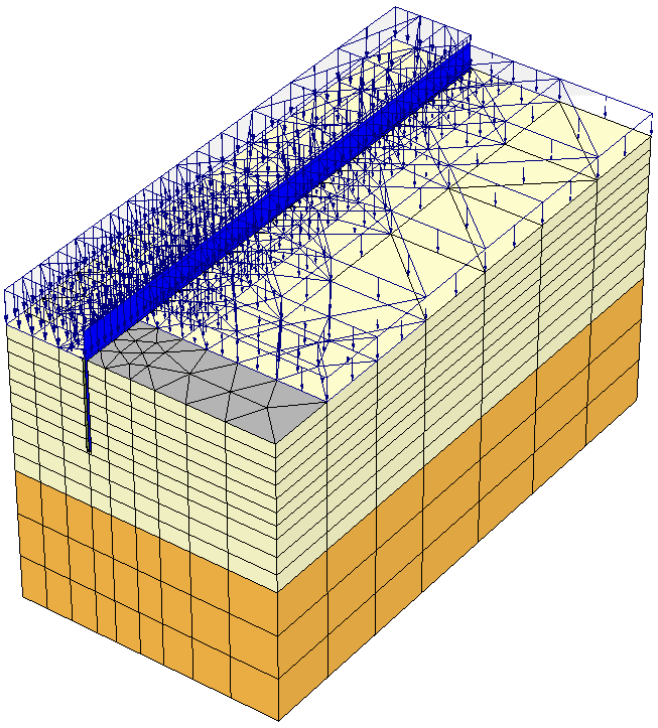

Figure 4.1 The finite element mesh of the model. The excavation area is marked.

Note that the mesh is finer in and around the excavation and along the sheet pile wall. This is because this is the area where most displacements are expected. The vertical mesh is finest at the level of the sheet pile wall, and just below. Chapter 3.5 also shows that a finer mesh will give more deformations. This is why it is important to

have a fine mesh in the excavation, where the deflection of the sheet pile wall has its maximum.

4.1.2 Soil

Values of material parameters are chosen so that the calculations could be valid for as many real case scenarios as possible, with emphasis for areas with similar geotechnical conditions as the Gothenburg area. The soil in the model has been chosen according to the conditions at Göta river valley, specifically at the area around Bohus. As the soils in this area are characterized by relatively soft clays, the strength of the soil is low. The uppermost layer consists of a one meter thick crust of silt. As mentioned earlier, this layer is replaced with an equivalent load, and thereby the effects in this specific layer are excluded in this study. Young´s modulus, E, is depending on the cohesion and is calculated by the empirical relation in Equation (4.1). This relation is equal at all depths in the clay.

$$\frac{E}{c'} = 261\ [kPa] \tag{4.1}$$

The cohesion, $c´$, of the clay is starting at 7 kPa, with an increment according to Figure 4.2, which also shows the E-modulus of the clay.

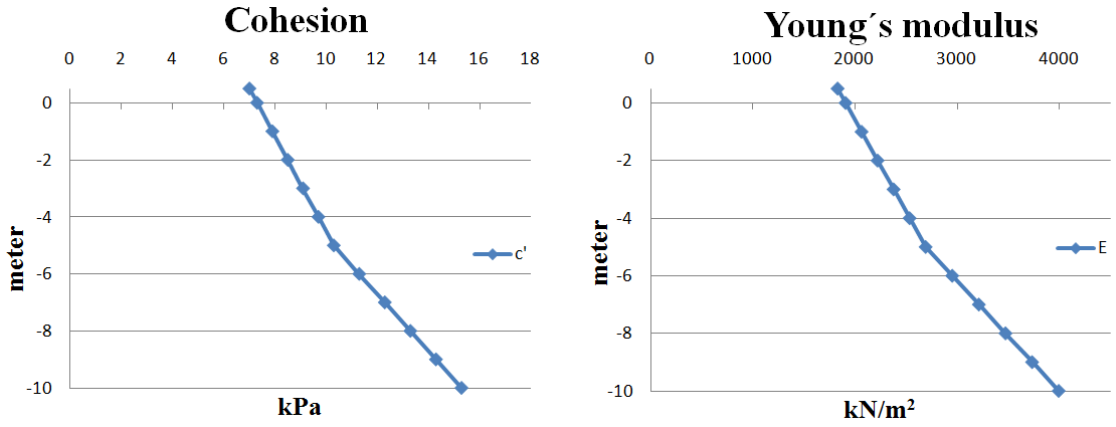

a) *b)*

Figure 4.2 *a) The cohesion, c', used in the model for different levels.*

b) The Young´s modulus, E, used in the model for different levels.

The interaction between the soil and the sheet pile wall is governed by the interface factor in PLAXIS, and is set for every soil type individually. For the clays, the roughness is assumed to be high, giving an interface factor equal to 1. For the top layer with silt, the roughness is much lower. The groundwater level is set to +1,5 meter, corresponding to the ground level. A complete list of the parameters used is shown in Table 4.1.

Table 4.1. Properties of the soil used in the model.

Parameter	Silt at 1,5 to 0,5m	Clay at 0,5 to -5m	Clay at -5 to -10m	Unit
Material type	Drained	Undrained	Undrained	-
$c´$	1	7	10,3	kPa
$c_{increment}$	0	0,6	1	kPa/m
φ	32	0	0	°
E	10000	1827	2691	kPa
$E_{increment}$	0	157	261	kPa/m
υ	0,3	0,3	0,3	–
ψ	0	0	0	°
$\gamma_{saturated}$	22	15,5	16	kN/m^3
$\gamma_{unsaturated}$	19	15,5	16	kN/m^3

4.1.3 Sheet pile wall

To determine required driving depth according to Swedish praxis, *Handbook for design of sheet pile walls* is used, (Ryner et al., 1996). The two dimensional calculation indicates that the sheet pile wall has to be driven to the level -3 meter, giving a wall lengths of 4,5 meter. This is valid for a safety factor of 1,5 if no additional load is acting on the surface. For a additional load of 10 kPa, the safety factor is just above 1,0. The maximum bending moment is 8 kNm/m. The complete calculation is presented in Appendix 1.

The wall chosen for the base case is a sheet pile wall, AU14. This is a relatively stiff wall, and should be able to withstand the stresses induced by the excavation, meaning that a possible failure in the system will be in the soil and not in the sheet pile wall. Specifications of an AU14 are presented in Figure 4.3 and Table 4.2.

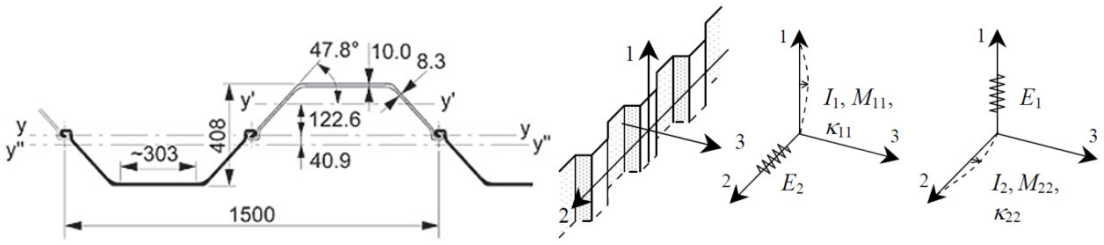

a) *b)*

Figure 4.3 *a) Sheet pile profile AU14 in plan including dimensions (ArcelorMittal, 2010)*
b) The local system of axes in the wall element and various quantities (Brinkgreve, 2007)

Table 4.2 *Technical specifications AU14 (ArcelorMittal, 2010).*

AU14	Sectional area cm^2	Mass/m kg/m	Moment of inertia cm^4	Elastic section modulus cm^3
Per m wall	132.3	103.8	28710	1410

When simulating in PLAXIS, the wall will have isotropic geometry, as the shape of a plate. This plate can however have anisotropic material properties. This means that the properties of the corrugated sheet pile wall must be transformed to an equivalent plate, with a certain thickness, *d*. Manufacturers does usually provide information about flexural rigidity in one dimension only, bending around the second axis. Values of E_1 and G_{13} can be determined according to Equation (4.2) and (4.3), given the moment of inertia and the sectional area from Table 4.2.

$$E_1 = \frac{12 \cdot E_{steel} \cdot I_1}{d^3} = \frac{12 \cdot 210e^9 \cdot 2{,}871e^{-4}}{0{,}01323^3} = 3{,}124 \cdot 10^{11}\ kPa \quad (4.2)$$

$$G_{13} = \frac{E_{steel} \cdot A_{13}}{2 \cdot (1+\upsilon) \cdot d} = \frac{210e^9 \cdot 4{,}41e^{-3}}{2 \cdot (1+o) \cdot 0{,}01323} = 3{,}5 \cdot 10^7 kPa \quad (4.3)$$

To decide the in plane shear modulus G_{12}, the moment of inertia against torsion, I_{12}, must be determined. Also I_1 and I_2 are needed to determine E_1 and E_2. This can be done in a number of ways and it is important to evaluate which value that gives the most realistic response of the sheet pile wall. It is the relation between I_1, I_2 and I_{12} that is of importance and an investigation of these relations is done below.

The PLAXIS user manual (Brinkgreve, 2007) recommends relations according to Alternative 1 in Table 4.3. These values can however be questioned, and this is why it needs to be further analysed. In this case a two dimensional model was created as presented in Section 3.7.2. A corrugated beam was modelled according to the manufacturer specification of the AU14 profile and the maximum deflection for a certain load was calculated. A solid plate was then simulated under the same conditions, with the equivalent values of E_1 and G_{13}. The idea was to make the deformations of the plate to match the deformation of the corrugated beam when

subjected for the same load. The value of I_2 was adjusted until a satisfying result was obtained. For sheet pile wall AU14, I_2 was set to $3{,}8 \cdot 10^{-8}$ m^4. This value is probably much closer the reality than the PLAXIS user manual recommendation.

To estimate the torsional rigidity against warping, I_{12}, needs to be determined. Equation (4.4) was used, based on *Theories and Applications of Plate Analysis*, (Szilards, 2004), described in Section 3.7.

$$I_{12} = \frac{s}{l} \cdot \frac{h^3}{6 \cdot (1-\nu)} = \frac{0{,}89}{0{,}75} \cdot \frac{0{,}009^3}{6 \cdot (1-0)} = 1{,}437 \cdot 10^{-7} m^4 \quad (4.4)$$

This value is used as a starting value when the 3D wall is tested in a PLAXIS 3D Foundation model, also described in Section 3.7, similar to the 2D model. This simulation gives $I_{12} = 4{,}78 \cdot 10^{-8}$ m^4. The difference from calculated values could originate from the fact that the Equation 3.15 is based on a sinus shaped plate, which differs from the shape of the sheet pile wall. These settings are tested in the soil/structure model as Alternative 3 in Table 4.3.

To investigate the behaviour of the sheet pile wall, a number of settings are tested in the soil/structure model. Alternative 2 uses value of I_2 according to the 2D simulation and the value of I_{12} recommended by the manual. Alternative 3 has both I_2 and I_{12} according to the simulations in PLAXIS 2D and 3D Foundation respectively. Alternative 4 has the same I_2 as Alternative 3, but a higher torsional rigidity against warping, I_{12}. For Alternative 5, the sheet pile wall properties are isotropic, which was the only available option in PLAXIS 3D Tunnel. These values are presented in Table 4.3. To simplify the comparison, the relation to I_1 is also presented within brackets in the table. The results from simulations with these values are plotted in Figure 4.4 and Figure 4.5.

Table 4.3. Properties of different sheet pile walls tested in the soil/structure model. Flexural rigidity is depending on the internal moments of inertia in different directions, which are presented. Relations to I_1 within brackets.

Alt	I_1 [m^4]	I_2 [m^4]	I_{12} [m^4]	
1	$2{,}871 \cdot 10^{-4}$	$1{,}436 \cdot 10^{-5}$ (I_1/20)	$2{,}871 \cdot 10^{-5}$ (I_1/10)	PLAXIS manual recommendations
2	$2{,}871 \cdot 10^{-4}$	$3{,}811 \cdot 10^{-8}$ (I_1/7533)	$2{,}871 \cdot 10^{-5}$ (I_1/10)	I_2 from PLAXIS 2D simulations
3	$2{,}871 \cdot 10^{-4}$	$3{,}811 \cdot 10^{-8}$ (I_1/7533)	$2{,}871 \cdot 10^{-7}$ (I_1/1000)	I_1, I_2 from PLAXIS 3D simulations
4	$2{,}871 \cdot 10^{-4}$	$3{,}811 \cdot 10^{-8}$ (I_1/7533)	$2{,}871 \cdot 10^{-6}$ (I_1/100)	I_{12} adjusted
5	$2{,}871 \cdot 10^{-4}$	$2{,}871 \cdot 10^{-4}$ (I_1/1)	$2{,}871 \cdot 10^{-4}$ (I_1/1)	Isotropic

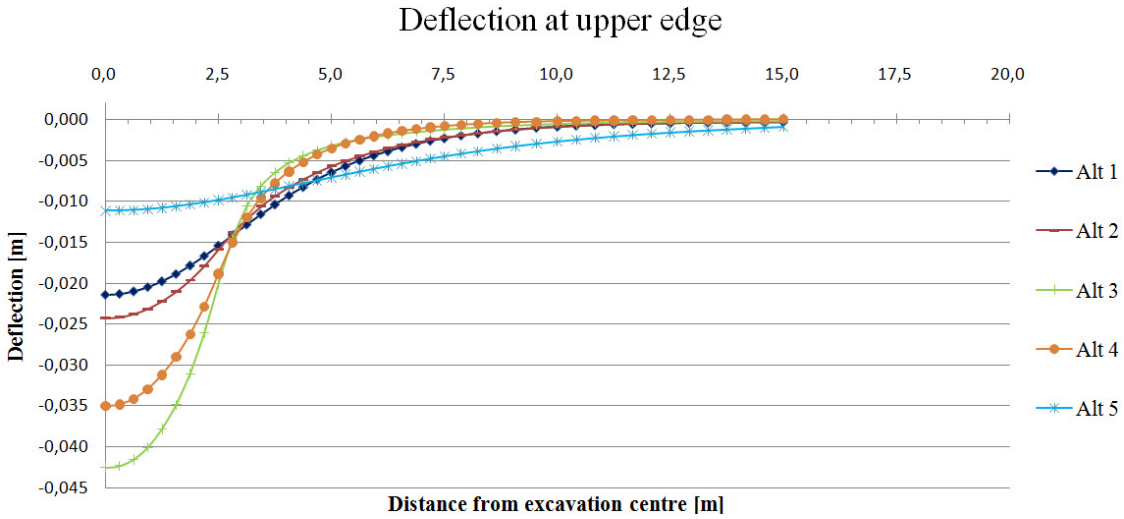

Figure 4.4 *The horizontal deflection at the upper edge of the sheet pile wall at different lengths from excavation centre. No wailing beam is used. Five wall settings are tested with different relations between the moments of inertia I_1, I_2 and the torsional rigidity against warping, I_{12}.*

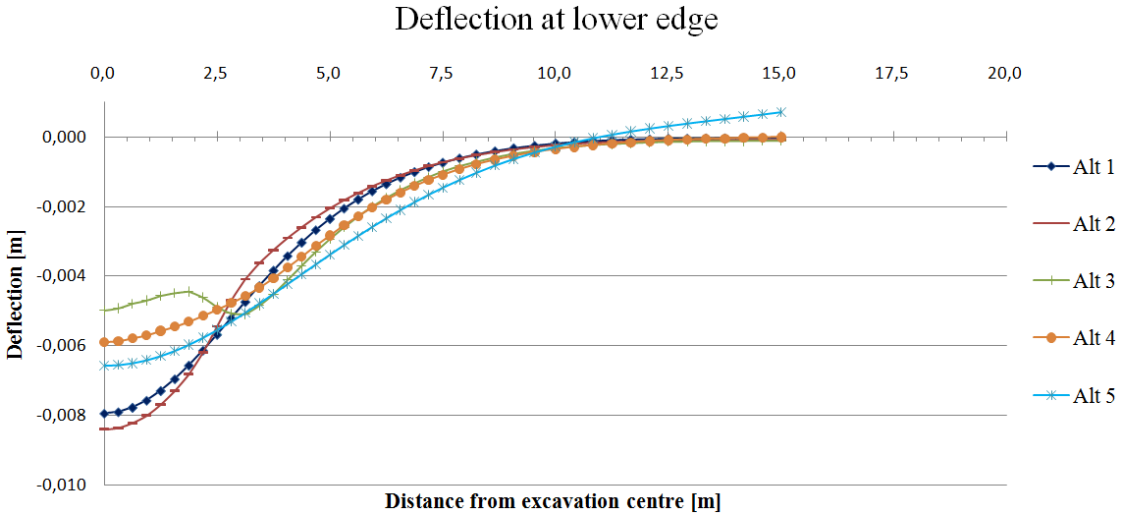

Figure 4.5 *The horizontal deflection at the upper edge of the sheet pile wall at different lengths from excavation centre. No wailing beam is used. Five wall settings are tested with different relations between the moments of inertia I_1, I_2 and the torsional rigidity against warping, I_{12}.*

The result shows that the recommended values from the PLAXIS user manual, Alternative 1, give a wall that is too stiff. This is also the case for Alternative 2 and 5. Alternative 3 was before the simulation the case that seemed most realistic, but looking at the deflections at the lower edge, this might not be the real behaviour of the wall. Instead, Alternative 4 gives the most realistic behaviour, with almost as large deflections at the top as Alternative 3, but with a smoother curve at the lower edge.

Two extreme cases were simulated in order to evaluate how much influence the sheet pile wall properties have. They were based on the input parameters in Alternative 4, but were adjusted according to the assumption that flexural rigidity around the vertical axis is close to zero. This means that slide and angle displacements in the interlocks are possible. In the first case, G_{23} was set to one. This resulted in a maximum

deflection of 41 mm at the upper edge of the sheet pile wall. At the lower edge, the behaviour was equal to the simulation of Alternative 3, i.e. an unrealistic curvature. In the second extreme case, E_2 was set equal to one. The maximum deflection was equal to the result from Alternative 4, i.e. 35 mm, but the behaviour was, as in previous case, unrealistic at the lower edge. This means that the behaviour of the chosen sheet pile wall is very similar to the extreme case.

The relations from Alternative 4 are from now on considered as a base case and are to be used later on in this thesis. A complete presentation of the material properties used in Alternative 4 is presented in Table 4.4. The values are calculated from given equations is Section 3.7 and with an equivalent thickness, d = 0,408.

Table 4.4 Material setting for the sheet pile wall AU14 used in PLAXIS.

Property	Value	Unit
d	0,408	m
E_1	$1{,}065 \cdot 10^7$	kPa
E_2	$1{,}414 \cdot 10^3$	kPa
G_{12}	$5{,}326 \cdot 10^4$	kPa
G_{13}	$1{,}135 \cdot 10^6$	kPa
G_{23}	$3{,}405 \cdot 10^5$	kPa

4.1.4 Wailing beam

The wailing beam used on site at contract E33 is a HEB300. This is a relatively stiff beam. In Ultimate limit state it probably would have been enough with a weaker beam, but since it was the deformations in Serviceability limit state that was of most concern this stiffer beam was chosen. Specifications of a HEB300 can be found in tables provided by steel manufacturer and the properties used in PLAXIS are presented in Table 4.5.

Table 4.5 The material setting for the wailing beam HEB300.

Parameter	Value	Unit
A	0,015	m^2
E	$2{,}1 \cdot 10^8$	kPa
I_3	$8{,}563 \cdot 10^{-5}$	m^4
I_2	$2{,}517 \cdot 10^{-4}$	m^4
I_{23}	0	m^4

4.1.5 Load

In the base case, an additional load is added on the active side of the sheet pile wall. The size of this load is 10 kPa, which could correspond to a normal surface load from construction traffic.

4.1.6 Excavation

A staged excavation is made in the length of the sheet pile wall, and is in the base case 5 meter wide and 1 meter deep. The complete excavation geometry is presented in Figure 4.6.

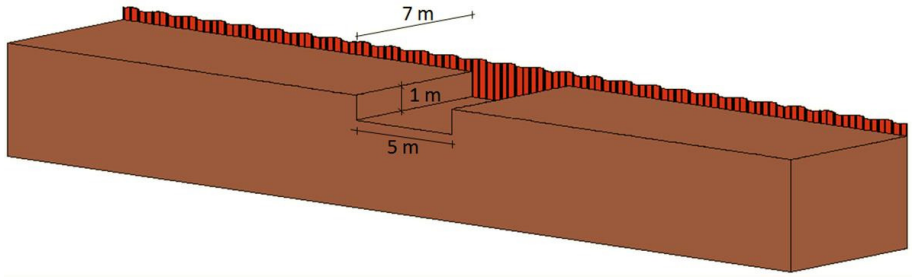

Figure 4.6 Geometry of the excavation.

4.2 Base case without wailing beam

Simulation of the deflections of the sheet pile wall in the model defined above is resulting in the deflection pattern shown in Figure 4.7.

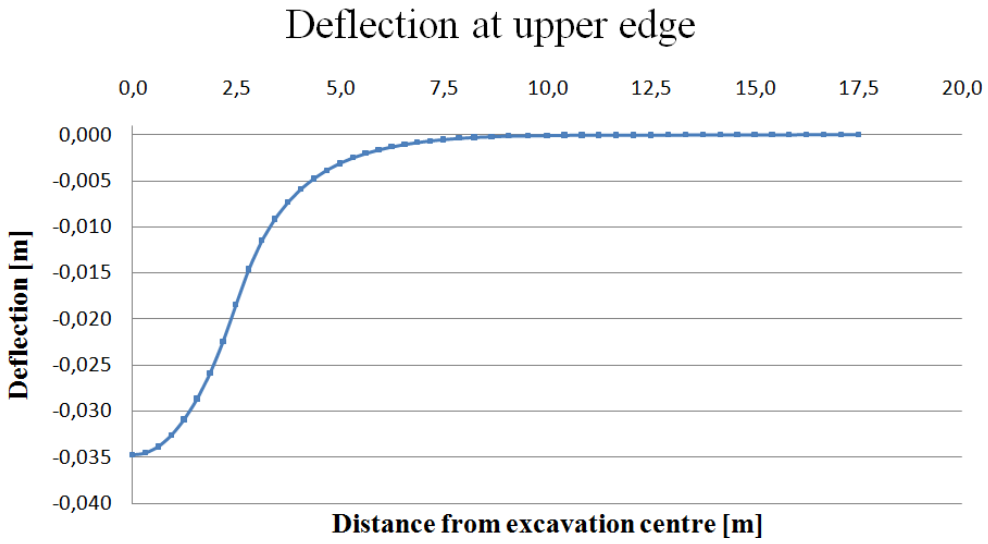

Figure 4.7 Horizontal deflection of the sheet pile wall at the upper edge.

The maximum deflection is 35 mm. The influence distance is 5 meter outside the excavation, i.e. 7,5 meter from the excavation centre. Beyond this point the sheet pile wall is unaffected by the excavation.

Starting from the base case, the parameters in this model are varied. The parameters are chosen according to what may influence the deformations and the safety factor.

The complete analysis is described in this section. An overview of the parameters that are to be studied is presented in Table 4.6.

Table 4.6 Parameters that are to be studied in this chapter and a short description of the purpose of each simulation.

Parameter	Question formulation
Crest length	What is the influence distance in the sheet pile wall? How long must the wall be outside the excavation?
Excavation width	How will the deflection pattern change when simulating different widths of the excavation?
E-modulus of the soil	What is the effect of the E-modulus of the soil?
Linear Elastic soil model	Will the result from a linear-elastic soil model considerably differ from the Mohr-Coulomb model?
Weaker sheet pile wall	What is the effect when using a weaker sheet pile wall? The chosen profile is a PU8R.

4.2.1 Crest length of the sheet pile wall

A fundamental question when designing a sheet pile wall is how long the wall must be extended outside the excavation, both in economical and geotechnical aspects. To investigate this, a number of sheet pile walls are simulated, each with different crest lengths. The definition of the sheet pile wall´s crest length is illustrated in Figure 4.8. When using the term crest length further on, the length is always measured from the excavation centre.

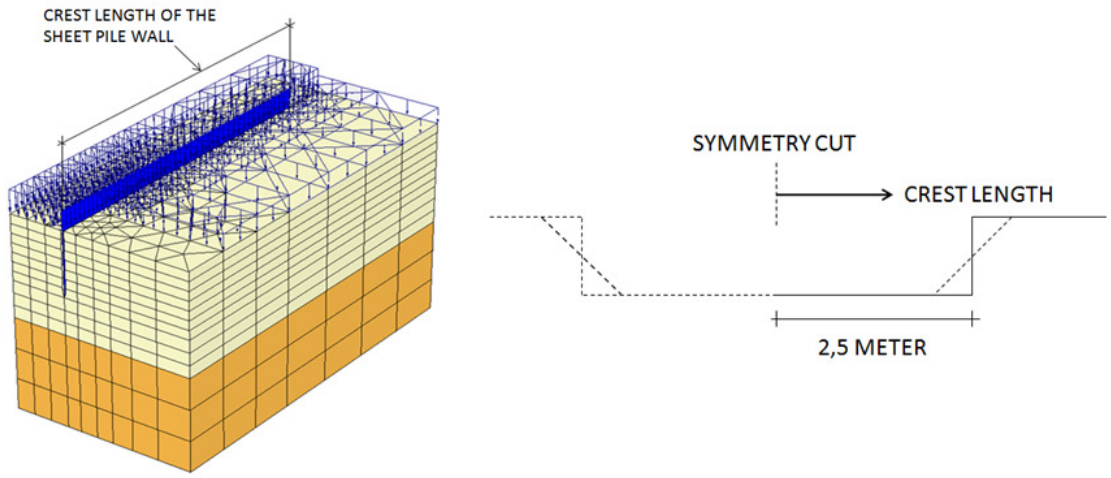

Figure 4.8 Definition of the crest length of the sheet pile wall.

A number of simulations are done, each with different crest lengths of the sheet pile wall. The deflections are then plotted and compared. The purpose is to determine how long the wall must be in order to get a satisfying deflection and get an acceptable safety factor. Results regarding deflections, bending moments and shear forces in the sheet pile wall can be analyzed and the soil behavior in different phases can evaluated regarding deformations and stresses. The results from the simulations are shown in Figure 4.9 and Figure 4.10. The horizontal deflection of the sheet pile wall is plotted at the upper edge, at level 1,5 meter, and at the lower edge, at -3 meter. Note that the sheet pile wall is seen from above.

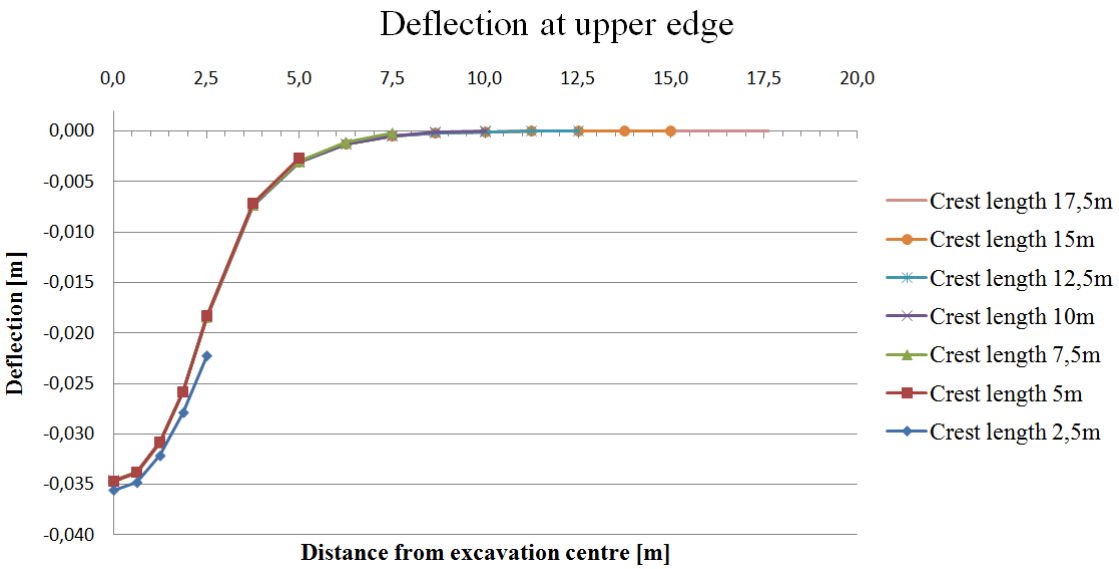

Figure 4.9 *The horizontal deflection at the upper edge of the sheet pile wall. Maximum deflection is 36 mm for the crest length 2,5 meter and 35 mm for crest lengths over 2,5 meter.*

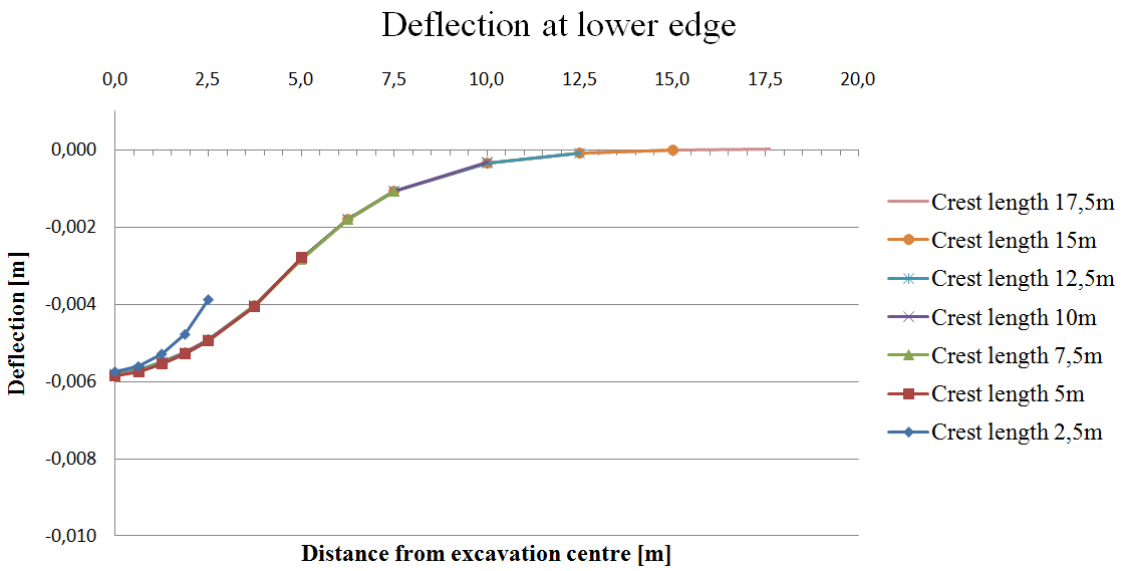

Figure 4.10 The horizontal deflection at the lower edge of the sheet pile. Maximum deflection for all crest length is 6 mm. Note that the scale differs from Figure 4.9.

The figure shows that the deflection curves follow the same pattern regardless how long the crest length is. Because of this, the deflection curves in Figure 4.9 and Figure 4.10 are stapled on each other. This is valid for all curves accept crest length 2,5 meter. The maximum deflection of the sheet pile wall longer than 2,5 meter is 35 mm in the upper edge and 6 mm in the lower. When the crest length is 2,5 meter, i.e. equal to the excavation length, the horizontal deflection gets larger in the upper edge of the sheet pile wall compared with the other crest length simulations. That can be explained by the fact that the sheet pile wall does not get as much support from the soil outside the excavation, when the crest length is 2,5 meter. The mechanical behaviour of the sheet pile wall with crest lengths longer than 2,5 meter has the same shape and the same maximum deflection. This means that the crest length can be relatively short to full fill the criteria's in Serviceability limit state. As long as the sheet pile wall can transfer the induced stresses to the soil, it fulfils its purpose regarding the deformations. For crest lengths from 7,5 meter, the deflection flattens out, and is close to zero, which could be seen as the influence distance. Outside this area the soil is unaffected.

The bending moments in the sheet pile wall are defined in Figure 4.11.

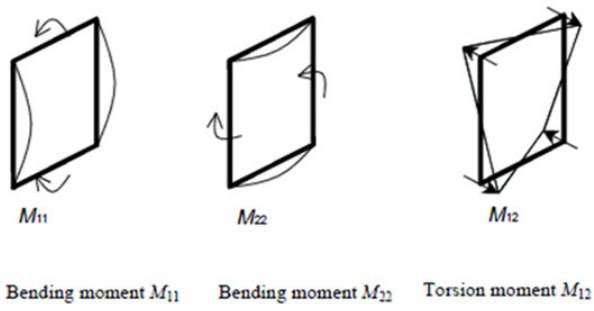

Figure 4.11 Definition of the bending moments M_{11}, M_{22} and the torsional moment M_{12}, (Brinkgreve, 2007)

The bending moment M_{11}, plotted in PLAXIS, is illustrated in Figure 4.12. The plot is from the simulation with 17,5 meter crest length and seen from the same side as the excavation pit.

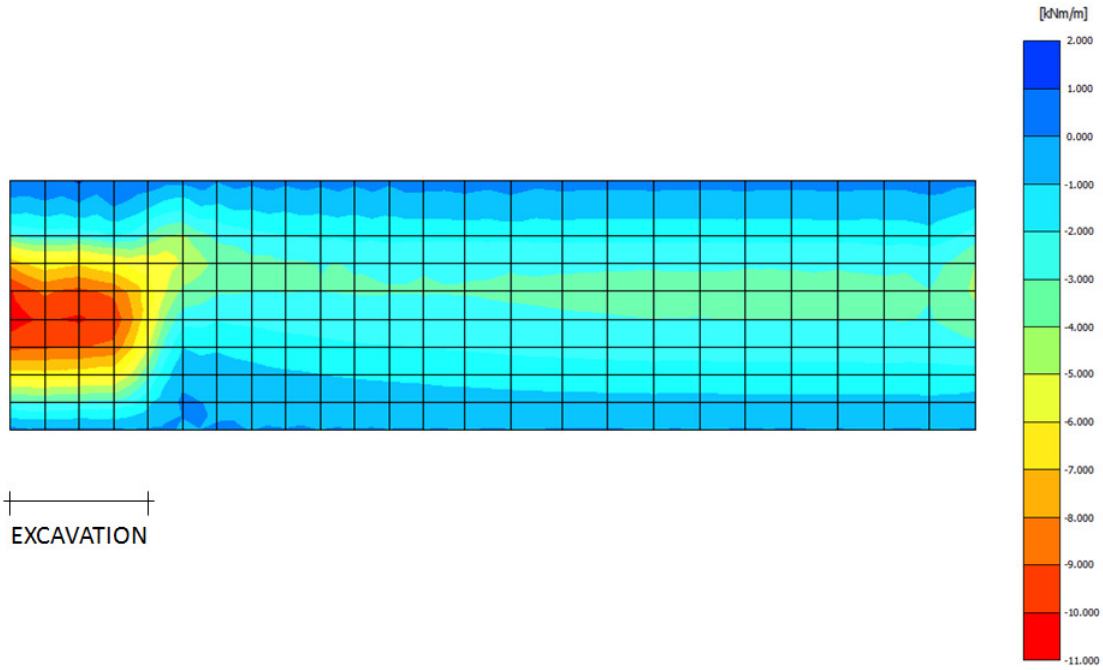

Figure 4.12 Bending moment, M11, at crest length 17,5 meter seen from the excavation side.

The maximum value of the bending moments M_{11}, M_{22} and the torsional moment M_{22} for the sheet pile wall with a crest length of 2,5 meter is presented in Table 4.7. Note that negative value is defined as out of plane, i.e. against the excavation pit.

Table 4.7 Maximum bending and torsional moments for crest length 2,5 meter.

Bending moment	M_{11}	M_{22}	M_{12}
M_{max} [kNm/m]	-23,0	$-70{,}0*10^{-3}$	1,5

For crest lengths from 5 to 20 meter the maximum moments are equal to each other and occur at same place in the sheet pile wall, see Table 4.8. Note that negative value is defined as out of plane, i.e. against the excavation pit.

Table 4.8 Maximum bending and torsional moments for crest lengths from 5 to 20 meter

Bending moment	M_{11}	M_{22}	M_{12}
M_{max} [kNm/m]	-11,0	$-70{,}0*10^{-3}$	-1,9

The design value of the moment capacity for bending around the second axis for a sheet pile wall is defined by Equation (4.5).

$$M_{Rxd} = \frac{W_x \cdot f_{yc}}{\gamma_m \cdot \gamma_n} \tag{4.5}$$

where W_x is the elastic section modulus and f_{yc} is the characteristic value of the steel quality of the sheet pile wall. The partial factors γ_m and γ_n is set to 1,0 and 1,2 respectively. For an AU14 profile with a steel quality of S270 GP the characteristic strength, f_{yc} , is 270 MPa and the elastic section modulus, W_x, is 1410 cm^3 per meter wall. The design value of the moment capacity is calculated in Equation (4.6).

$$M_{Rd} = \frac{(1{,}41\times10^{-3})\cdot(270\times10^{3})}{1{,}0\cdot1{,}2} = 317 kNm/m \tag{4.6}$$

Required profile in this case can be much weaker than the AU14 profile. After each phase of different crest length follows a *phi/c reduction* in order to determine the factor of safety in the soil. The results are presented in Figure 4.13.

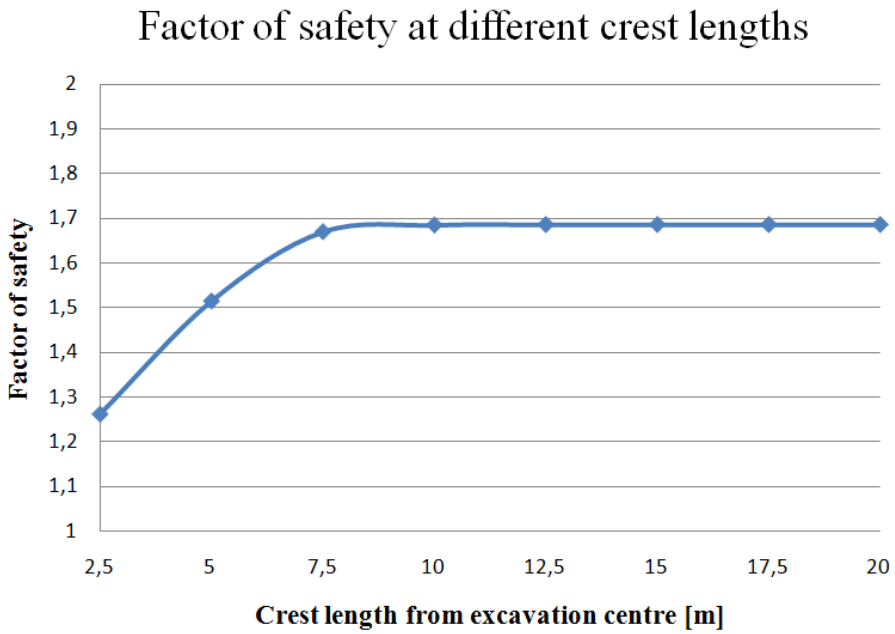

Figure 4.13 Factor of safety of the soil at different crest lengths.

The factor of safety is increasing until the crest length of the sheet pile wall reach 7,5 meter from the excavation centre, where the curve flatten out. This can be compared with influence area of the deflection that flatten out at 7,5 meter from the excavation centre and verifies that there is no impact on the surrounding soil outside this boundary. It should be clarified that the factor of safety only concerning the soil and not the sheet pile wall. The sheet pile wall is simulated with linear elastic behavior, i.e. it is not possible for the sheet pile wall to go to failure.

4.2.2 Excavation width

When the excavation length along the sheet pile wall is varied the deflection in the centre is affected. To investigate how large this effect is, and if the influence distance outside the excavation is affected, a number of different excavation lengths is tested in the model. This is then compared to the base case. A simulation equivalent to a 2D model is also performed, where no side effects are included. Here, the excavation is made along the entire sheet pile wall. This corresponds to a simulation made in PLAXIS 2D, which also is performed. Simulating with the same input values for the 2D model as in the 3D model, the result shows good correlation, verifying the accuracy. The displacement in the 2D model is also the value to which the displacement is approaching when increasing the excavation width in the 3D model. Excavations are made with 2,5, 5, 8 and 15 meter width respectively. The results are presented in Figure 4.14.

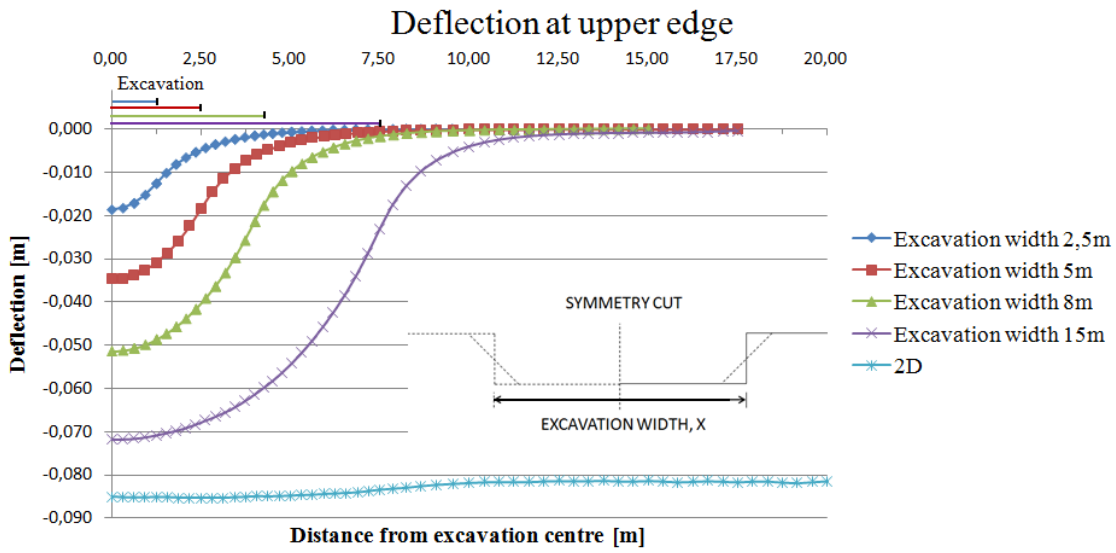

Figure 4.14 The horizontal deflection pattern for four different excavation lengths. The horizontal lines shows where the different excavations end.

The horizontal lines above the deflection curves mark the excavation width. For the curve in the 2D case, the deflection is not exactly the same along the sheet pile wall. The reason for this is that the mesh is made finer in and just around the excavation since this is the area of most concern. This makes the deflection larger to the left in Figure 4.14.

4.2.3 Variation of E-modulus in the soil

The effect of decrease and increase the properties related to the stiffness in the sheet pile wall has shown relatively large differences in magnitude of the deformations.

In order to evaluate the influence of the clay properties, a variation of the E-modulus is done. In the first simulation the E-modulus is divided by a factor two and in the second it is multiplied by the same factor. The result is compared to the simulation done with the soil parameters used in the base case. The input properties are presented in Table 4.9 and

Table 4.10. Note that only the E-modulus and its increment by depth in the clay are changed in the different simulation.

Table 4.9 Values of halved E-modulus during the simulation

	Clay at level +0,5 to -5	Clay at level -5 to -10
E [kPa]	914,0	1345,0
$E_{increment}$ [kPa/m]	79,0	131

Table 4.10 Values of doubled E-modulus during the simulation

	Clay at level +0,5 to -5	Clay at level -5 to -10
E [kPa]	3654,0	5381,0
$E_{increment}$ [kPa/m]	314,0	522,0

The simulations were done with a crest length of 15 meter and the result is presented in Figure 4.15 and illustrates the deflection of the upper edge of the sheet pile wall.

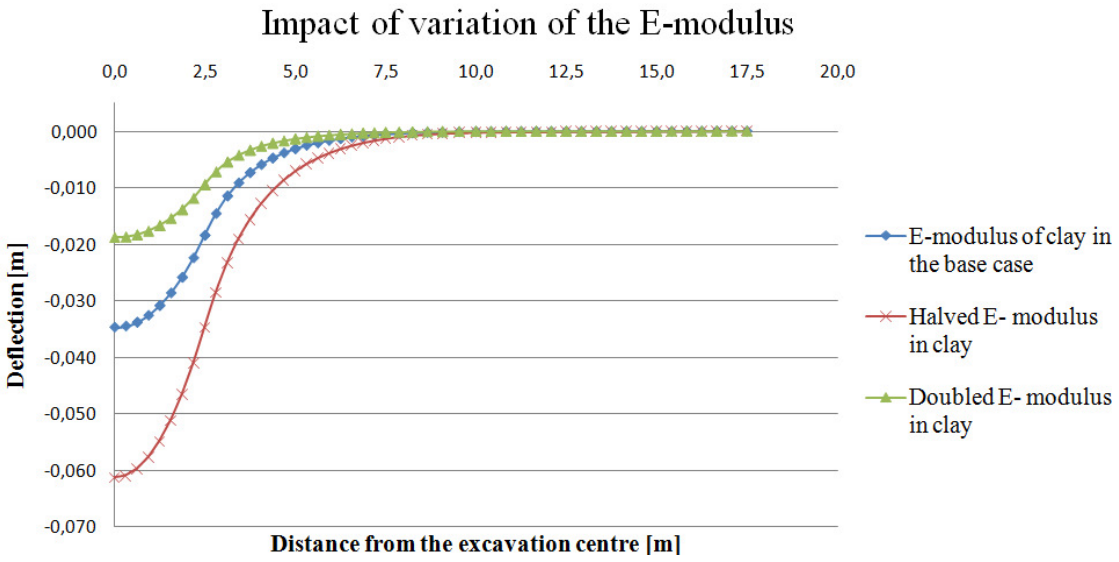

Figure 4.15 The horizontal deflection at the upper edge of the sheet pile wall when simulate with different E-modulus in the clay.

The result verifies clearly that the deflection of the sheet pile wall differs when E-modulus of the clay is changed. In the case where the E-modulus in the clay was halved, the deflection was increased by approximately a factor two compared with the base case. The deflection was decreased by about a factor two in the simulation where the E-modulus was doubled. If the stiffness in the soil increases, the sheet pile wall will be exposed by lower stress. In the same way, when lowering the E-modulus of the soil, the sheet pile wall will take up more stresses and thereby increase the influence distance.

4.2.4 Linear- Elastic soil model

The soil is, as described in Section 3.6, simulated with the *Mohr-Coulomb model* in the base case. This is one of the most frequently used soil models and is a linear elastic, perfectly-plastic model. This means that the material is behaving ideal elastic until all the shear strength has been mobilized. When the plastic state is reached in a soil element, plastic deformations occur. Stresses are also redistributed to other soil elements until a new equilibrium state is found. The total strain consists of a plastic and an elastic part, which is shown in Equation (4.7).

$$\varepsilon^{tot} = \varepsilon^{e} + \varepsilon^{p} \tag{4.7}$$

For a simulation in PLAXIS, the points where plastic deformations exist can be plotted, as shown in Figure 4.16.

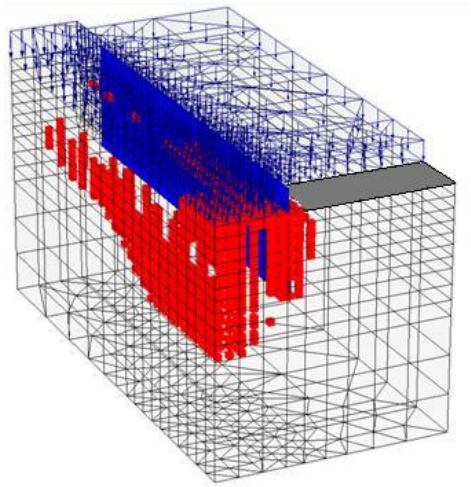

Figure 4.16 View of a 3D model, the red points show where the plastic deformations occur.

According to Figure 4.16, plastic deformations occur in many points, especially in the area around the excavation. To investigate how large these deformations are, the soil model is changed to *Linear- Elastic*. In this soil model, only elastic deformations are possible. The result from this calculation is shown in Figure 4.17.

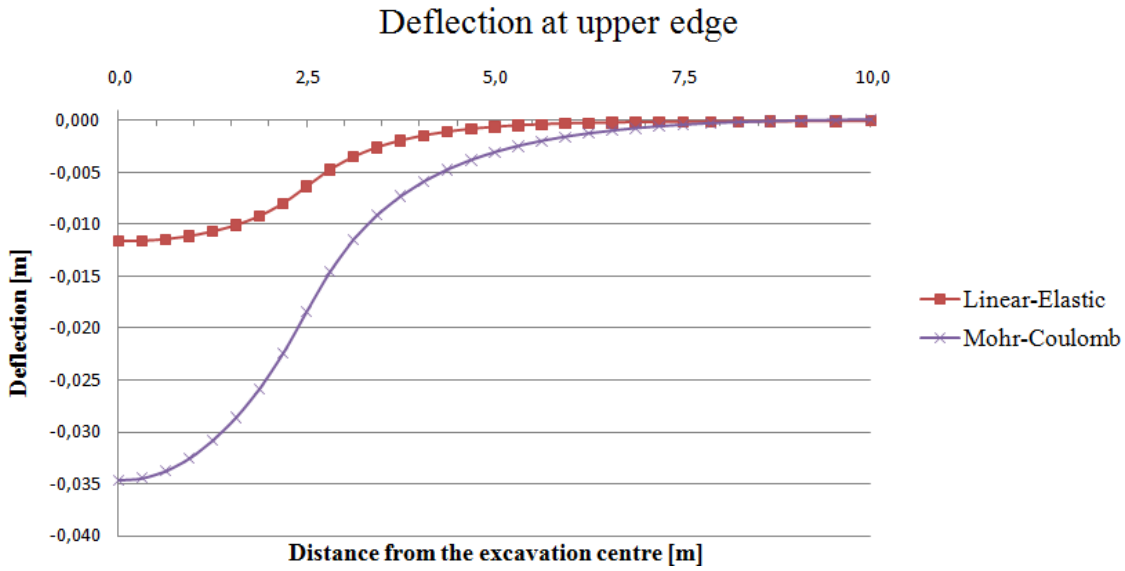

Figure 4.17 Horizontal deflection from Linear-Elastic model compared to Mohr-Coulomb model.

The plastic deformations are the difference between the *Mohr-Coulomb* deformations and the *Linear-elastic* deformations. The figure shows that most of the deformations, 66 %, are plastic which indicates that the soil body is highly stressed.

4.2.5 Simulation with a weaker sheet pile wall

In order to evaluate the effect of a weaker sheet pile wall, the profile AU14 is replaced by a PU8R profile. Due to the fact that the properties of the sheet pile wall was complicated to estimate, a relation between the moment of inertia, I_1, for AU14 and PU8R made a base which decided the properties of the PU8R profile. The relation is given in Equation (4.8).

$$\frac{I_{1,AU14}}{I_{1,PU8R}} = \frac{28710\ [cm^4/m]}{10830\ [cm^4/m]} = 2{,}65 \tag{4.8}$$

The input properties from AU14, except the equivalent thickness, are divided with the factor 2,65 which can be seen as a rough estimation. The purpose of the simulation is to analyze the effect of a sheet pile wall with weaker properties concerning the deflection of the sheet pile wall. The properties of the sheet pile profile PU8R is presented in Table 4.11.

Table 4.11 Material properties for a PU8R profile.

Property	Value	Unit
d	0,408	m
E_1	$4{,}02 \cdot 10^6$	kPa
E_2	533,60	kPa
G_{12}	$2{,}01 \cdot 10^4$	kPa
G_{13}	$4{,}283 \cdot 10^5$	kPa
G_{23}	$1{,}285 \cdot 10^5$	kPa

The result is compared with simulation of the sheet pile profile AU14 concerning the deflections. The shape of the deflection of the PU8R is equal for crest length from 5 to 20 meter from the excavation centre. This was also the case in the simulation of AU14 profile. A comparison will therefore be done at the crest length 17,5 meter from the excavation centre. The result is presented in Figure 4.18 for deflections at the upper edge and Figure 4.19 at the lower edge. Note the scale in both figures.

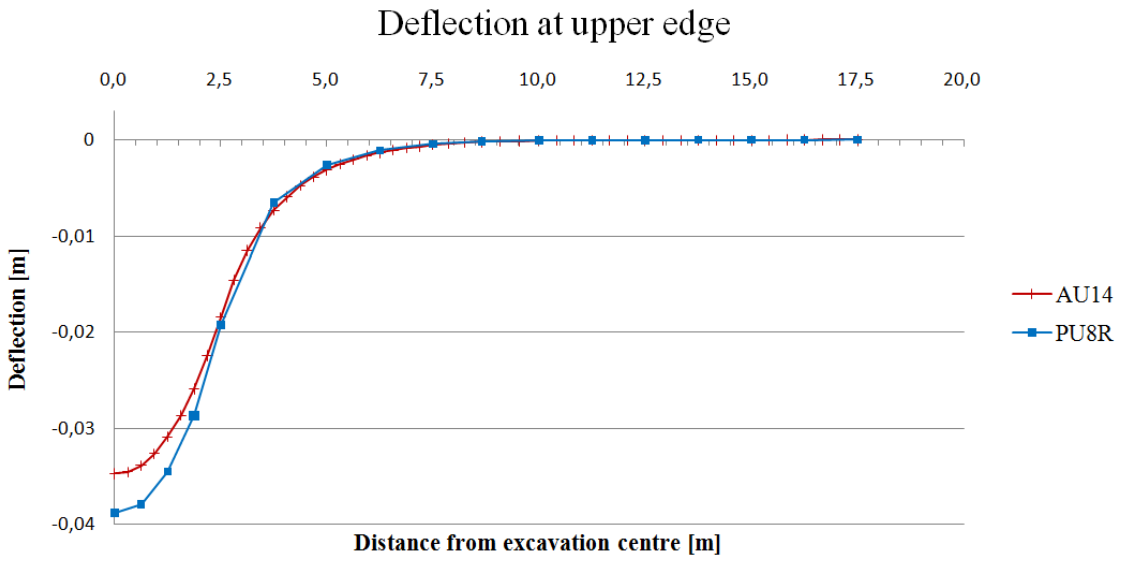

Figure 4.18 Horizontal deflection of the sheet pile profile PU8R at the upper edge compared to AU14.

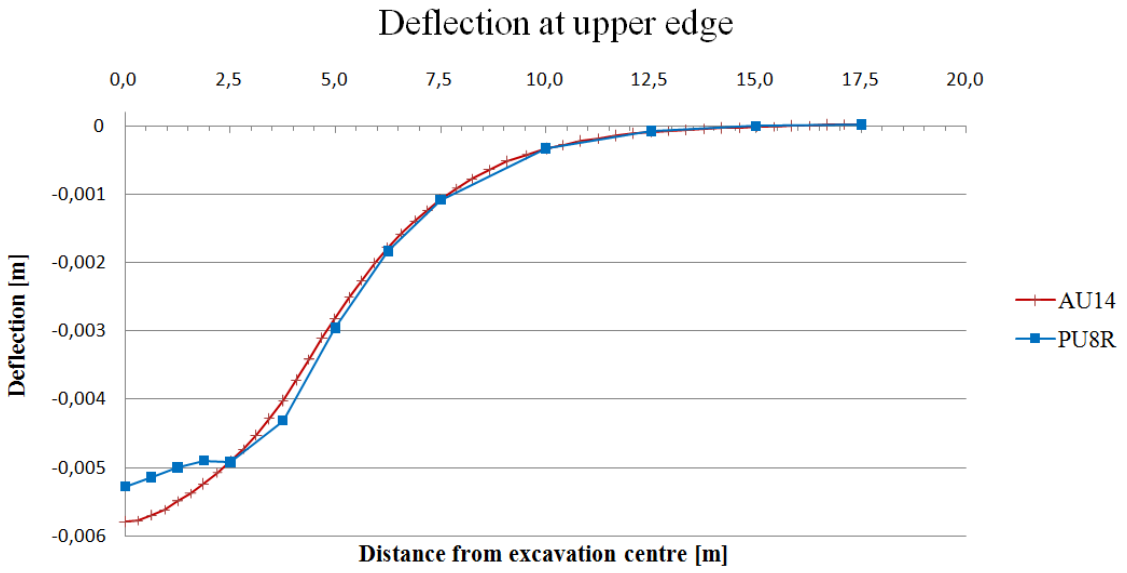

Figure 4.19 Horizontal deflection of the sheet pile profile PU8R at the lower edge compared to AU14.

According to the results, the properties of the sheet pile wall seem not to affect the deflection in a larger magnitude when reducing the properties with a relatively low factor. This can be compared with the simulations of different sheet pile wall properties in chapter 3.7. The maximum deflection at the upper edge of the PU8R profile is 39 mm in the excavation centre compared to 35 millimeter for the AU14 profile. At the lower edge the shape of the sheet pile wall is similar to the simulation of Alternative 3 in Section 0 and might not be the real behaviour of the wall. The influence distance is equal for both sheet pile wall profiles, i.e. 7,5 meter from the excavation centre.

The design value of the moment capacity around the second axis for a PU8R with the steel quality S270 GP is 174 kNm per meter of wall. The bending moments and torsional moment in the sheet pile wall is defined in Figure 4.20.

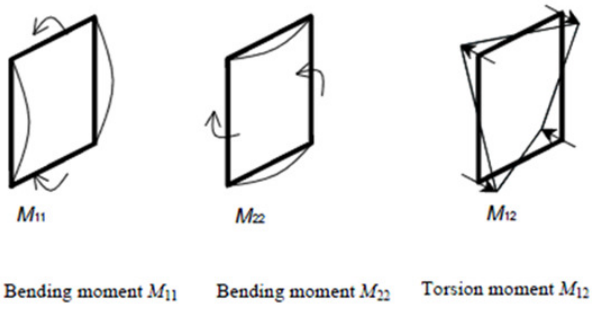

Figure 4.20 Definition of bending moments M_{11}, M_{22} and the torsional moment M_{12}, (Brinkgreve, 2007).

The maximum bending moments and the torsional moment that the sheet pile wall is exposed for in current simulation is presented in Table 4.12 and Table 4.13.

Table 4.12 Maximum bending and torsional moments for crest length 2,5 meter.

Bending moment	M_{11}	M_{22}	M_{12}
M_{max} [kNm/m]	-17,0	$-70{,}0*10^{-3}$	1,5

Table 4.13 Maximum bending and torsional moments for crest lengths from 5 to 17,5 meter.

Bending moment	M_{11}	M_{22}	M_{12}
M_{max} [kNm/m]	-12,0	$-41{,}0*10^{-3}$	1,2

Weaker profiles than PU8R could be used and still have acceptable deformations, for a additional load of 10 kPa and when the excavation depth is relatively shallow. As for the AU14 profile, the low value of the bending moment M_{22} can be explained by the fact that the sheet pile wall is very weak in this direction and cannot take moments of a high magnitude.

The factor of safety in the simulation with PU8R at different crest lengths are compared with the results from the simulations with AU14 and presented in Figure 4.21. Note that the factor of safety concerns the soil, not the sheet pile wall.

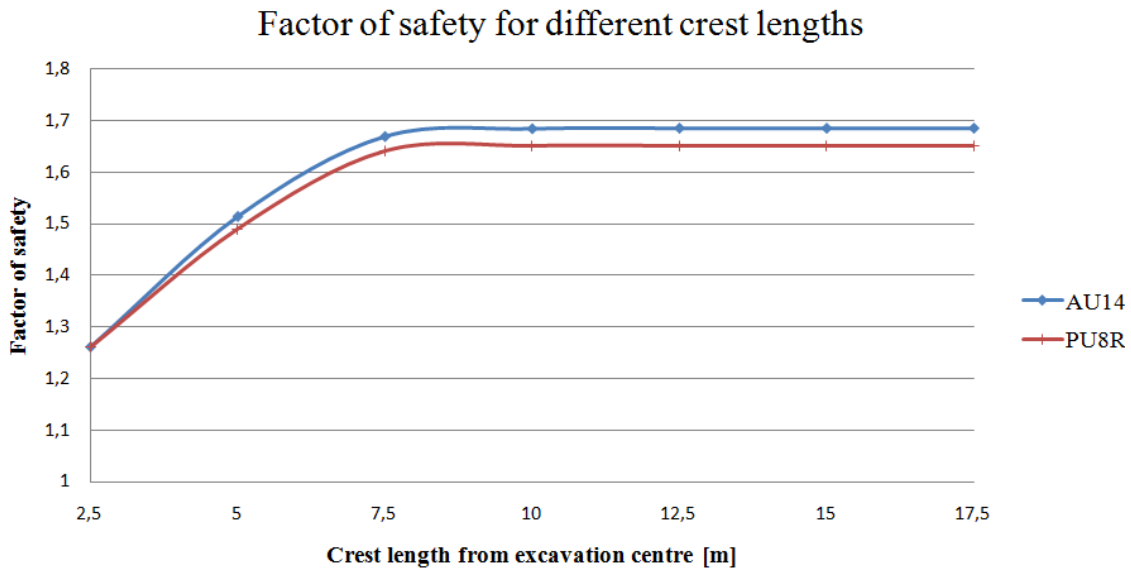

Figure 4.21 Factor of safety for soil at crest lengths 2,5 to 17,5 meter outside the excavation centre.

The factor of safety is equal for PU8R and AU14 at crest length 2,5 meter. This can be explained by the fact that the sheet pile wall is exposed for less side effects from the surrounding soil, compared to crest lengths longer than the excavation width. Also the differences between the two sheet pile profiles are relatively small concerning the safety factor. For the other crest lengths, 5 to 17,5 meter, the AU14 profile can distribute more forces laterally than the PU8R profile why the safety factor of the soil is lower when simulating with the PU8R profile.

4.3 Base case with wailing beam

The purpose by adding a wailing beam to the sheet pile wall is to decrease the maximum deflection at the centre of the excavation. It is hard to predict which effect the wailing beam will have when adding it to the sheet pile wall, why simulations in PLAXIS are done.

The wailing beam is welded at the upper edge of the wall, at level +1,5 meter. The profile of the wailing beam is a HEB300, which is the beam used on site at the project at contract E33. The input parameters in PLAXIS for a HEB300 are presented in Table 4.14. I_{23} defines the moment of inertia against oblique bending and is zero for symmetric beam profiles.

Table 4.14 Material parameters for HEB300

Parameter	Unit	Value
A	m^2	0,015
E	kPa	$2{,}1 \cdot 10^8$
I_3	m^4	$8{,}563 \cdot 10^{-5}$
I_2	m^4	$2{,}517 \cdot 10^{-5}$
I_{23}	m^4	0

Simulation of the model resulted in the deflection pattern presented in Figure 4.22.

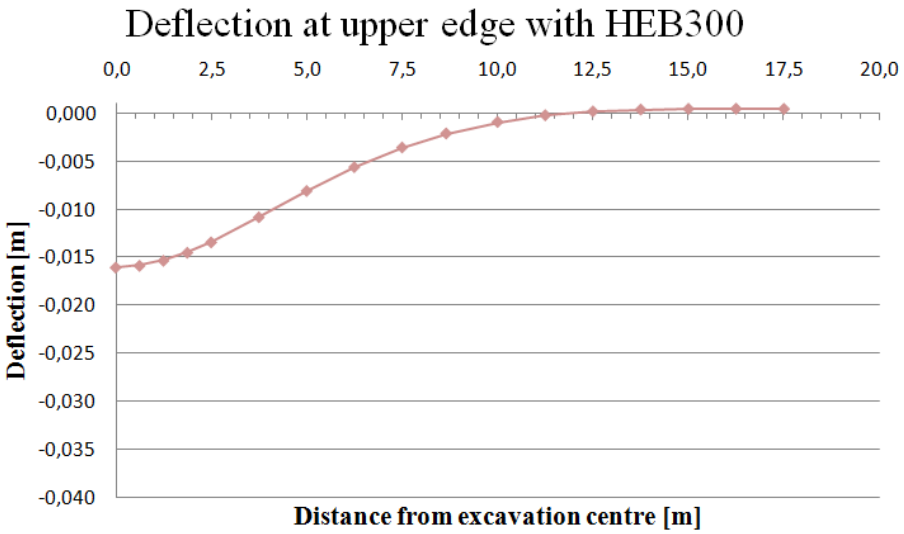

Figure 4.22 Horizontal deflection at the upper edge of the sheet pile wall with a wailing beam.

The maximum deflection is 16 mm and the influence distance is 10 meter outside the excavation centre.

In Figure 4.23 the deflection with and without wailing beam is compared. The plot shows the deform pattern for the entire sheet pile wall, in a symmetry cut in the excavation centre.

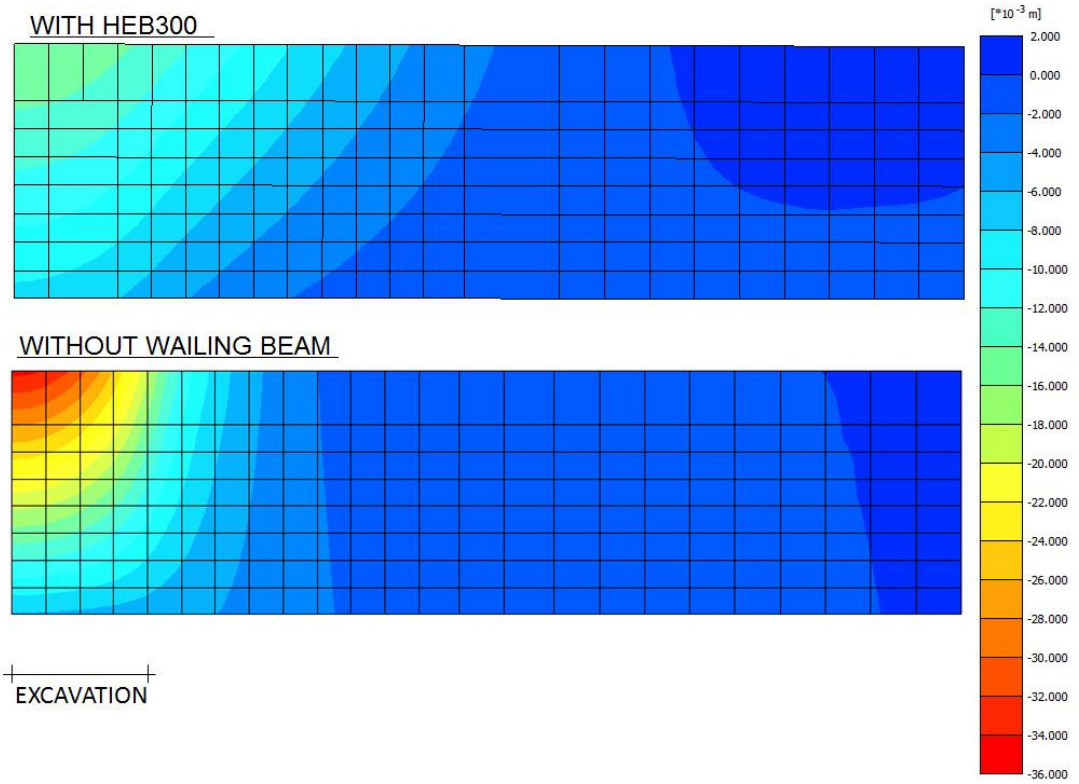

Figure 4.23 Elevation of the horizontal deflection for the sheet pile wall, both with and without wailing beam. The wall is 17,5 meter long from the excavation centre, to the left in the figure.

The fundamental question is how the wailing beam affects the mechanical behaviour of the retaining structure. Starting from the base case, the parameters in this model are varied. The parameters are chosen according to what may influence the deformations and the safety factor. An overview of the parameters that are to be studied are presented in Table 4.15.

Table 4.15 Parameters that are to be studied in this chapter and a short description of the purpose of each simulation.

Parameter	Question formulation
Crest length	What is the influence distance in the sheet pile wall? How long must the wall be outside the excavation?
Excavation width	How will the deflection pattern change when simulating different widths of the excavation?
E-modulus of the soil	What is the effect of the E-modulus of the soil?
Linear Elastic soil model	Will the result from a linear-elastic soil model considerably differ from the Mohr-Coulomb model?
Weaker wailing beam	What is the effect when simulating with weaker wailing beams?

4.3.1 Crest length of the sheet pile wall

In order to investigate how the wailing beam is affecting the mechanical behavior of the retaining system, the simulations will be compared to the results from the simulation with the AU14 profile without a wailing beam. The comparison will concern mechanical behavior at different crest lengths including deflection pattern, shear forces, bending moments and safety factor.

The results from the simulation of different crest lengths with the AU14 profile with HEB300 are presented in Figure 4.24.

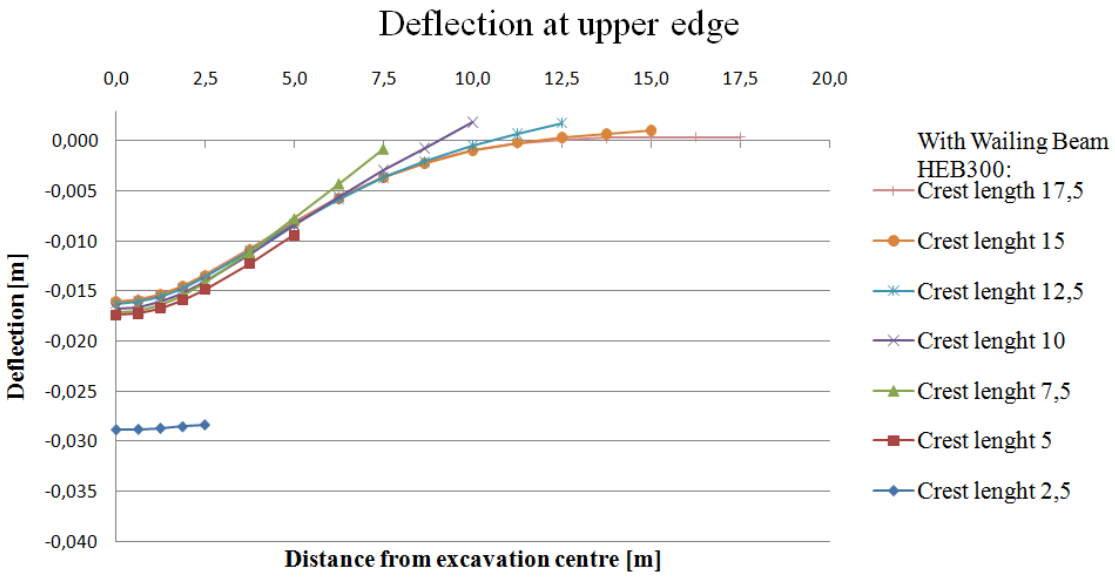

Figure 4.24 The horizontal deflection at the upper edge of the sheet pile wall versus distance from the excavation centre. The deflection curve without wailing beam is included for comparison.

The most obvious effect is that the maximum deflection is reduced. The deflection of the sheet pile wall at the crest length 2,5 meter is 29 mm and almost constant. This should be compared to the case without wailing beam where the curvature of the sheet pile wall was smooth with a maximum deflection of 36 mm, see Section 4.2.1. The maximum deflections at crest lengths from 5 to 17,5 meter is within an interval from 16 to 17 mm. For the sheet pile wall with the crest length 7,5 meter, almost no deflection occurs at the end. This means that it is only necessary to use a sheet pile wall that is elongated 5 meter outside the excavation. A comparison of the result from the base case without a wailing beam is presented in Figure 4.25 and regards the crest length 17,5 meter.

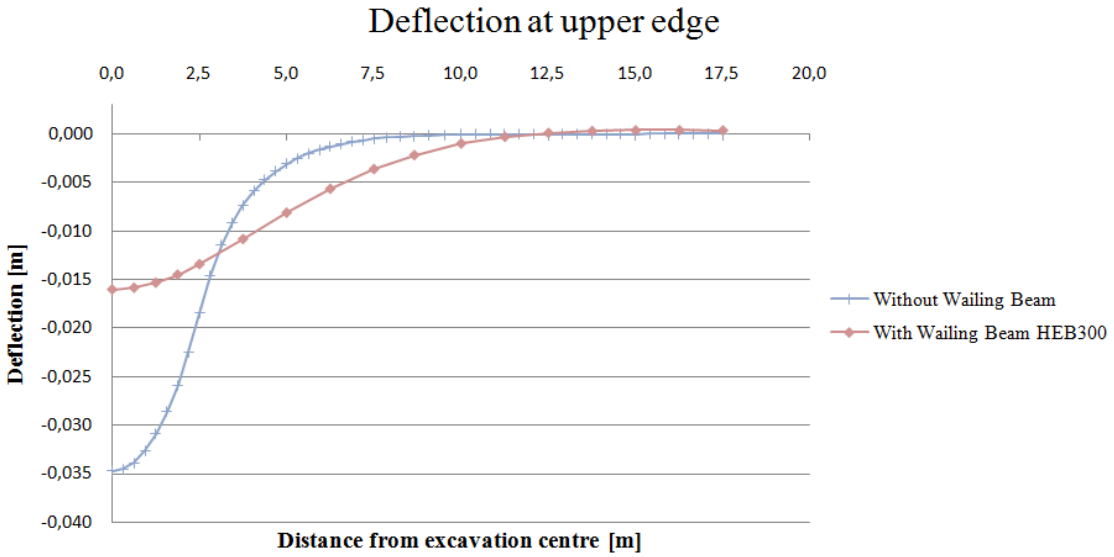

Figure 4.25 Horizontal deflection for crest length 17,5 meter with and without wailing beam.

The simulations show a clear effect of the wailing beam. Without the wailing beam, the maximum deflection of the sheet pile wall at the upper edge is 35 mm. By adding the wailing beam, the maximum deflection is decreased to 16 mm. This is a reduction of about 50%. These effects are valid for the upper edge. In Ultimate limit state it would probably have been enough with a weaker beam, but since it was the deformations in Serviceability limit state that was of most concern a stiffer beam was chosen at contract E33.

Another important aspect is to evaluate how the influence distance of the sheet pile wall will be affected when the wailing beam is added. The simulations with different crest lengths have the same pattern of the curvature.

The influence distance increase when simulating with a wailing beam from 5 to 9 meter outside the excavation pit. Using the wailing HEB300, the horizontal deflection is reduced with 50 %, and this leads to an increased influence distance with 50 %.

The beam, as well as the wall are modelled as elastic and cannot go to failure. Because of this, it is important to look at the stresses in these elements separately, and compare them to their corresponding capacity in Serviceability limit state. The definition of the quantities of the wailing beam is illustrated in Figure 4.26.

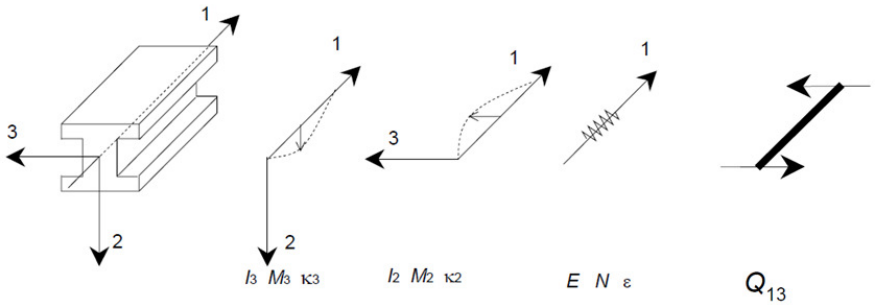

Figure 4.26 Definition of moment of inertia (I), positive bending moment (M), positive curvature (κ), stiffness (E) and the shear force Q_{13} for a horizontal beam based on local system of axes (Brinkgreve, 2007)

The distribution of the shear force, Q_{13}, for different crest lengths is presented in Figure 4.27.

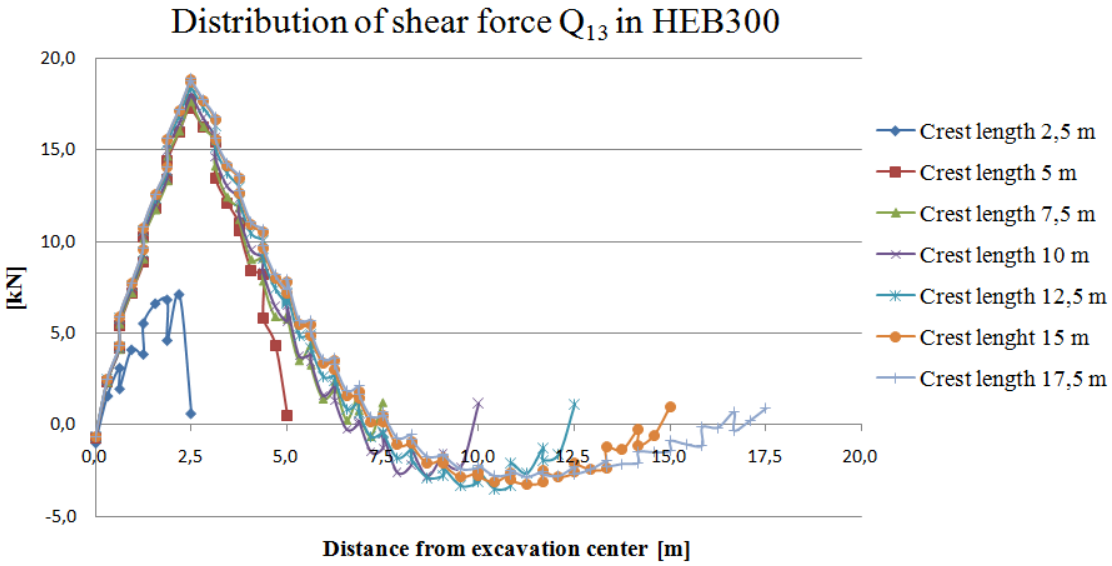

Figure 4.27 Distribution of the shear force Q13 in the beam profile HEB300.

For the crest length 2,5 meter, the shear forces are considerably smaller than for higher crest lengths. The shear force decrease fast when it has reached its maximum. The distribution of the shear forces in the wailing beam at this crest length is probably because of the wall is not getting that much support from the surrounding soil volumes.

The shear force distribution for crest lengths from 5 meter has the same pattern even though the sheet pile wall with 5 meter crest length decrease faster when it has reached its maximum compared to the other. The maximum shear force is inside an interval from 17 to 19 kN and occurs at the edge of the excavation.

The force in the wailing beam is relatively small and should be compared to the design shear force capacity which is defined in Equation (4.9). Input values are found in specifications from manufacturer.

$$V_{Rd} = \frac{A_w \cdot f_{yc}}{\gamma_m \cdot \gamma_n} \quad (4.9)$$

where A_w is the area of the web and f_{yc} is the characteristic strength of the used steel quality, equal to 270 MPa. The partial factors γ_m and γ_n are set to 1,0 and 1,2 respectively. The comparison of the action effect and the capacity of the HEB300 are presented in Table 4.16.

Table 4.16 Comparison of the action effect and the capacity regarding Q_{13} of the wailing beam profile HEB300.

	Unit	Action effect	Capacity
Q_{13}	kN	19	648

As shown in Table 4.16, the shear force capacity of the beam is much higher than the action effect. This means that the use of the wailing beam is mostly for lowering the deflections in Serviceability limit state.

The inclination of the shear force distribution curve gives the distributed reaction force against the wailing beam. When the inclination is constant, the intensity of the reaction force is the same inside the interval. The distributed shear force at crest length 17,5 meter is illustrated in Figure 4.28.

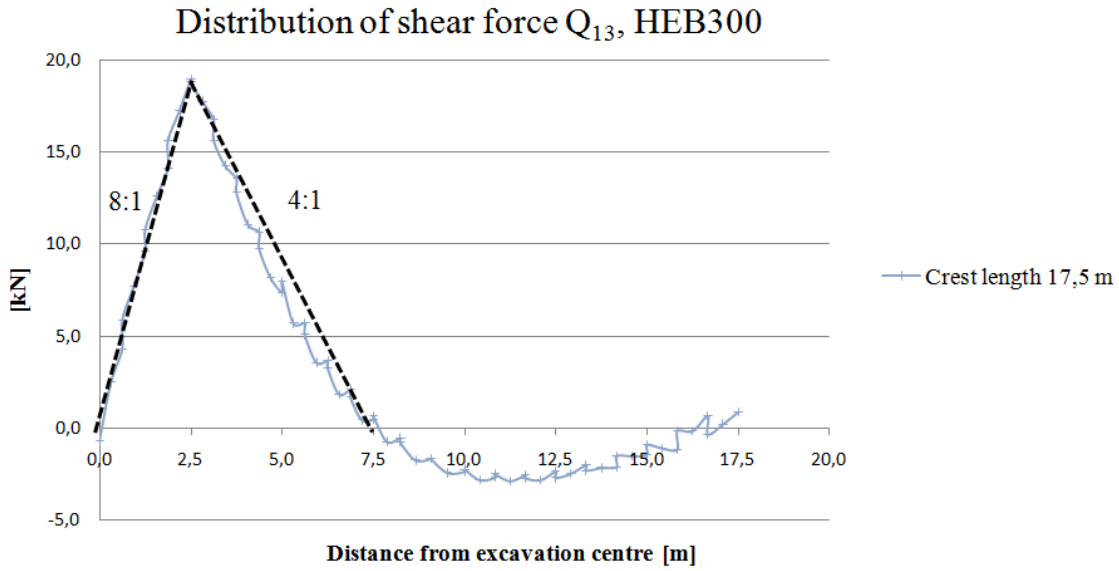

Figure 4.28 The inclination of the distributed shear forces gives de reaction force on the wailing beam.

The first 2,5 meter from the excavation centre, i.e. inside the excavation, the positive inclination is 8:1 which means that the intensity of the reaction force is 8 kN/m. Outside the excavation the negative inclination is 4:1 until it flatten out 5 meter outside the excavation. This means that the reaction force on the wailing beam is 4 kN/m. This gives a distribution of the reaction force illustrated in Figure 4.29. The shear force distribution outside 7,5 meter are neglected in this thesis.

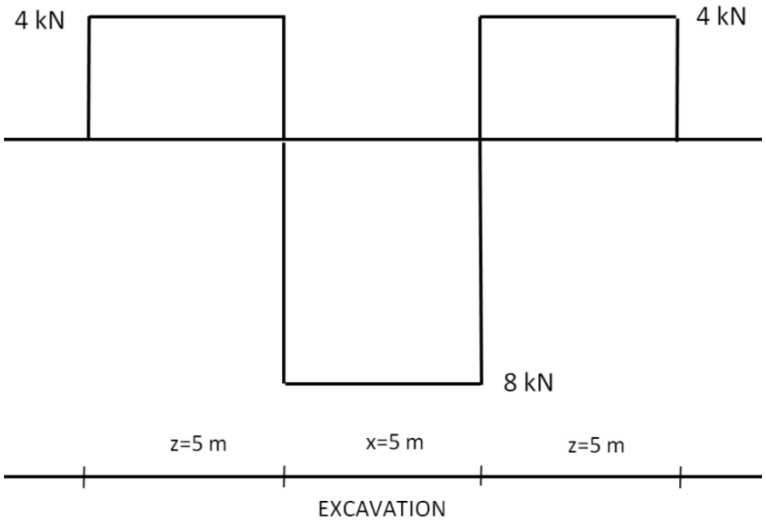

Figure 4.29 The distributed reaction force in the wailing beam. The value x is the excavation width and z is the distribution distance of the reaction force on both sides outside the excavation.

The reaction force in the wailing beam has a constant distribution, both inside and outside the excavation. In the case with the HEB300 profile, the reaction force due to the staged excavation is 8 kN/m inside the pit and 4 kN/m on both sides of the excavation respectively. This gives equilibrium of the distributed reaction forces. This should be compared to what was assumed in the design phase, see Section 2.2.1. The assumed distribution of the reaction force would according to this, decrease with the distance from the excavation, see Figure 4.30.

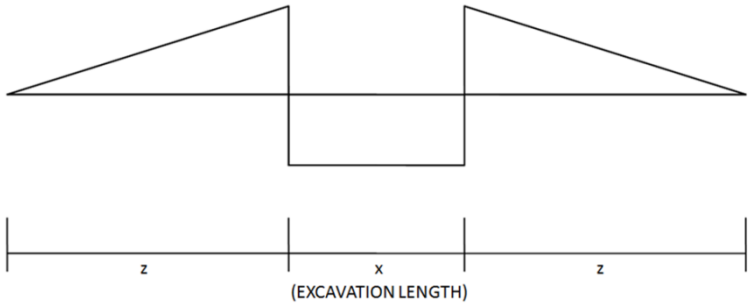

Figure 4.30 The assumed distribution of the reaction force in the wailing beam during design phase.

The reaction force was assumed to be constant inside the excavation, which also was shown in the simulations. Outside the excavation, the assumption was not fully correct. The result also shows that the distribution distance, z, is equal to the excavation width, x in the case when simulation with a HEB300, and that the reaction force is constant.

The distribution of the bending moment, M_2, in the wailing beam at different crest lengths is presented in Figure 4.31.

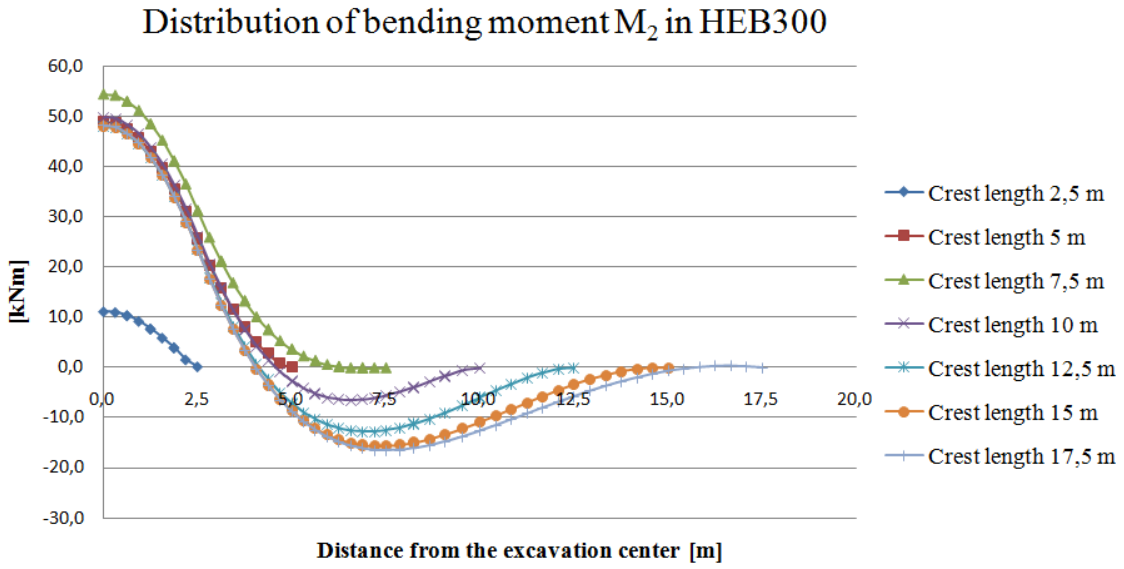

Figure 4.31 Distribution of the bending moment M_2 in the wailing beam at different crest lengths.

The distribution of the bending moment at crest length 2,5 meter is considerably smaller than for the other crest length. This has the same explanation as for the shear force distribution, i.e. the sheet pile wall does only get small support from the surrounding soil volumes. The other crest lengths follow the same pattern and shows small differences in maximum and minimum values. At the end of the wailing beam, in every crest length, the bending moment is zero, which means that the wailing beam can be seen as freely supported. This is the opposite compared to the symmetry cut, in the excavation centre, where the retaining structure is fully fixed.

The moment capacity of the wailing beam HEB300 is calculated from Equation (4.10).

$$\boldsymbol{M_{Rd}} = \frac{\boldsymbol{W_t \cdot f_{yc}}}{\boldsymbol{\gamma_m \cdot \gamma_n}} \tag{4.10}$$

where W_t is the elastic section modulus, f_{yc} is the characteristic strength of the used steel quality, equal to 270 MPa, $\gamma_m = 1$ and $\gamma_n = 1{,}2$. The comparison of the action effect and the capacity of the HEB300 is presented in Table 4.17.

Table 4.17 Comparison of the action effect and the capacity regarding M_2 of the wailing beam profile HEB300 in Serviceability limit state.

	Unit	Action effect	Capacity
M_2	kNm	55	378

As shown in Table 4.17, the moment capacity of the beam is much higher than the action effect. This means, as mentioned earlier, that the use of the wailing beam is mostly for lowering the deflections in Serviceability limit state.

Evaluating the safety factor in the soil at different crest lengths, the safety factor in the soil is increased when adding a wailing beam, see Figure 4.32.

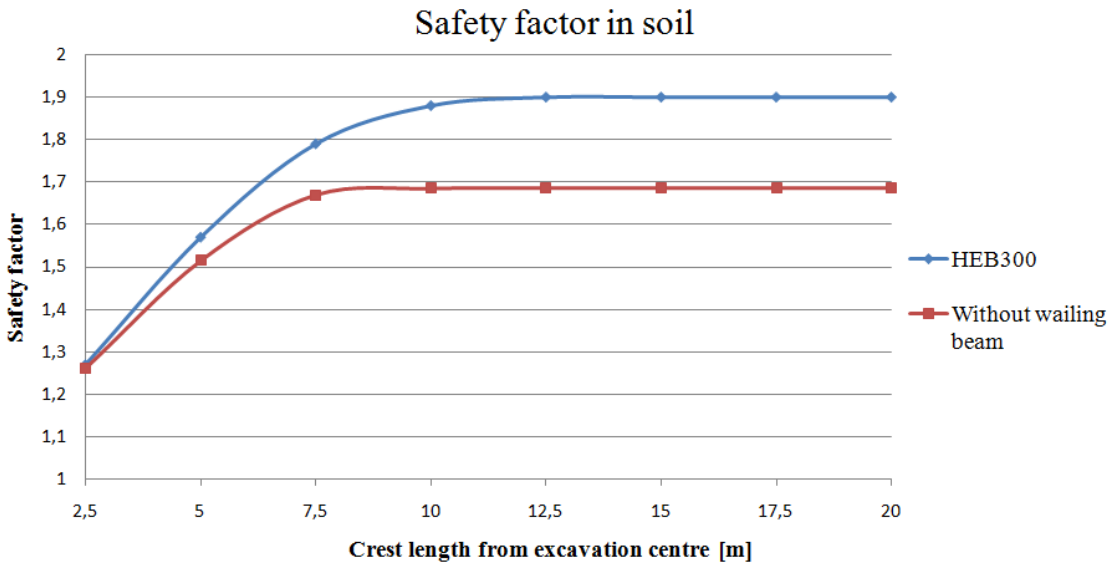

Figure 4.32 The safety factor in the soil.

The comparison shows that the wailing beam HEB300 has a good effect on the retaining system. This agrees with the statement that the sheet pile wall itself is relatively weak around the vertical axis. The beam is transferring load from the sections in the excavation over to the soil where it is distributed over a larger area. This behaviour, called horizontal arching, explains why the influence distance is larger when using a stiffer beam.

4.3.2 Excavation width

The effect of the wailing beam when increasing the excavation width, concerning the horizontal deflection and the influence distance, is an important aspect. This because an optimization of the width of the staged excavation is often preferable on the construction site due to practical and economical reasons. The chosen excavation width to simulate is 8 meter. The result from the simulation, which also includes the results from the simulation without a wailing beam, is presented in Figure 4.33.

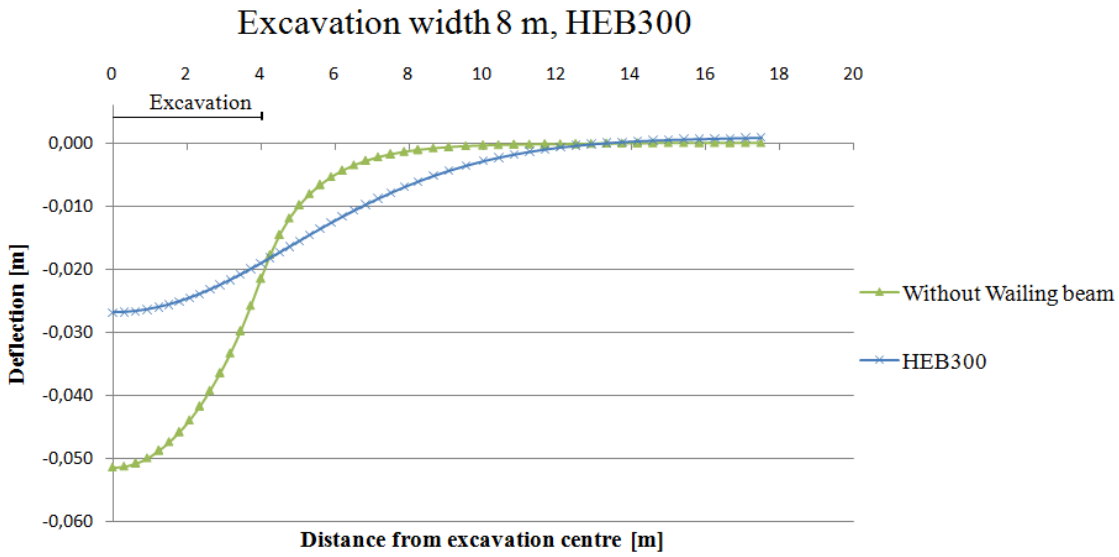

Figure 4.33 Horizontal deflection of the sheet pile wall at upper edge, with and without wailing beam.

The wailing beam has a large effect of the deflection of the sheet pile wall. It reduces the deflection with about 50 % compared with not using a wailing beam. The influence distance increase with about 50 %, from 5 to 9 meter outside the excavation pit. As in Section 4.2.1, the reduction with 50 % of the deflection leads to an increased influence distance with 50%. Whether this can be seen a rule of thumb or not can be discussed, but more simulations has to be done in order to prove that this is not only a coincidence. However, this study lies outside the delimitations of this thesis.

4.3.3 Variation of E-modulus in the soil

In Section 4.2.3 it was established that the deflection was reduces by a factor two when doubled the E-modulus in the soil. And when simulated with halved E-modulus, the deflection increased with a factor two, see Figure 4.34. The result from the simulations with the E-modulus as in base case is added as a comparison.

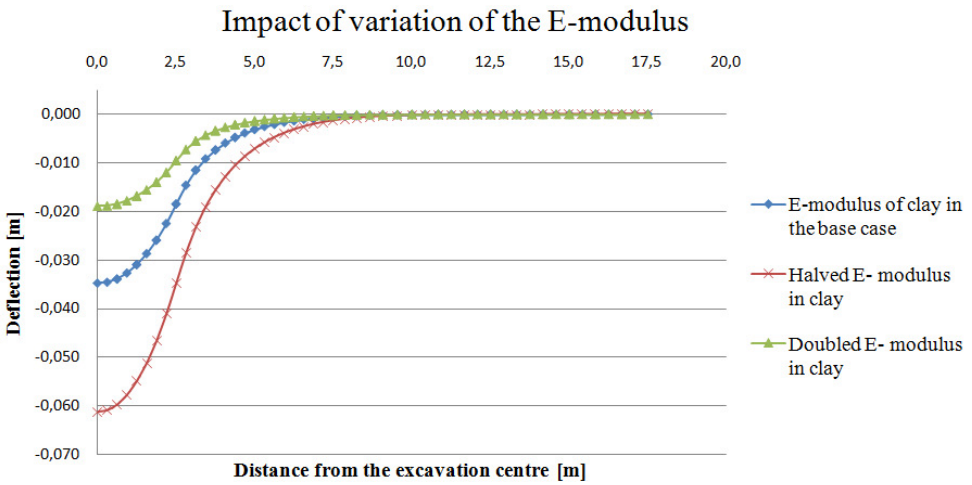

Figure 4.34 The horizontal deflection at the upper edge of the sheet pile wall when double and halved the E-modulus in the soil. The plot regards simulation without a wailing beam.

The effect of adding a wailing beam HEB300 into the simulations is presented in Figure 4.35. The result from the simulations with the E-modulus as in base case with wailing beam is added as a comparison.

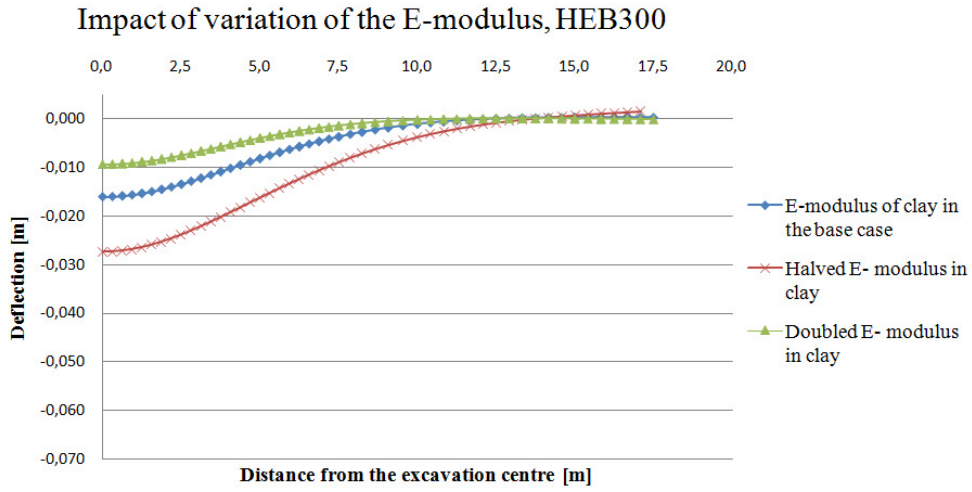

Figure 4.35 The horizontal deflection of the wailing beam when double and halve the E-modulus in the soil, compared with the simulation with the E-modulus as in base case with wailing beam.

The deflection of the wailing beam is reduced by approximately a factor two when doubled the E-modulus in the soil. When simulate with halved E-modulus, the deflection is increased with a factor two. The simulations show relatively small differences concerning the influence distance. In the case with halved E-modulus, the stresses in the sheet pile wall are higher since the soil is much weaker. The result shows that the relative differences are equal between the simulation without a wailing beam and by adding a wailing beam.

4.3.4 Simulation with weaker wailing beams

The simulations with the wailing beam profile, HEB300, showed that the sheet pile wall became much stiffer. It improved the safety factor in the soil since the sheet pile wall could transfer higher forces when it is stiffer. A weaker wailing beam could be used instead, and still probably get satisfying mechanical behavior of the retaining system. In order to investigate the effect of using a weaker beam profile, two different wailing beams will be simulated in the model, HEB100 and HEB180. The definition of the quantities of the wailing beam is illustrated in Figure 4.36.

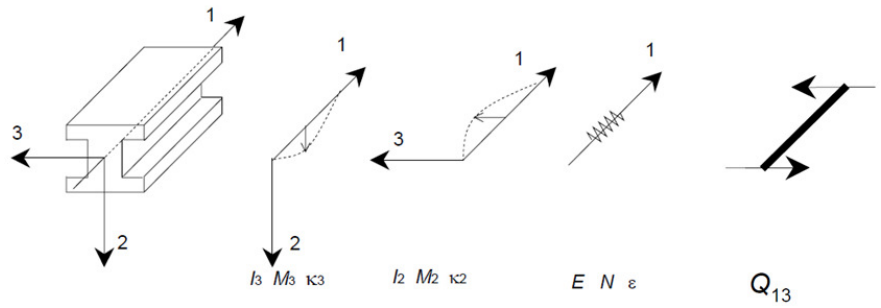

Figure 4.36 Definition of moment of inertia (I), positive bending moment (M), positive curvature (κ), stiffness (E) and the shear force Q_{13} for a horizontal beam based on local system of axes (Brinkgreve, 2007).

The material parameters that are used as input values in PLAXIS are presented in Table 4.18. It also includes the input parameters for HEB300 for comparison.

Table 4.18 Material parameters for the wailing beam HEB300, HEB180 and HEB100.

Parameter	HEB300	HEB180	HEB100	Unit
A	$15{,}0\cdot10^{-3}$	$6{,}525\cdot10^{-3}$	$2{,}604\cdot10^{-3}$	m^2
E	$2{,}1\cdot10^{8}$	$2{,}1\cdot10^{8}$	$2{,}1\cdot10^{8}$	kPa
I_3	$8{,}563\cdot10^{-5}$	$1{,}362\cdot10^{-5}$	$1{,}673\cdot10^{-6}$	m^4
I_2	$2{,}517\cdot10^{-4}$	$3{,}831\cdot10^{-5}$	$4{,}495\cdot10^{-6}$	m^4
I_{23}	0	0	0	m^4

The horizontal deflection of the sheet pile wall, without wailing beam and with the three profiles that are used in this thesis is presented in Figure 4.37. It is valid at the upper edge of the sheet pile wall, where the wailing beam is welded, for the crest length 17,5 meter.

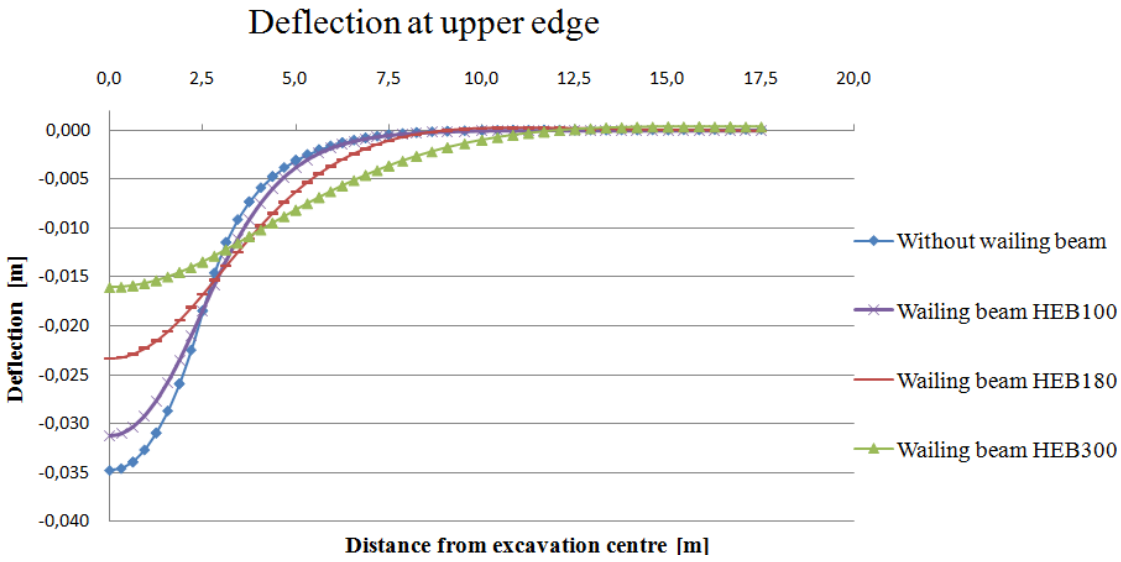

Figure 4.37 The horizontal deflection at the upper edge of the sheet pile wall without and with different wailing beams. The plot regards simulations at the crest length 17,5 meter.

The most obvious effect is that the maximum deflections at the centre of the excavation are increased incrementally when simulated with weaker retaining structures. The differences in the horizontal deflection between the case without a wailing beam and with different wailing beams are presented in Table 4.19.

Table 4.19 Maximal horizontal deflections.

	Without wailing beam	HEB100	HEB180	HEB300
Deflection [m]	0,035	0,032	0,023	0,016

The results show that the mechanical behavior when using a HEB100 is close to the case without a beam. This is because the beam profile has much weaker properties than the other profiles used in the simulations and is one of the smallest HEB profiles on the market. The HEB180 has a relatively high effect of the retaining system and increase the horizontal deflection effectively.

Another important aspect is to evaluate if the influence distance of the sheet pile wall is affected when adding wailing beams with different properties. For the case without a wailing beam and the simulations with a HEB100, the pattern is almost the same. The influence distance differs more, approximately one meter, when adding a HEB180 and the deflection curve is straighter.

To illustrate the different behavior for the different wailing beams, the deflection is plotted in cross-sections at four different distances from the excavation centre, see Figure 4.38. These figures shows how the deflection of the walls varies with depth, and that the wall with HEB300 has much lower deflection at the excavation centre, but also larger deflection 7,5 meter from the excavation centre. At distance 12,5 from the excavation centre, all walls are unaffected by the excavation.

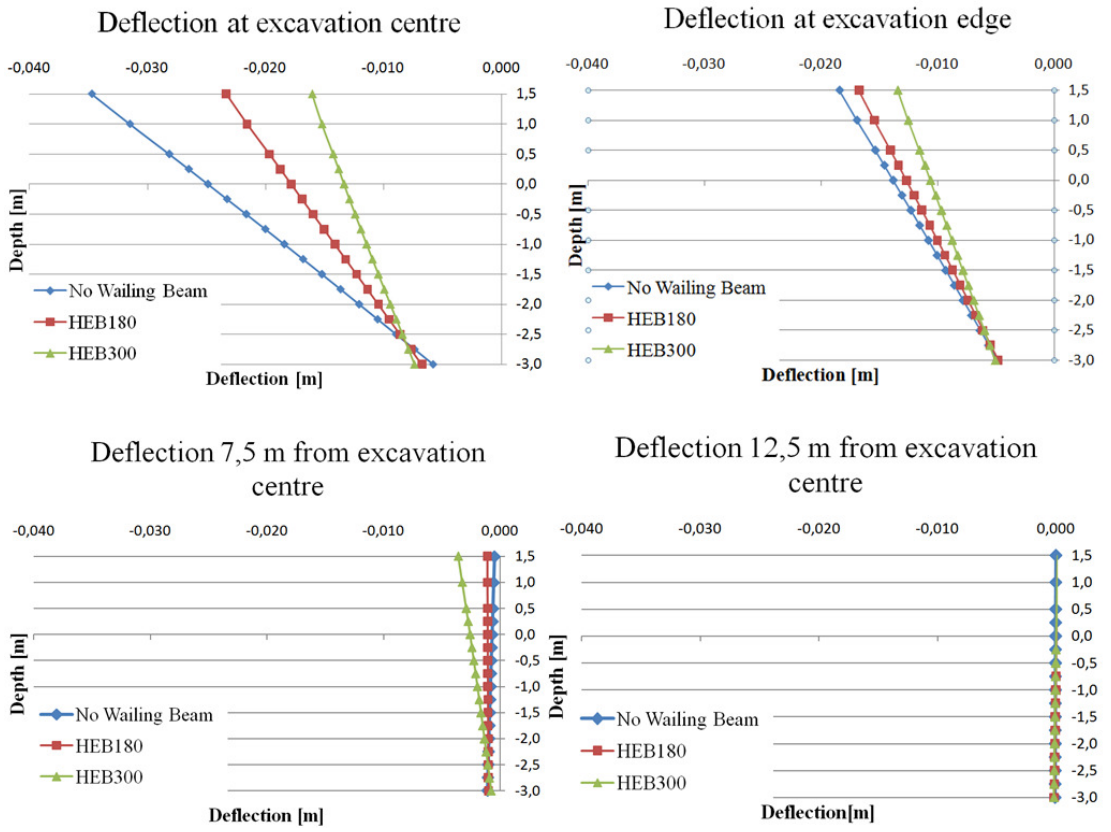

Figure 4.38 Cross section of the horizontal displacement of the sheet pile wall at four different distances from the excavation centre. The excavation edge is 2,5 meter from the excavation centre.

The distributions of the shear force, Q_{13}, in the simulated wailing beams are illustrated in Figure 4.39. The figure only concerns the distribution at crest length 17,5 meter.

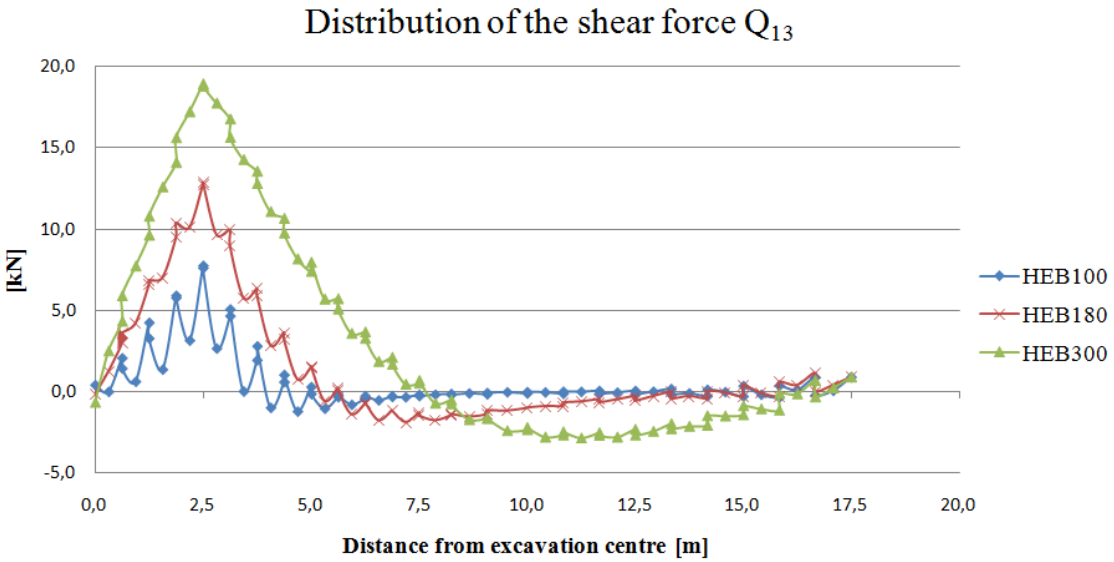

Figure 4.39 The distribution of the shear force, Q_{13}, in HEB100, HEB180 and HEB300 at crest length 17,5 meter.

The maximum action effect of the shear force and the capacity of the wailing beams is presented in Table 4.20.

Table 4.20 The action effects of shear force and the calculated capacity of the different wailing beams.

	HEB300		HEB180		HEB100	
	Action effect	Capacity	Action effect	Capacity	Action effect	Capacity
Q_{13} [kN]	19	648	13	291	8	108

The maximum value of the shear forces decrease with approximately 60 % when simulating with the HEB100 compared with the maximum value for HEB300. The difference between the HEB300 and HEB180 is about 30 %.

The distributed reaction force in the wailing beams HEB100 and HEB180 is calculated in the same way as in Section 4.3.1 for HEB300. Shear forces with negative values is neglected and the result is presented in Figure 4.40 and Figure 4.41.

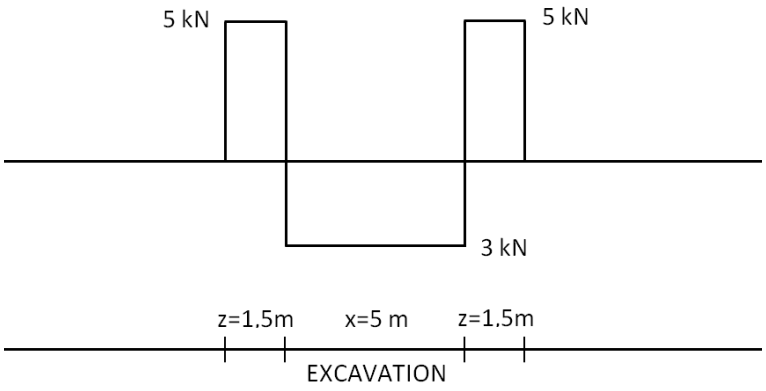

Figure 4.40 The distribution of reaction force in HEB100.

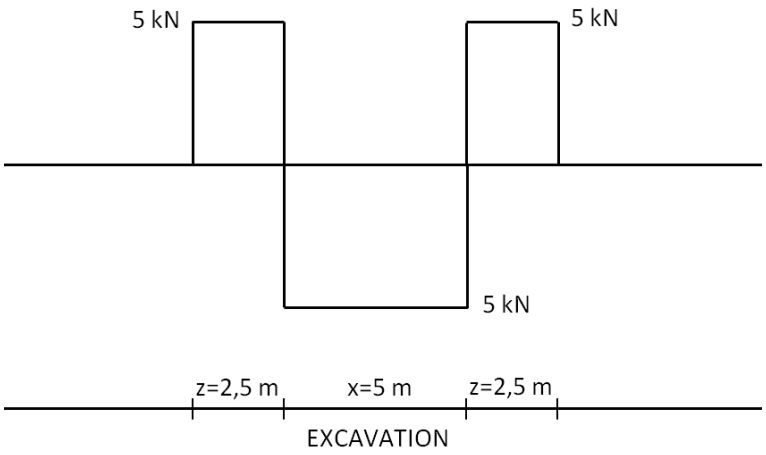

Figure 4.41 The distribution of reaction force in HEB180.

As in the case with HEB300, the reaction force against HEB100 and HEB180 is constant both inside and outside the excavation. The influence distance of the reaction forces differs from each other but an equilibrium state occurs in both cases.

The distribution of the bending moment, M_2, is illustrated in Figure 4.42. The distribution concerns HEB100, HEB180 and HEB300 at crest length 17,5 meter.

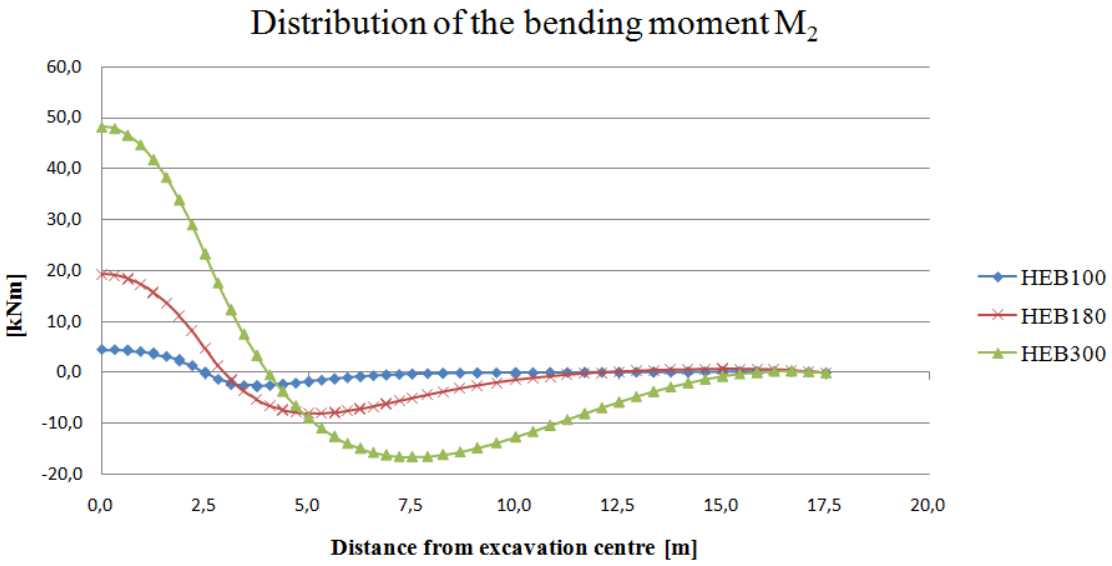

Figure 4.42 The distribution of bending moment M_2 at crest length 17,5 meter.

A comparison between the maximum bending moment, M_2, and the capacity is presented in Table 4.21.

Table 4.21 The maximum bending moment, M_2, and the calculated capacity of the different wailing beams.

	HEB300		HEB180		HEB100	
	Action effect	Capacity	Action effect	Capacity	Action effect	Capacity
M_2 [kNm]	48	378	19	96	5	20

There are relatively large differences between maximum bending moments in the wailing beams. The HEB100 cannot take any high moments, compared to HEB180 and HEB300, due to the beam has a lower flexural rigidity. The magnitude of the moment distribution curve is low, which means that the HEB100 do not support the sheet pile wall in a higher extent. This can be related to the deflection curve of the sheet pile wall with HEB100, which had almost the same curvature as when simulated without a wailing beam. At the end of the wailing beam, as mentioned in Section 4.3.1, the bending moment is zero, which means that all the wailing beams can be seen as freely supported. In the symmetry cut, in the excavation centre, the wailing beams are fully fixed.

A *phi/c reduction* was done in order determine the differences in the safety factor of the soil when simulate with different wailing beams. The result is presented in Table 4.22.

Table 4.22 The safety factor for the model, concerning failure in the soil and how it is affected by the use of different wailing beams. These safety factors is valid for a crest length longer than 12,5 meter.

	Without wailing beam	HEB100	HEB180	HEB300
Safety factor	1,69	1,90	1,90	1,90

As seen in the table, there is no difference using HEB100, HEB180 or HEB300, concerning the safety factor. The reason why the safety factor is equal in the simulations with the different wailing beams is that the failure mechanism is changed. In the case without a wailing beam, the failure mechanism is developed as a slip surface under the sheet pile wall, see Figure 4.43 a). When simulating with the different wailing beams, the failure mechanism occurs as a result of the distributed load that is replacing the silt, see Figure 4.43 b).

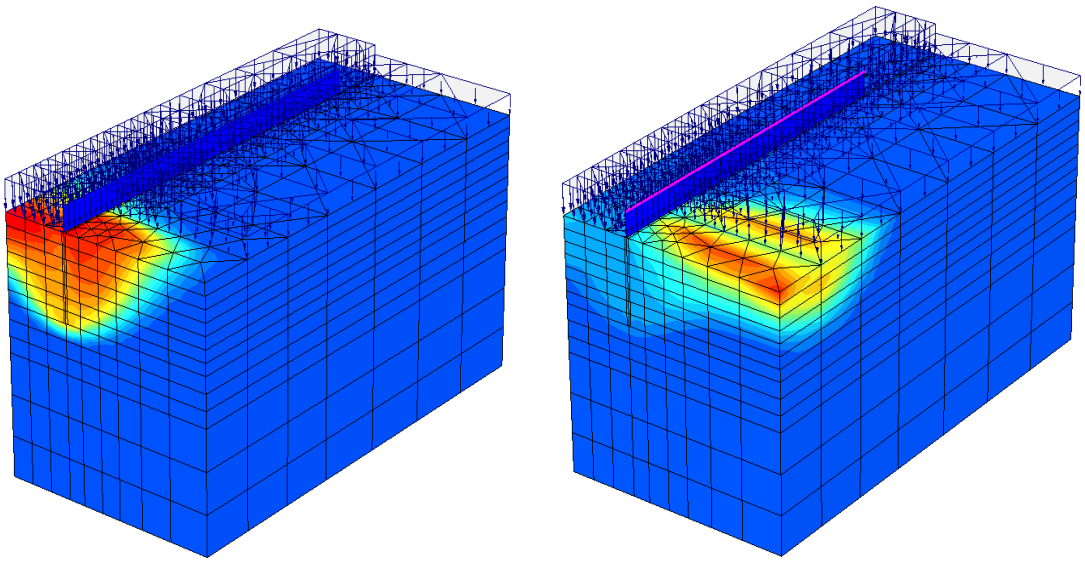

a) *b)*

Figure 4.43 Failure mechanisms in the soil

a) Without wailing beam

b) With wailing beam

The failure mechanism in the case with the wailing beam will probably not be developed in a real case, since it is caused by the fictive load, representing the silt. In a real scenario, there will be a resisting soil volume, as a slope with a sufficient inclination, which will prevent this slip surface to occur. During the *phi/c reduction,* PLAXIS will find the point with the lowest safety factor in the model. This means that

the safety factor for the slip surface under the sheet pile wall is higher than 1,9. It should be noted, as mentioned earlier, that the safety factor is only regarding failure in the soil body.

5 Studied object

The planning of the infrastructure project BanaVäg i Väst has been discussed over a long time. The project includes a new double track railway and a four lane highway with increased standard between Göteborg and Trollhättan, along the Göta river, see Figure 5.1. The purpose is to meet the increased amount of cargo trains, and to make the road safer for the road users and also to improve the environment in the area.

Figure 5.1 Stretch of the project BanaVäg i Väst (Banverket och Vägverket, 2008)

The railway is designed for velocities up to 250 km/h which set high demands on the foundation of the railway. The geotechnical conditions are relatively poor. Ground improvements as lime/cement columns have to be installed along most of the stretch. The project is divided into 16 stages and the entire project is planned to be finished in 2012.

5.1 Project description

The contract E33 is located between Bohus and Nödinge and includes 3,2 kilometer of double railway track and highway. The contractor is Skanska Sverige AB and responsible for all the temporary geotechnical structures is Skanska Teknik.

Before the construction of the new railway embankment, lime/cement columns are installed and these have to be surveyed. This is to verify that the columns have a satisfying quality, that they are homogenous and have an inclination which does not exceeds the limits. The columns are often of poor quality the first meter, why this part of the columns often is taken away so a fresh end surface occurs. This includes excavation of clay material and refilling with crushed material that will form the sub base of the railway embankment. In the southern part of contract E33 the new railway track will be built close to the existing railway track. In order to keep the existing railway track open for traffic during the construction, a retaining structure is used. A cantilever sheet pile wall will be installed and the excavations down to fresh columns will be done as a staged excavation after which the pits are re-filled with crushed material. One part of the wall is reinforced with a wailing beam, and in one part satisfying stability and deflections below the limits are achieved without wailing beam. A section is shown in Figure 5.2.

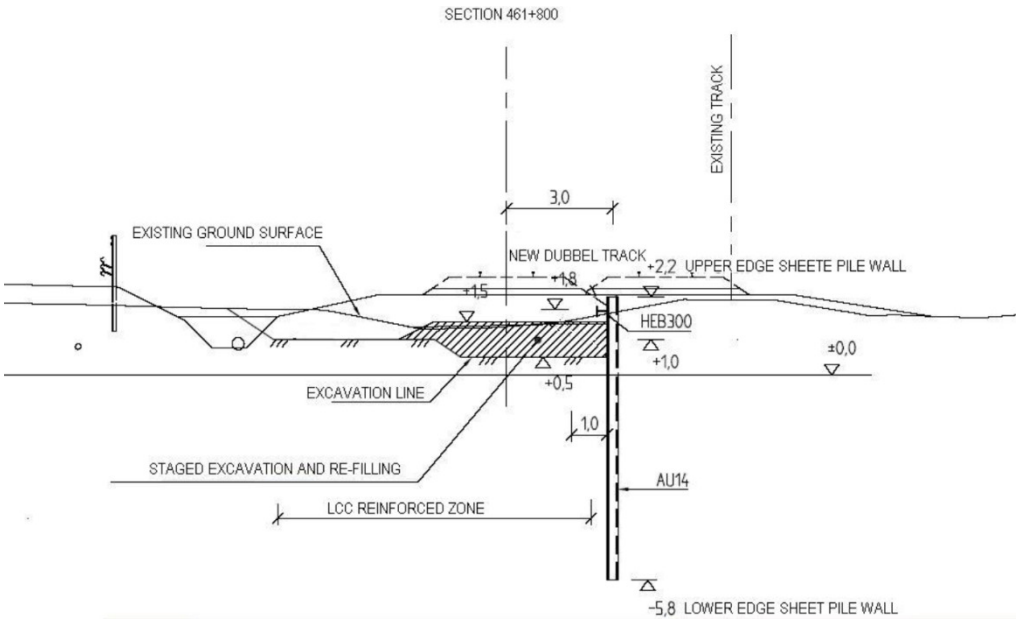

Figure 5.2 Cross section of construction phase 1 (Skanska Teknik AB, 2009)

The geometry corresponds to what is modeled in previous chapters, but the characteristic load is somewhat hard to define. In the design, the load from the existing track was set to 37,4 kPa. This is what is prescribed from the Swedish Traffic Administration, but is considerably higher than the weight of the trains that normally operates the stretch. The design load is instead calculated from the weight of the heaviest cargo train that could pass within 50 years, multiplied with factors concerning dynamic effects and partial factors. What load the excavation in reality is subjected to is hard to predict.

The soil properties are also somewhat different to what was used in the model, since some simplifications were done to generalize the model. On site, the newly installed lime/cement columns will increase the strength parameters of the soil, an effect that is not considered in the model. Also the length of the sheet pile wall differs. In the model, the wall reaches a depth of -3 meter, instead of -5,8 at the project site. The reason for choosing the smaller depth is that when designing for the smaller load, 10 kPa, the required depth in a 2D model is -3 meter. This gives a safety factor just above 1.0, excluding the addition from the side effects.

5.2 Measurements

To evaluate the results of the simulations, a field study was carried out at contract E33. Instrumentation was installed at two sections, where the horizontal and vertical deflection of the sheet pile wall was measured. One of the sections had a wailing beam and one section did not. The mandatory monitoring program at site was extended, and measured the deflections on every second sheet pile. This corresponds to every 1,5 meter. These measurement were made in 15 points along the wall, giving the deform pattern for 22,5 meter wall. This gives information about movements in three dimensions and has an accuracy of ± 2 mm/m. The position of the wall was measured before the excavation was made and used as a reference called the zero setting. After excavation, the deflection was measured repeatedly during a couple of days, until the values of the deflection had stabilized. During the time, about 70 train

per day passed by the excavation. Unfortunately, the excavations could not be done in both sections at the same time due to practical reasons at the construction site. The section without wailing beam was excavated at February 4th, 2010, and refilled one week later after four measurements. The results are presented in Figure 5.3. At this time, the ground frost reached a depth of over 1 meter below surface, due to a extremely cold winter. The other section, with wailing beam, was excavated May 7th, 2010, when the ground frost was gone long-time. In total, six measurements were done at this section before the shaft was refilled May 15th, 2010. The result is presented in Figure 5.4.

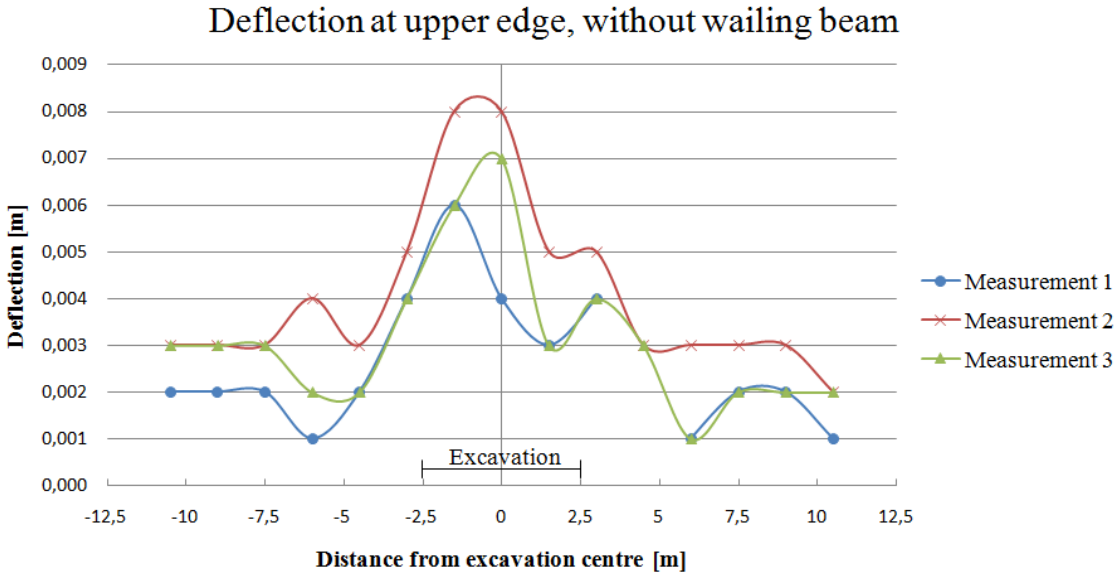

Figure 5.3 *Measured horizontal deflection at upper edge of the sheet pile wall without a wailing beam at three different times.*

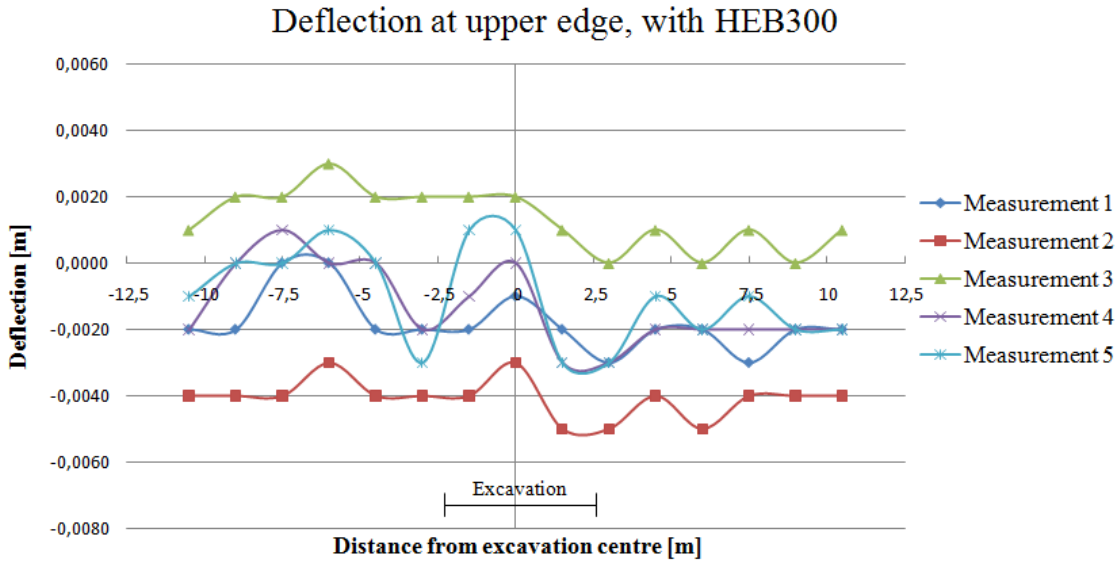

Figure 5.4 *Measured horizontal deflection at upper edge of the sheet pile wall with a HEB300 at five different times.*

For the section without wailing beam, Figure 5.3, the measured values show clear correlation and the three curves all have the same pattern. Even if the absolute value differs up to 4 mm, most of them are within 2 mm range, and many of the points within 1 mm range. The deflections measured for the section with the wailing beam in Figure 5.4 is however harder to interpret. The curves are more scattered, and the values are smaller. For many of the values in these sections, the deflection of the wall is negative, i.e. the wall is moving towards the railway. Many of the curves show the same pattern, but are displaced up or down. Studying measurement 1 and 5, the difference is relatively large. However, if the shapes of these two curves are studied, it is easy to see that they are following the same pattern. It is likely that this deflection could originate from errors in measurement. When setting up the measurement equipment, the device is placed in front of the wall and the position of the device is calculated using three reference points where the location is known. This procedure is made every time the measurements are done, and if the location of the device is not exact, the deflection curves could be displaced. The errors could also be caused by movements of the device after positioning. Since the ground is soft, it is possible that the tripod where the measuring device is placed is disturbed. This could explain a displacement up or down of the curves.

To even out the differences between the curves in each section and get a representative value from the measurements, the mean value is calculated for each section. This is presented in Figure 5.5.

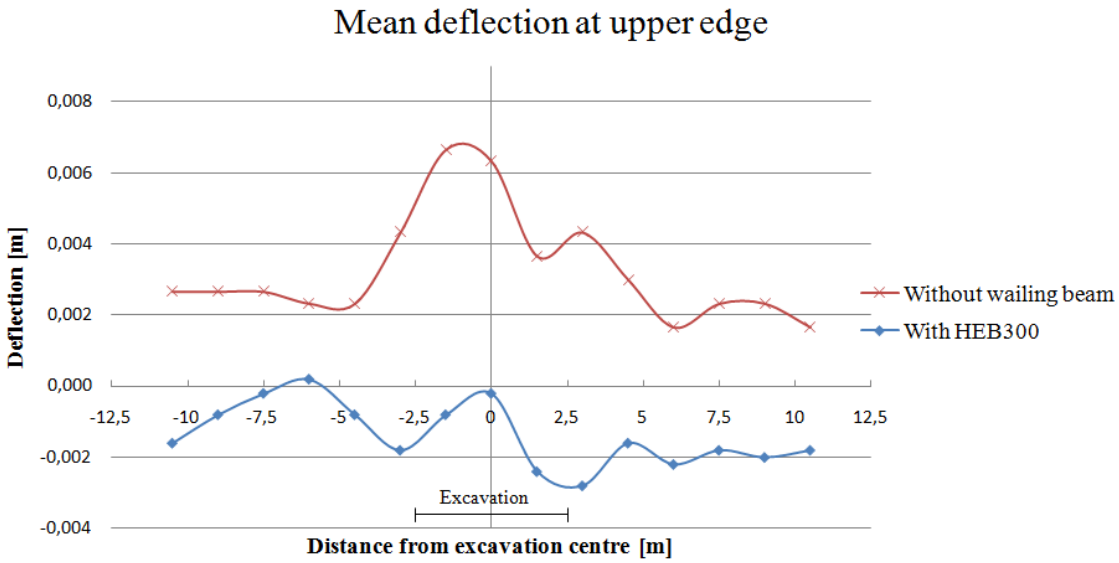

Figure 5.5 *Mean values for the measured horizontal deflection at upper edge of the sheet pile wall for sections with and without wailing beam.*

For the section without wailing beam there is a clear deflection inside the excavation. The maximum deflection occurs in the middle of the excavation and has a value of around 6 mm. From this value, the deflections decreases and at a distance of about five meter outside the excavation, the displacement approaches the error margin. It is possible that the curve has been displaced one or two millimetres upward due to measurement error, and that the real deflection curve should be adjusted downwards.

For the section with wailing beam HEB300, the deflection curve is almost entirely within the 2 mm margin. Since the curve does not show any uniform pattern, it is

likely that no measurable deflection occur. What the curves show should in that case only be noise. It is clear that there is a difference between the two cases, with and without wailing beam and this is a proof that the waling beam has an effect, at least for this particular case.

5.3 Evaluation

To evaluate the deflections calculated in PLAXIS 3D Foundation, the result is compared with the measured values of the deflection from the sheet pile wall at the project site at contract E33. The outer parameters differ in many ways, which was discussed in previous section. Because of this, the absolute value of the deflection differs. To make these results comparable, the deflection curves are normalized. This is done by dividing the deflection in every point by the maximum deflection of the curve. By doing this, the maximum deflection gets the value one and the deflection are then decreasing towards zero. The measured curve is also adjusted so that the points where the defections flatten out, about 5 meter from the excavation and out, is considered to be unaffected. In other words, the whole curve in Figure 5.5, is moved 2,3 mm downwards before it is normalized. This is to compensate a possible displacement of the zero setting, caused by error in measurements, see Figure 5.6. Since the section with wailing beam did not show any deflection, only the curve from the section without wailing beam is plotted.

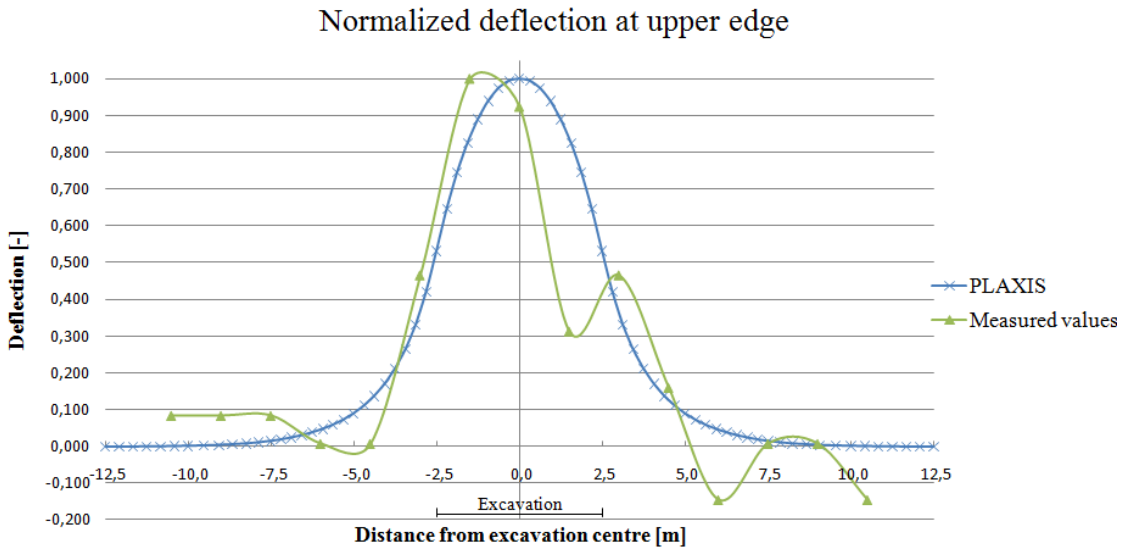

Figure 5.6 *Normalized horizontal deflections of the sheet pile wall. The curve from the measured values is adjusted so that the deflections outside the influence distance approaches zero.*

6 Conclusions

The knowledge of the three dimensional behavior of a corrugated sheet pile wall is limited. The reason for this is probably that it is seldom necessary to consider positive side effects in 2D calculations, why the effects are neglected. It is much easier to extend the driven depth of the sheet pile wall to achieve required stability. But in some cases, the addition from these effects could be of significant matter for the design, and be the difference whether it is necessary to use e.g. ground anchors or not. Since this method brings high costs, the profit with staged excavation is obvious. With the development of three dimensional softwares, the side effects can be modeled. This requires more detailed knowledge of the sheet pile wall´s properties in different directions.

6.1 Modeling process

In order to perform a parametric study, a generalized model was created in PLAXIS 3D Foundation. Much effort was put in the creation process of the model since it is of great importance to analyze the validity of the model. This includes verification that the boundary conditions are valid for the simulations as well as the simplifications and assumptions done in the model. In order to evaluate how the mesh affected the calculation results, a study was done. This study showed how the calculation results were affected by the coarseness of the mesh and how this affected the calculation time. The study also showed the importance of evaluating the level of the coarseness and how a too coarse mesh could give misleading results. A finer mesh will give larger deformations and a lower safety factor, but only until a certain point. When reached a certain coarseness in the model, the result no longer differs when refining the mesh. A finer mesh will only increase the calculation time, and not more than marginally increase the accuracy of the calculations. Where this level is, differs and has to be evaluated from case to case. This aspect is especially important when using 3D software, since the calculation time is considerably higher than using 2D software. It is tempting to choose a coarse mesh to save calculation time, since a detailed calculation with a fine mesh could take several hours for one phase, but this will also affect reliability of the result. That is why it is important to consider these aspects, and at least in some calculations remake the simulations with a different mesh and evaluate possible differences.

6.2 Flexural rigidities of the sheet pile wall

The most complex process in this thesis was to estimate the three dimensional properties of the sheet pile wall. The flexural rigidity around a vertical axis is hard to estimate, as well as the torsional rigidity against warping. When designing a sheet pile wall for staged excavation, it is essential to at least have a rough estimation of these properties. These assumptions are often based on qualified guessing from experienced geotechnical engineers, but there are also recommendations from user manuals of modeling softwares such as PLAXIS. The assumptions and the guidelines are many times pointing in different directions.

Basic assumptions regarding slide in interlocks and angle displacement are affecting the result in some extent. In attempt to estimate the impact of these parameters, a FE-model was created in PLAXIS 3D Foundation, where a corrugated sheet pile wall was subjected for bending in different directions. These simulations were made with the assumption that the interlocks do not slide or allow angle displacement. The

simulations showed that the flexural rigidity of the corrugated sheet pile wall is considerably weaker for bending around a vertical axis, than bending around a horizontal axis. Using these parameters when calculating the deflections of the sheet pile wall in a soil/structure model, the result shows that the wall is so weak against bending around a vertical axis that it gives deflections in the same magnitude as if the flexural rigidity was absent. This means that it is almost the same as using the assumption that angle displacement is possible. This is an interesting conclusion, since the value that is recommended in the user manual for PLAXIS 3D Foundation is completely different. The simulations also show that the torsional rigidity against warping is considerably lower than what is recommended in the user manual. This relation is also verified by theories from plate analysis.

6.3 The effect of a wailing beam

In the design of the sheet pile wall for the stage excavation at contract E33, the profit of using a wailing beam was discussed. Since no anchors were used, the idea was to transfer the loads from the excavation in the retaining structure to the soil outside the staged excavation. The maximum deflection would then be depending on the stiffness of this structure. To increase the stiffness, a wailing beam was used, and a relatively stiff profile, HEB300 was chosen. Using only two dimensional models, the effect of the wailing beam was hard to estimate. In this study, simulations in PLAXIS 3D Foundation have shown that the use of a wailing beam in an effective way decreases the maximum deflection of a retaining structure. Using a HEB300, the maximum deflection of the sheet pile wall is decreased with 50%. This result is valid even if some parameters such as excavation width or the E-modulus of the soil is changed. Reducing the dimension of the wailing beam, the effect was not as obvious as when using a HEB300. It was shown that the HEB100 almost did not have any effect at all on the deflections. It can therefore be concluded, that a stiffer wailing beam is required if the purpose is to lowering the deflections. On the other hand, if the global factor of safety in the soil is of most concern, also a weaker wailing beam can be effective. The HEB100 had almost the same effect on the safety factor of the soil as the HEB300. In these cases it is important to manually control the capacities of the beams, since the *phi/c reduction* in PLAXIS only reduces the strength parameters of the soil. Structural elements such as walls and beams are modeled as elastic and can never go to failure, why these have to be evaluated separately in Ultimate limit state.

A fundamental question in the design process was the influenced distance, which would determine the extension of the wall outside the excavation. For the case without wailing beam the deflections are much higher but the influence distance is relatively short. Since the wall is so weak for bending around a vertical axis, the wall cannot transfer stresses lengthwise in any larger scale. This means that it is enough to elongate the wall a few meters outside the excavation edge. Using a wailing beam will increase the influence distance due to its stiffness. In the simulations, the influence distance increases with 50 % using a wailing beam, same value with which the deflection was reduced. For the case with a HEB300 the rule of thumb is that the sheet pile wall has to be elongated outside the excavation edge with the same distance as the excavation is wide. This means that for a five meter excavation, the total length of the sheet pile wall has to be the excavation width, 5 meter, plus 5 meter at each side, giving a total length of 15 meter.

6.4 Measuring results

To evaluate the result of the calculations, a field study was performed at the construction site at contract E33. A staged excavation was performed and the deflection of the sheet pile wall was measured. For the section with wailing beam, no clear displacement where measured. The section without wailing beam showed a clear deflection pattern. Since the outer conditions were hard to define, the results where normalized so that the deflection pattern could be compared with a normalized deflection curve from the simulations in PLAXIS. The results showed good agreement, verifying that the flexural rigidities achieved from previous simulations, were realistic. There was also a clear difference compared to the section with wailing beam which means that the wailing beam do have a significant effect.

7 Future research

In this report, the three dimensional properties of the sheet pile wall is studied, and a method for finding the flexural and torsional rigidities are presented. This method can be developed and refined and a deeper study in this specific subject would be of great interest. It would also be preferable to perform more field measurements in order to determine the real behavior of the sheet pile wall. In the field study in this master's thesis, the load induced by the trains was hard to estimate. Therefore it would be preferable to do a field study where the specific additional load would be easier to determine.

In order to simplify the design process, it would be preferable to use a simplified model in two dimensions. Therefore a method needs to be developed to transform the three dimensional side effects to the two dimensional case.

8 References

ArcelorMittal, 2010. *ArcelorMittal Projects*. [Online] Available at: http://www.arcelorprojects.com/EN/sheet_piling/U_sections/AU14.htm [Accessed 22 April 2010].

Banverket och Vägverket, 2008. *BanaVäg i Väst*. [Online] Available at: www.banavag.se [Accessed 31 Mars 2010].

Brinkgreve, R.B.J., 2007. *PLAXIS, Finite Element Code for Soil and Rock Analyses*.

Edstam, T., 2010. *Beräknings PM*. Göteborg: Skanska Teknik Skanska Sverige AB.

Gabrielsson, J., 2007. *Numerisk simulering av stabilitet för vägbank på sulfidjord-Jämförelser med fältmätningar*. Luleå: Luleå University of Technology.

Gustafson, G., 2008. Course litterature "Modelling and problem solving in civil engineering". Gothenburg, 2008. Chalmers university of technology.

Kort, D.A., 2002. *Sheet Pile Walls in Soft Soil*. Delft: DUP science.

Kullingsjö, A., 2007. *Effects of deep excavations in soft clay on the immediate surroundings*. Gothenburg: Chalmers University of Technology.

Oskarsson, R. & Thorén, T., 2004. *Studie av 3-Dimensionella sidoeffekter vid etappvis schaktning i Götatunneln, J2*. Gothenburg: Chalmers University of Technology.

Potts, D. et al., 2002. *Guidlines for the use of advanced numerical alalysis*. London: Thomas Telford.

Potts, D.M. & Lidija, Z., 2001. *Finite element analysis in geotechnical engineering - Application*. London: Thomas Telford.

Rankine, W., 1857. *On the stability of loose earth*. London: Philosophical Transactions of the Royal Society of London.

Ryner, A., Fredriksson, A. & Stille, H., 1996. *Sponthandboken. Handbok för konstruktion och utformning av sponter*. Stockholm: Byggforskningsrådet.

Skanska Teknik, 2009. *Blueprint 302G223f (modified)*. Göteborg: Skanska Teknik.

Szilards, R., 2004. *Theories and application of plate analysis*. New Jersey: John Wiley & Sons.

Sällfors, G., 2001. *Geoteknik, Jordmateriallära – Jordmekanik*. Gothenburg.

Sällfors, G., 2009. Course litterature in "Infrastructural Geo Engineering". Gothenburg, 2009. Chalmers University of Technology.

Sällfors, G., 2009. *Handbook - Sheet pile wall design*. Course literature in Geotechnics BOM045. Gothenburg: Chalmers University of Technology Division of Geo Engineering, Geotechnical engineering.

Wiberg, N.E., 1974. *Finita Elementmetoden- en datorbaserad beräkningsmetod för ingenjörsproblem*. Malmö: LiberLäromedel.

Appendix

2D calculation of required driven depth of the sheet pile **Appendix 1**

This calculation was done in order to determine the required the required driven depth of the sheet pile wall which gives the safety factor of 1,0 the including a additional of 10 kPa. This calculation match the 2-D simulations done in PLAXIS 2D.

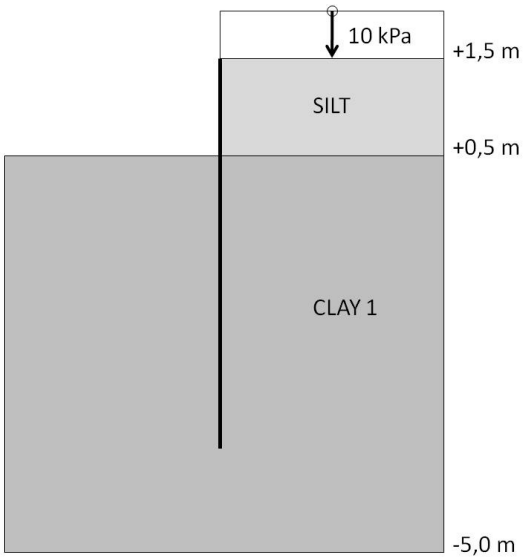

Input data:

Safety class 1

γ_n= 1,0 (valid for SLS and ULS)

γ_m= 1,0 (valid for SLS and ULS)

γ_{Sda}= 1,0

Silt: (1,5-0,5 meter)

$\gamma_{drained}$= 19 kN/m^3

$\gamma_{undrained}$= 22 kN/m^3

φ= 32°

K_A= 0,31

Clay (0,5-5,5 meter)

$\gamma_{undrained}$= 15,5

c_{ud}= 7+0,6·z

Active earth pressure

Friction soil $p_{ad} = \gamma_{Sda} \cdot \sigma'_v \cdot K_A + p_w$

Clay $p_{ad} = \gamma_{Sda} \cdot (\sigma_v - 2 \cdot c_{ud})$

Net earth pressure

The ground below the excavation bottom consists of clay. The net earth pressure is calculated by:

$$p_{net} = N_{cb} \cdot c_{ud} \cdot \gamma_{Sd,Ncb} \cdot (\gamma \cdot H + q_d - P_d)$$

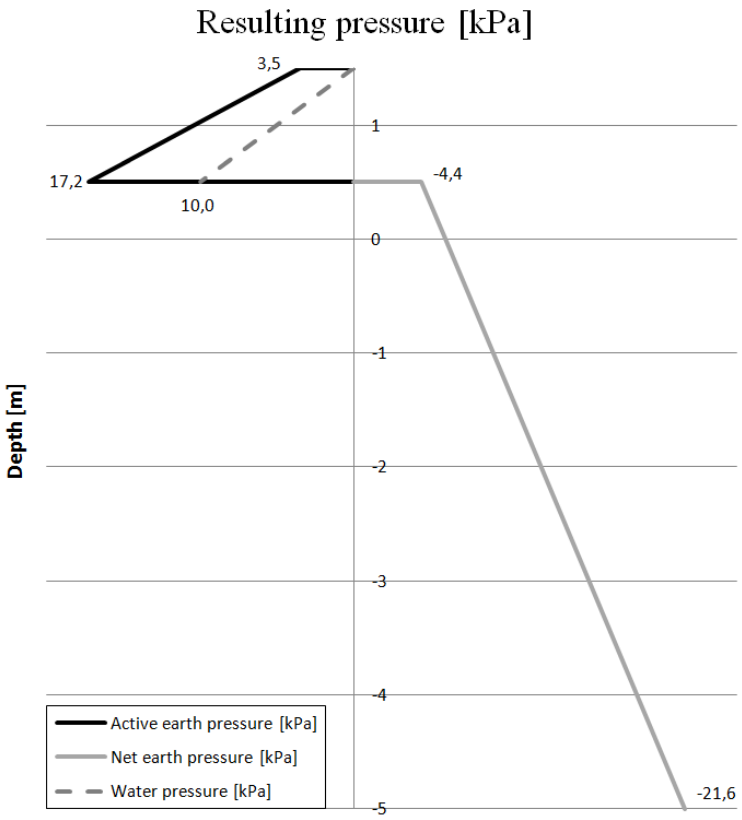

Required driven depth of the sheet pile wall, D = $D + 0{,}2 \cdot D$ = 3,5 meter

Level of driven depth= -3 meter

Total required length of the sheet pile wall= 4,5 meter

Phases during the simulations in PLAXIS

Appendix 2

Identification	Phase no.	Start from	Calculation type	Loading input	Time	First	Last
Initial phase	0	N/A	K0 procedure	Staged construction	0,00 day	N/A	N/A
Replace silt with load	1	0	Plastic	Staged construction	0,00 day	N/A	N/A
Additional loading 10kPa	2	1	Plastic	Staged construction	0,00 day	N/A	N/A
Instalation of sheet pile wall	5	2	Plastic	Staged construction	0,00 day	N/A	N/A
Excavation	3	2	Plastic	Staged construction	0,00 day	N/A	N/A
Safety factor	4	3	Phi/c reduction	Incremental multipliers	0,00 day	N/A	N/A

Results from the PLAXIS simulations

Appendix 2

Note that the scale differs between the figures

Results from Serviceability limit state design

Sheet pile profile AU14, without a wailing beam

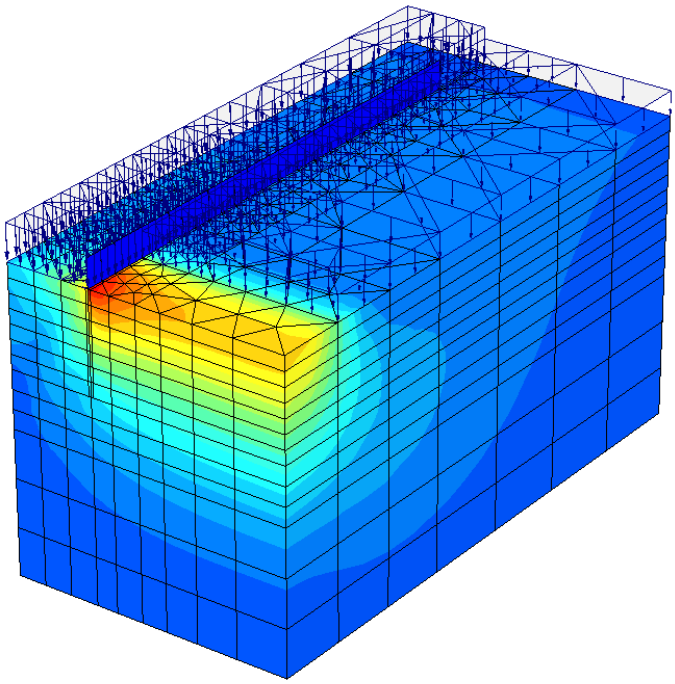

Sheet pile profile AU14, wailing beam profile HEB100

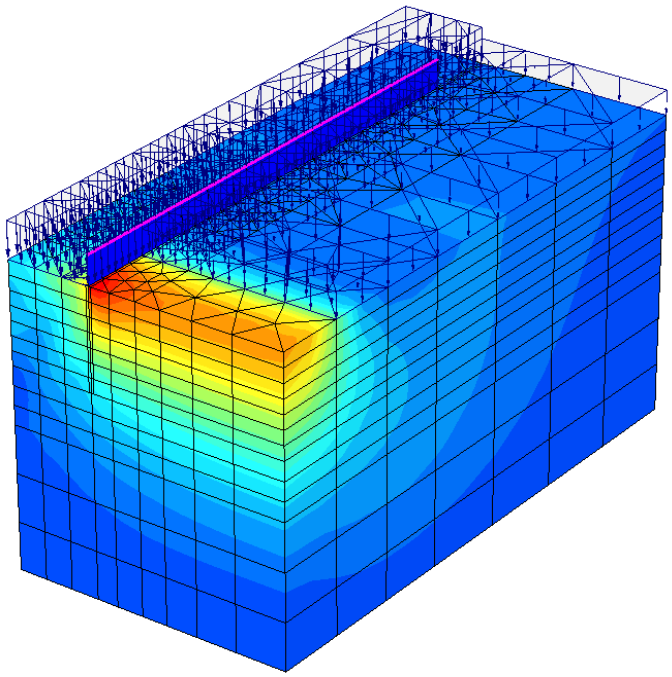

Sheet pile profile AU14, wailing beam profile HEB180

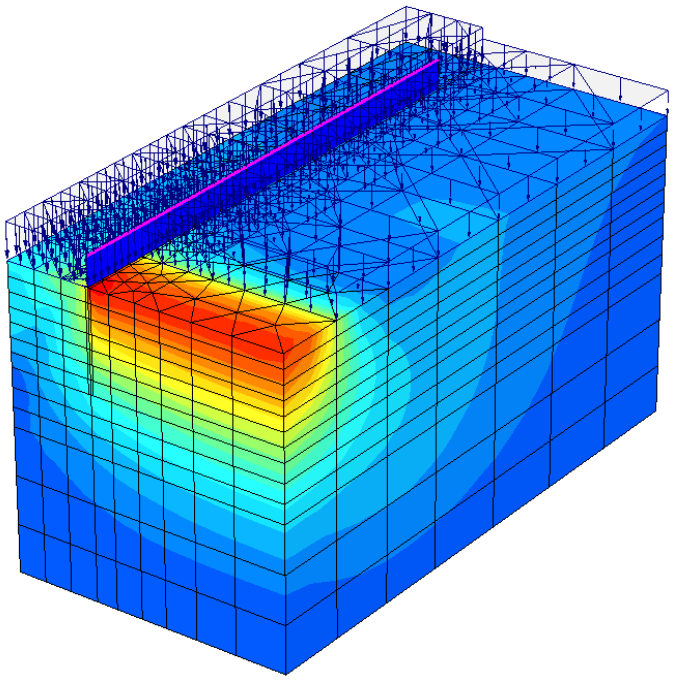

Sheet pile profile AU14, wailing beam profile HEB300

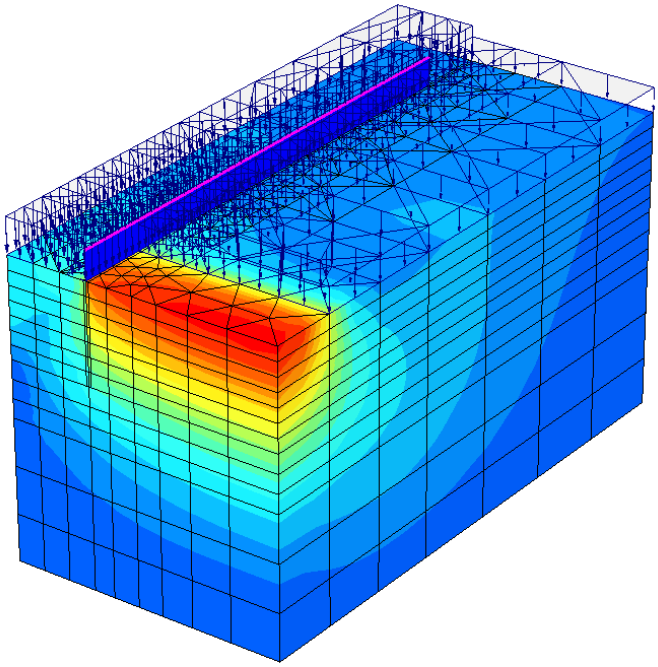

Results from the Phi/c reduction

Sheet pile profile AU14, without a wailing beam

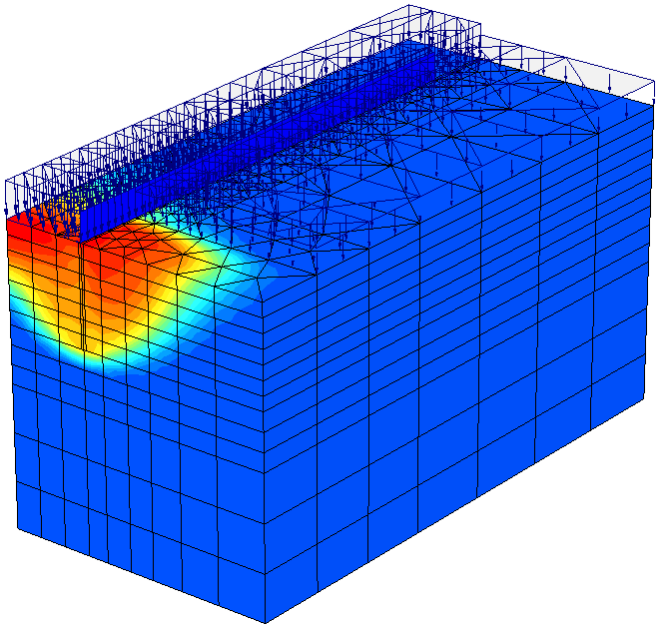

Sheet pile profile AU14, wailing beam profile HEB100

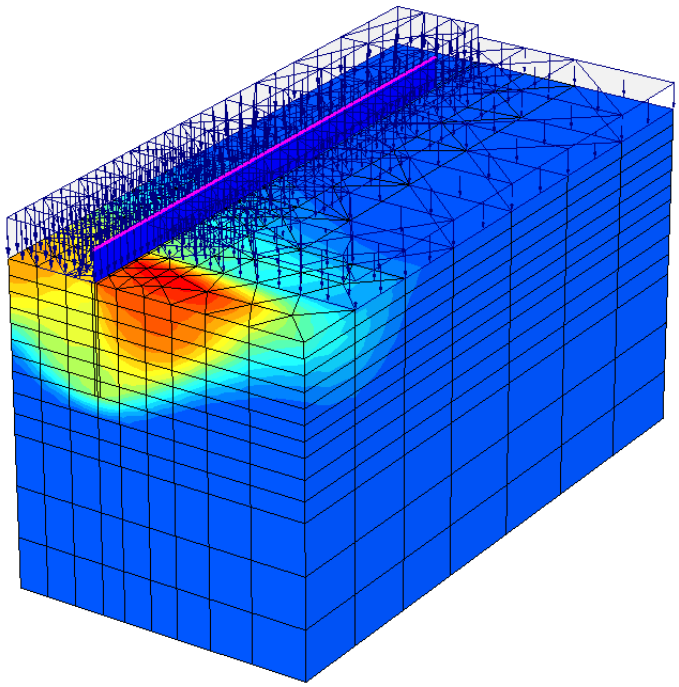

Sheet pile profile AU14, wailing beam profile HEB180

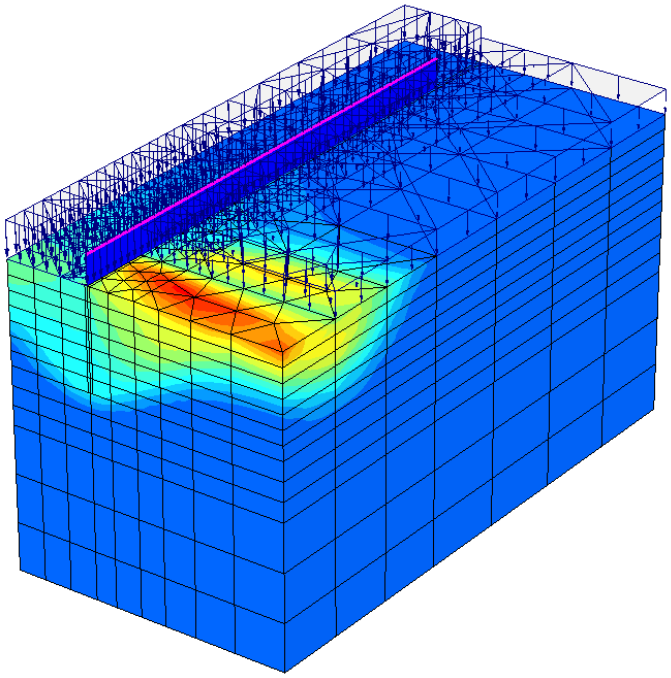

Sheet pile profile AU14, wailing beam profile HEB300

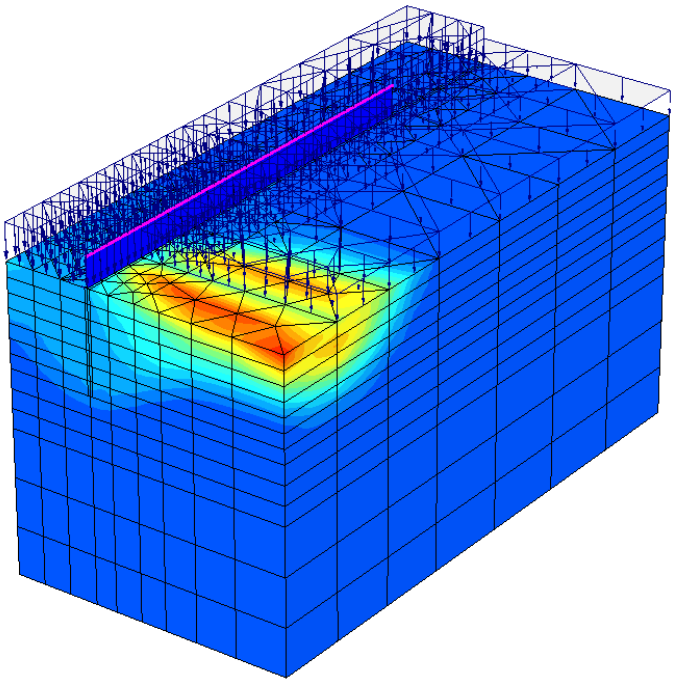

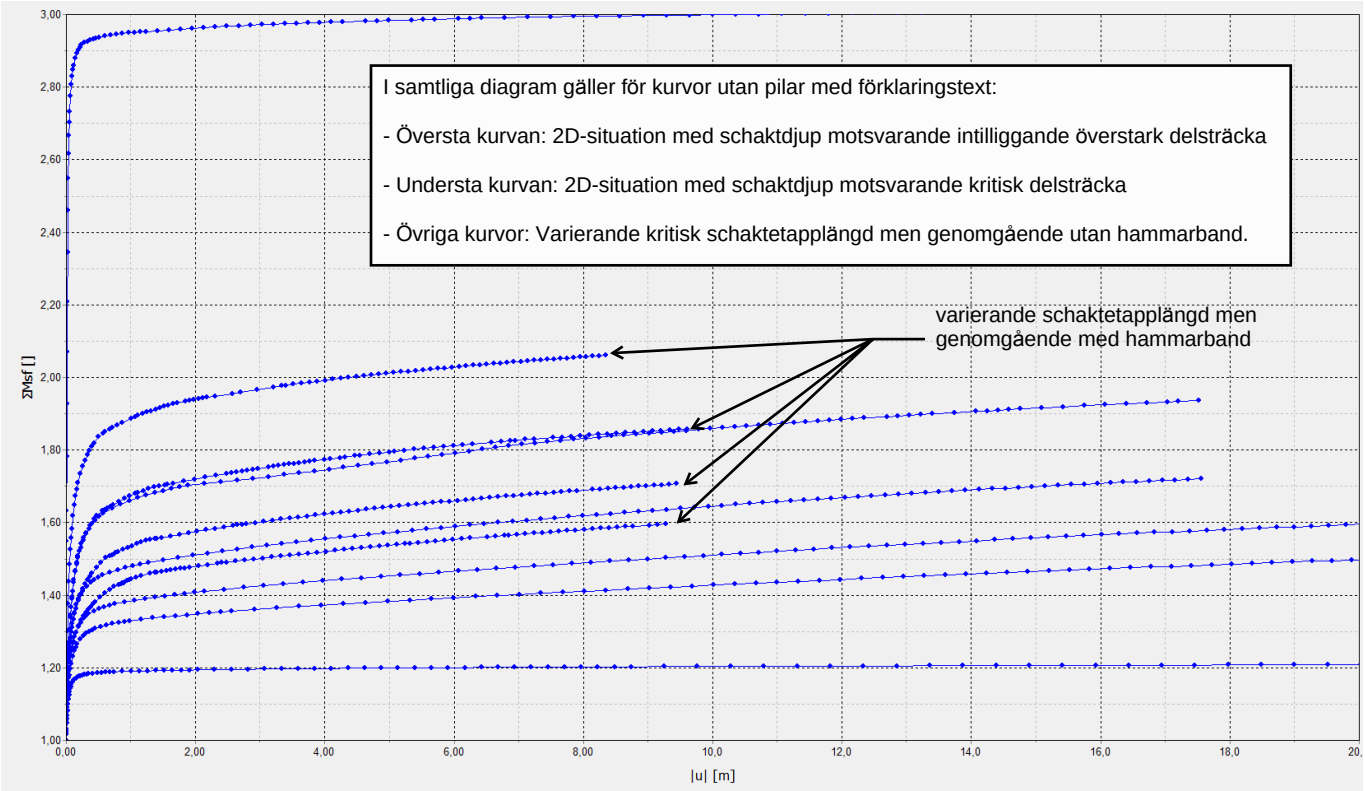

Hållfasthetsprofil: 10 kPa; Schaktdjup: 0,5 m och lokalt 2,0 m.

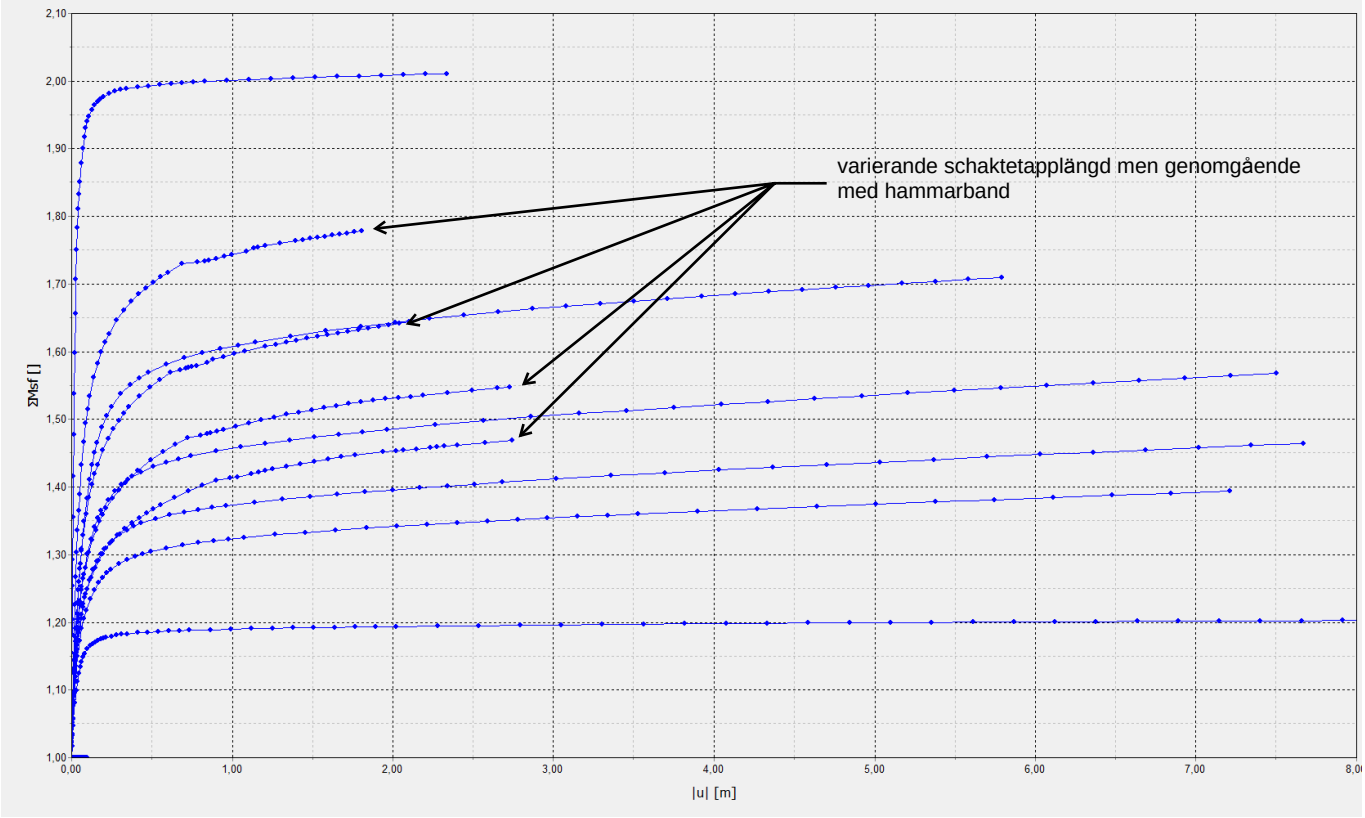

Hållfasthetsprofil: 10 kPa; Schaktdjup: 1,0 m och lokalt 2,0 m.

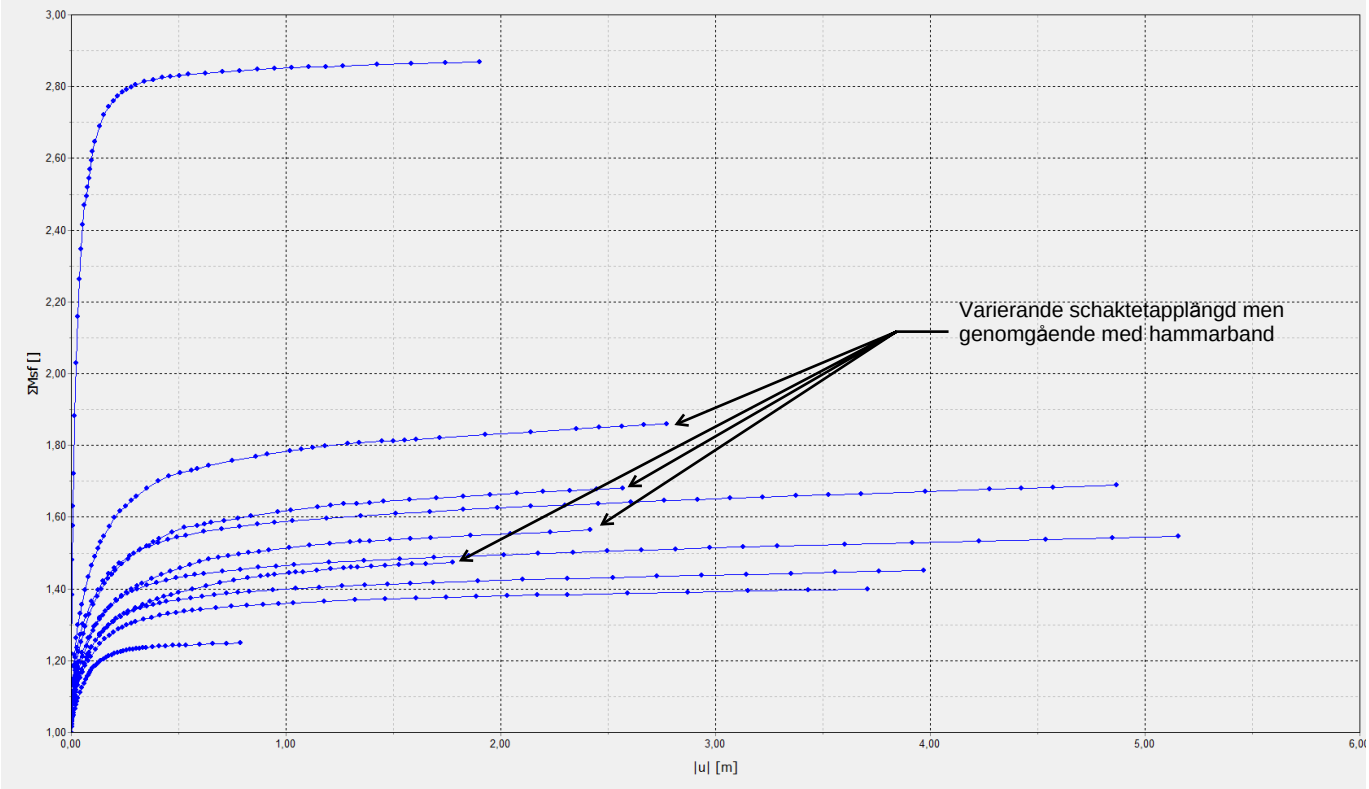

Hållfasthetsprofil: 10+1z kPa; Schaktdjup: 1,0 m och lokalt 3,0 m.

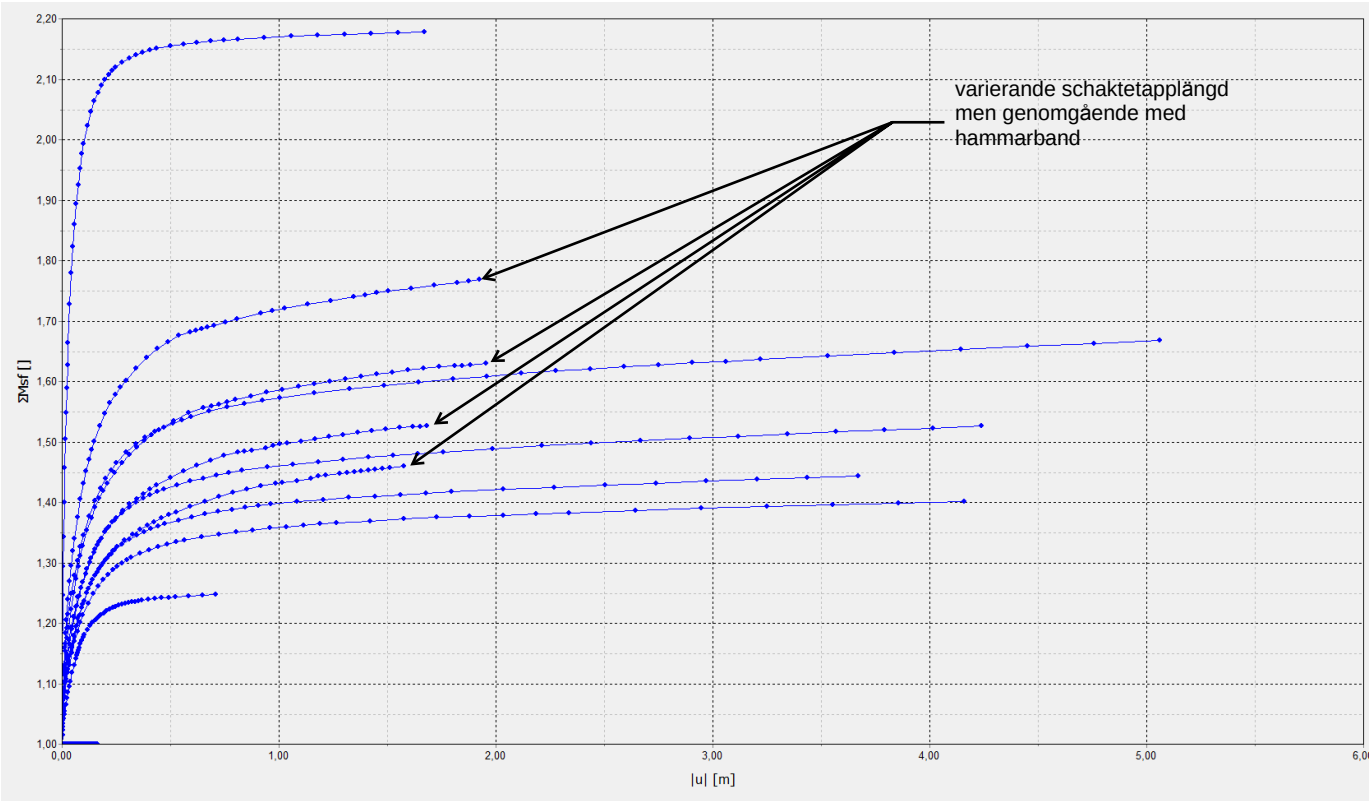

Hållfasthetsprofil: 10+1z kPa; Schaktdjup: 1,5 m och lokalt 3,0 m.

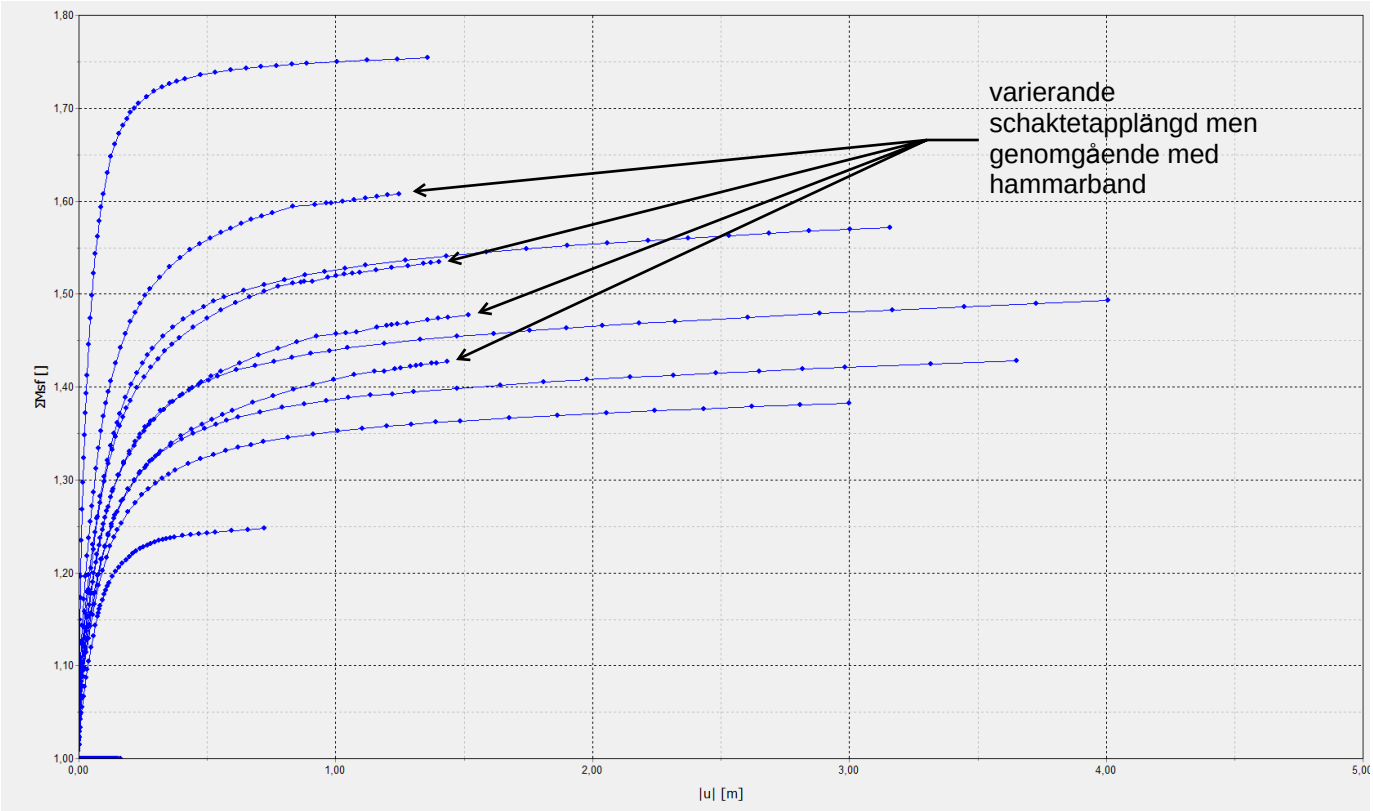

Hållfasthetsprofil: 10+1z kPa; Schaktdjup: 2,0 m och lokalt 3,0 m.

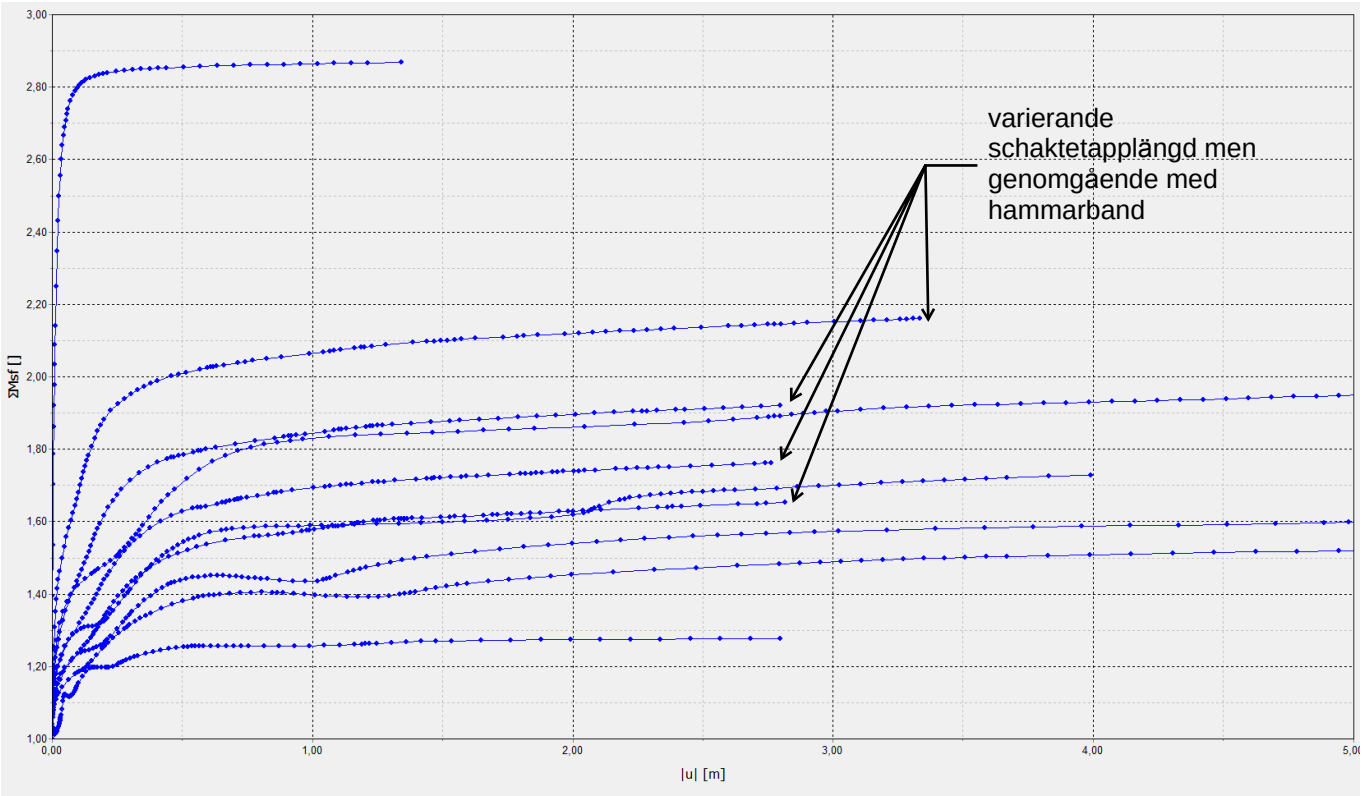

Hållfasthetsprofil: 20 kPa; Schaktdjup: 1,6 m och lokalt 3,6 m.

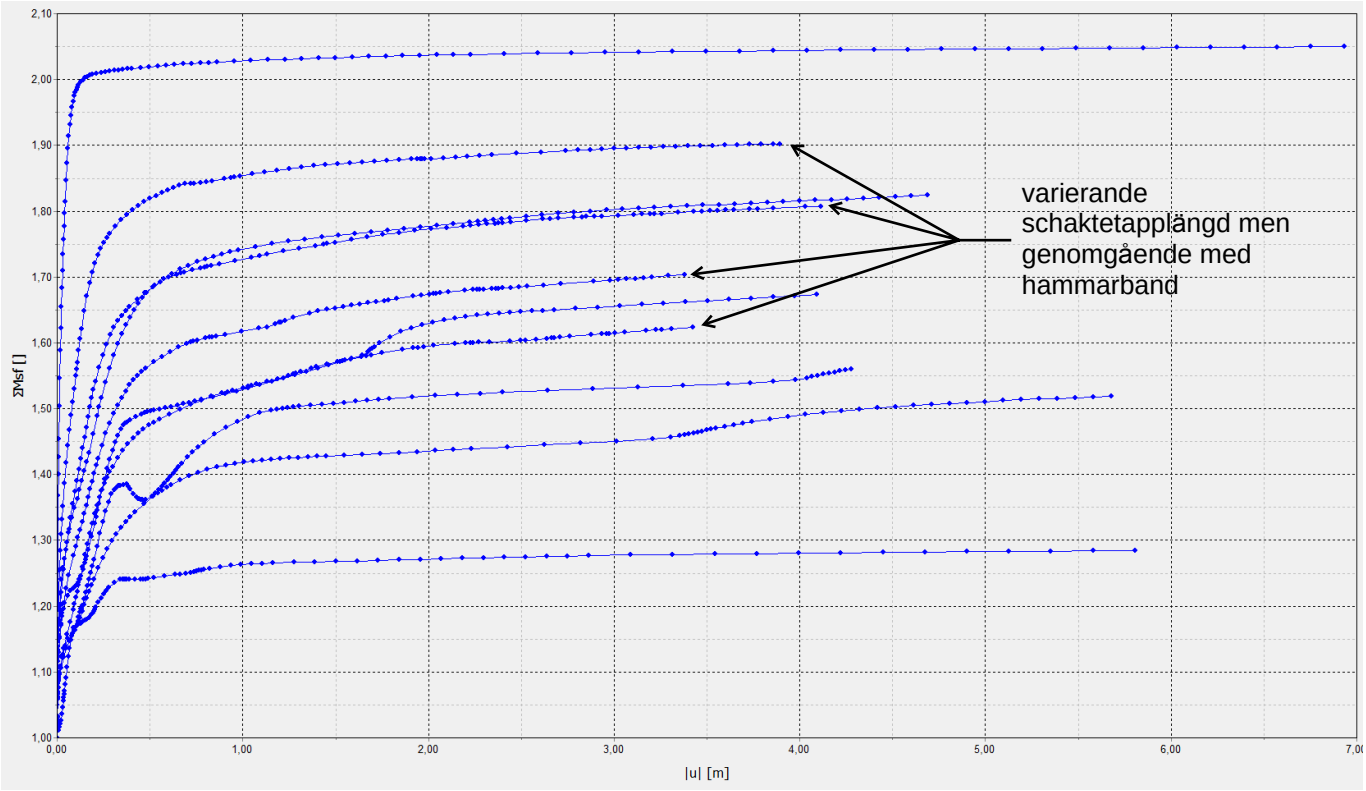

Hållfasthetsprofil: 20 kPa; Schaktdjup: 2,4 m och lokalt 3,6 m.

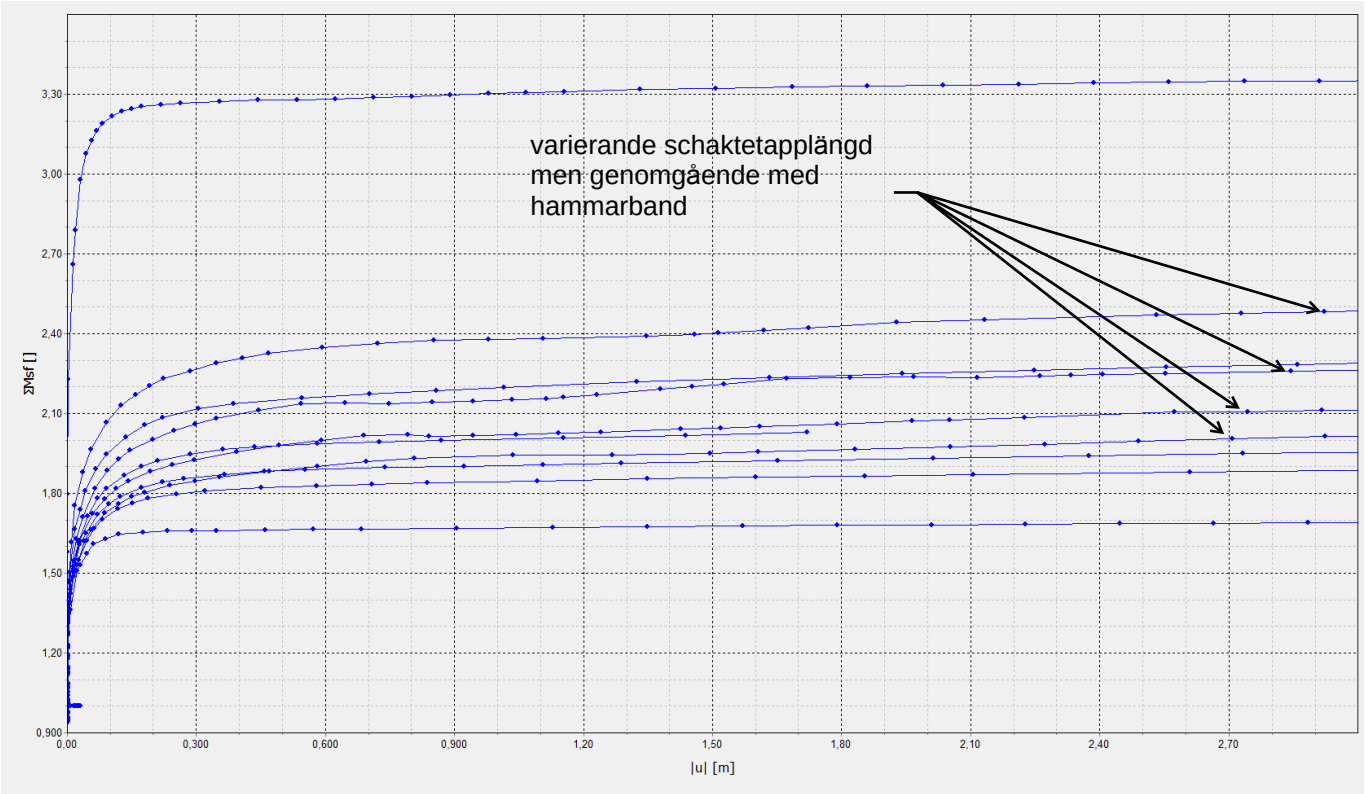

Hållfasthetsprofil: 20 kPa; Schaktdjup: 1,6 m och lokalt 3,6 m; ej i-face